UniS

University of Surrey

SCHOOL OF ENGINEERING
&
POSTGRADUATE MEDICAL SCHOOL

Applications of dielectrophoresis in oncology

by

Fatima H. Labeed

Submitted as part of the requirements for the degree of Doctor of Philosophy

September 2004

Abstract

Malignant cancers are a major cause of morbidity in the UK, accounting for a quarter of all deaths. Chemotherapy is considered to be the most effective treatment; however, cancer cells can become simultaneously resistant to different chemotherapeutic drugs that have no common structure- a phenomenon called multidrug resistance (MDR). This is a serious impediment to the successful treatment of many human cancers and is responsible for many tens of thousands of deaths each year. Cells can acquire MDR via more than one route. The more widely studied MDR mechanism involves the overexpression of membrane proteins such as P-glycoprotein (P-gp), which is thought to eject the drug from within the membrane before it exerts its cytotoxic effects. The second mechanism is mediated by other ion transporters, and results in changes in the pH of various compartments of the cell which allows the cell to sequester and subsequently eject drugs before they act.

This thesis presents a study of the biophysical properties of cancer cells in a range of pharmacological scenarios, focusing on the effects of pharmacological agents both on drug-sensitive and multidrug resistant leukaemic and breast cancer cell lines. In this work, *dielectrophoresis* has been used as a non-invasive technique to examine dielectric properties of drug resistant and sensitive cancer cells before and after treatment with anti cancer drugs, and with a chemosensitiser. These results provide a better understanding of the physiology of different types of cancer cells, and allowed direct comparisons of dielectric properties of the membrane and cytoplasm. Specifically, this work examines the

biophysical changes in both P-gp and non-P-gp mediated MDR cell lines, and at different stages of apoptosis (programmed cell death). In all three, cellular processes are characterised by changes in the ionic state of the cells, as well as changes in the physiology of the membrane.

CONTENTS

Chapters

To my parents,

family and friends

Acknowledgements

I have been indebted in the preparation of this thesis to my supervisors, Dr. Mike Hughes and Dr. Helen Coley, whose support, patience and academic experience have been invaluable to me. Words can not describe my gratitude to them. To Mike: thank you for your kindness and enthusiasm, and for always helping me whenever am on your office door, as well as your humour which always lightened up the atmosphere. To Helen: thank you for your enthusiasm, for being there to answer my cries of help, for teaching me and opening up my eyes to science and cancer, for taking good care of me in conferences abroad and all your lengthy and expensive mobile calls to advise me. I would also like to thank Prof. Hilary Thomas and Dr. David Ewins for their support.

I am very grateful for the help and ideas that have kindly been provided by Dr. George Kass and for the practical assistance given by Mr. Michael Salako and Mrs. Patricia Pirard. My thanks are also due to Mr. David Gould for his urgent technical assistance, as well as Mrs. Christine Shotton and Mr. Ayaz Mehar for practical help and proof reading chapters of my thesis.

I would also like to thank from the bottom of my heart my close friends who have supported and cheered me up from near and far. From far including, Dr. Michele Peters and Mrs. Melanie Rae Nickolaus Stevens, for their continuous understanding and support even when they are miles away, and who have made me feel as if they were near, and Dr. Suha Al-Naimi (for her comforting

phone calls). From near including, Miss. Yvonne Hübner (for having me as her room mate and always lending me the 'listening ear'), Mr. Thomas Wells, Mr. David Moser, Mr. Henry Fatoyinbo, Mr. Fil Horta, Miss Paola Catalfalmo, Mr. Salim Al-Ghoussayni, Mr. Lei Su, Mr. Fei Shao, Mr. Jing Kai Zhang, Mr. Issam Flaieh, Miss. Karla Bustamante (supporting me while she was writing up), Miss. Louisa Lewis, Mrs. Liz Roberts, Miss. Josie De Jesus, Dr. Chris Stevens and Dr. Kai Hoettges.

I would like to thank the EPSRC for funding this project.

Last but by no means least, my heart full of thanks goes to my mother, father, brother and all my sisters, nieces and nephews. They have been a constant source of moral and emotional support.

1. Introduction

Malignant cancers are a major cause of morbidity in the UK, over 245, 000 new cases were registered in 1995. They account for a quarter of all deaths. 1 in 3 people are considered at risk in his/ her lifetime and over 65% of all new cases are diagnosed in people over 65 years of age (The Cancer Research Campaign, 1998- 99). There are over 200 types of cancer, the most common of those are lung, breast, bowel and the leukaemias. The latter accounts for a third of all cases (The Cancer Research Campaign, 1998-99). The usual ways of treatment were reported to involve, local excision and/or radiation, chemotherapy for patients with haematological malignancies, immunotherapy and biological-response modifiers (as reviewed in Gottesman et al, 2002). Cancers are classified according to the tissue and cell type from which they arise. Those arising from epithelial cells and connective tissue are termed *carcinomas* and *sarcomas*, respectively. Those that do not fit into any category are the *leukaemias* and arise from different haemopoietic cells (Alberts et al, 1994).

Chemotherapy is considered to be the most effective treatment for metastatic tumours. However, cancer cells can become simultaneously resistant to different chemotherapeutic drugs that have no common structure- a phenomenon called multidrug resistance (MDR). This is a serious impediment to the successful treatment of many human cancers and is responsible for many tens of thousands of deaths each year, as reviewed by Gottesman et al (2002) and Rosenberg et al (1997). MDR causes an increase in drug efflux, and in turn, lowers the intracellular drug concentrations, as reviewed by Ford (1996). The resistance of

neoplastic cells to cytotoxic drugs may be intrinsic (present before the drug is first given) or 'acquired' (developed during drug treatment). The acquired resistance may either be due to adaptation of the tumour cells or to mutation (Rang et al, 1995).

1.1. Mechanisms of Multi-Drug Resistance (MDR)

Cells can acquire MDR via more than one route. The way some MDR cells operate can involve one or more mechanisms. The more widely studied MDR mechanism involves the overexpression of membrane proteins which are thought to eject the drug from within the membrane before it reaches the cytoplasm. These proteins form a family known as the ATP binding cassette (ABC or ABCC) proteins. The second method is mediated by other ion transporters, and results in changes in the pH of various compartments of the cell which allows the cell to sequester and subsequently eject drugs before they act. We will now consider these in more detail.

1.1.1. ABC-related MDR

Over 40 years ago, it was recognised that certain proteins were able to transport substances across cellular membranes and against a concentration gradient. It was early realised that these processes require the input of energy and the hydrolysis of ATP, directly or indirectly. A large subclass of these proteins has been described, known as the ABC proteins (ATP- binding cassette), named for their distinctive domains that bind ATP. These sequences, known as Walker A

and Walker B, reside in the nuclear binding domain (NBD) and are highly conserved across many species (Litman et al, 2001).

Classic MDR generally results from the expression of ATP- dependent efflux pumps with drug specificity. Resistance results because increased drug efflux lowers the intracellular drug concentrations. An example of the group of drugs that is affected by MDR is the *anthracyclines* (that includes doxorubicin), as well as other natural product agents such as vincristine, paclitaxel (Taxol) and VP-16 (Gottesman et al, 2002 and Ford, 1996).

The MDR phenotype was first linked to the over- expression of a 170 kDa membrane glycoprotein, named as P- glycoprotein (P- gp, P for permeability). This protein was found by Juliano and Ling (1976), and was the first known human ABC protein capable of transporting drugs out of the cell. P- gp is the product of the (*MDR1*) gene, made from 12 transmembrane regions that bind hydrophobic, either neutral or positively charged, drug substrates. It has been demonstrated by immunohistochemistry that P- gp is highly expressed in colon, kidney, adrenocortical and hepatocellular cancers (Gottesman et al, 2002).

In non-MDR cells, cytotoxic agents such as doxorubicin can permeate through the plasma membrane, exert their cytotoxic effects which leads to cell death. In MDR cells, the drugs are effluxed from the lipid phase and cannot accumulate in the cell. Reports reviewed (Higgins and Gottesman, 1992) and (Higgins and Linton, 2001) that P- gp acts as a 'flippase', whereby the drug interacts with the membrane lipids before it interacts with the actual protein, and drug that is

intercalated into the inner leaflet of the lipid bilayer is either pumped directly into the extracellular space or is flipped by the protein into the outer leaflet. P- gp function was reported to require two ATP hydrolysis events to transport one drug molecule. The binding of substrate to the transmembrane regions stimulates the ATPase activity causing a conformational change that releases the substrate to either the outer leaflet of the membrane or the extracellular space. Hydrolysis at the second ATP site seems to be needed to re- set the P- gp to bind the substrate again, thus completing one catalytic cycle (Gottesman et al, 2002).

The flow diagram (Figure 1.1) summarises the possible roles of P- gp, beyond its protective functions, suggested in recent literature (Ferte, 2000):

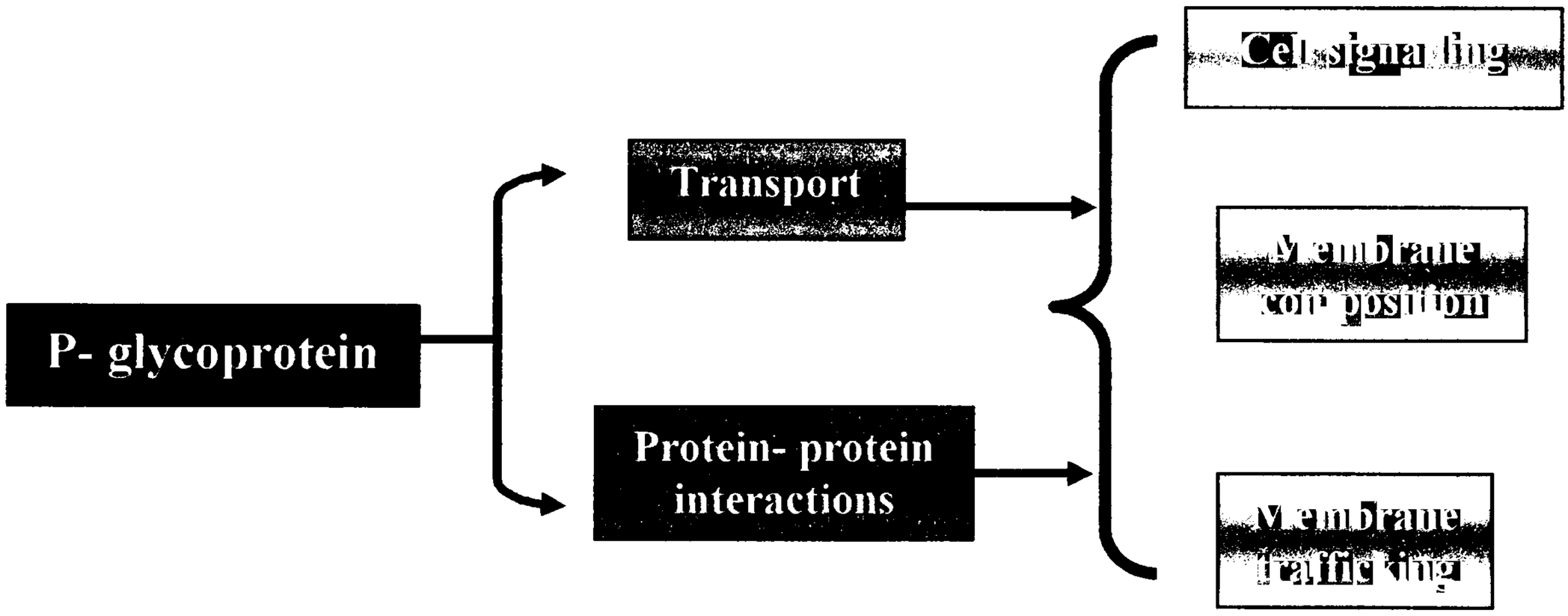

Figure 1.1: Summary of P- gp role

Paclitaxel (Taxol) is a commonly used anticancer agent, excreted from the intestine via P-gp. Gene- targeting studies have demonstrated that P- gp is responsible for fecal excretion of 85% of orally administered Taxol (Scuetz, and Strom, 2001). P- gp can be found in normal tissues, it is located in the luminal surface of endothelial cells of capillaries forming the blood- brain- barrier and

preventing the penetration of cytotoxins across the endothelium (Gottesman et al, 2002).

As not all MDR cells express P- gp, a search for other efflux pumps was initiated leading to the discovery of multidrug- resistance- associated protein 1 (MRP1), which was identified and characterised by Cole et al (1992) and Grant et al (1994). This 190 kDa protein is another ABC transporter and is similar to P- gp in structure, with the exception of an amino terminal extension containing five membrane- spanning domains attached to a P- gp-like core. Human P- gp and MRP1 share 15% amino acid homology. MRP1 transports drugs such as vincristine and Taxol. MRP was discovered because of its over- expression in a number of MDR human cell lines that do not over- express P- gp. In addition, MRP1 has been shown to be expressed in several normal tissues including the liver (Jedlitschky et al, 1996). In addition MRP1 proteins have been shown to be localised to the basolateral membrane of choroids plexus, where they serve to pump the metabolic waste products of cerebrospinal fluid (CSF) into the blood (reviewed in Gottesman et al, 2002). Other ABC transporters associated with MDR and the breast cancer resistance protein (BCRP) and the lung resistance protein (LRP) (Maliepaard et al, 1999; Izquierdo et al, 1995).

1.1.2. Non-ABC MDR Mechanisms

Another mechanism has been suggested for the acquisition of MDR, which does not require the expression of ABC transporter overexpression. Instead, this mechanism is related to the sequestration of drugs within vesicles and

cytoplasmic organelles away from the target site (Sognier et al, 1994; Slapak et al, 1992; and reviewed in Dietel, 1991).

These cells are reported to have an alkaline cytoplasmic pH (Warburg, 1956; Simon and Schindler, 1994), while the vesicular pH is more acidic in resistant than sensitive cells. Schindler et al (1996) explained that sensitive cells exhibited a diminished capacity to remove cytotoxic drugs from the cytoplasm by sequestration of protonated drugs within the vesicles. The group suggested that protonation of anti-cancer drugs causes them to be sequestered in vesicles, allowing them to be secreted later and thus preventing them reaching their target.

1.1.2. MDR modulators

Recent literature (Litman et al, 2001) reviewed how this transport could be blocked, and MDR reversed by the addition of substrate analogues, the so-called *MDR modulators* or *chemosensitisers*. Many have been developed, such as the PSC833 (one of the second generation modulators) and XR9576 (a third generation modulator that has reached phase III in clinical trials). However, their precise mechanism of their action remains unclear, although a good deal of research has been carried out thus far.

A large number of drugs have been identified which inhibit the function of P- gp. Just as the anticancer substrates are diverse in chemical structure and function, so too are MDR "modulators". They fall into six broad categories: a) calcium

channel blockers, b) calmodulin antagonists, c) cyclic peptides, d) steroids and hormonal analogues, e) dipyrimadole, and f) miscellaneous other compounds (Ford, 1996). Most of these modulators (such as verapamil and cyclosporin A, known as "First generation MDR modulators") are themselves non- specific, weak inhibitors and substrates for the P- gp pump (Fisher et al, 1996). An exception to this is the cyclosporin analogue PSC833, one of the "Second generation modulators". Its intracellular accumulation is not altered by expression of P- gp and is less toxic (Krishna et al, 2000). A recent review (Litman et al, 2001) supported the notion that PSC833 is a substrate of P- gp, and when it competes with the anticancer drug (such as verapamil or daunorubicin), it will win out due to its higher affinity. However, since the transport rate is slower, it will slow down the turnover rate, which will decrease the ATPase activity. It might, therefore, be better to regard PSC83 as partial antagonist, as it does not completely block P- gp, but slows it down; PSC833 is a bulky molecule that will act as an obstructive substrate. Second generation P-gp modulators have a better pharmacologic profile than the first generation compounds, but they also retain some characteristics that limit their clinical usefulness. In particular, these compounds have been suggested to significantly inhibit the metabolism and excretion of cytotoxic agents, thus leading to unacceptable toxicity that has necessitated chemotherapy dose reduction in clinical trials (reviewed in Thomas and Coley, 2003) The development of more potent and selective P- gp inhibitors remained a goal, which has resulted in the discovery of a potent and a specific P- gp inhibitor, anthranilamide based, XR9576 (Xenova Ltd, Slough, UK) (Roe et al, 1999).

1.2. Apoptosis

Cells that die accidentally as a result of an injury degenerate by a process called *necrosis* that is characterised mainly by swelling and bursting of the cells, which would together induce an inflammatory response in the surrounding tissue. *Apoptosis* on the other hand was the term first described by Kerr et al (1972), but the authors were grateful to Professor James Cormack of the department of Greek at the University of Aberdeen, who suggested the name. Apoptosis was suggested as a genetically regulated process, mechanisms of which appear to play a complementary but opposite role to mitosis in the regulation of cells in the animal and plant kingdom as examples. Kerr et al (1972) first described the changes in morphology in apoptotic cells as being of a "programmed" nature, initiated by stimuli such as the environment. These structural changes were suggested by the authors to take place in two stages, the first comprises a nuclear and cytoplasmic condensation, and breaking up of the cell into membrane-bound 'apoptotic bodies'. The second stage involves the apoptotic bodies shedding from the surfaces.

Apoptosis seems to be involved in the cell turnover in many healthy adult tissues and is responsible for the focal elimination of cells during the normal embryonic development. It can occur spontaneously and has been implicated in physiological atrophy of various tissues and organs (Kerr et al, 1972).

Programmed cell death is a highly regulated process but has been described as a "double-edged" sword (Hughes and Mehmet, 2003). It is crucial to the

developmental processes in multi-cellular organisms, but loss of regulatory control is implicated in a growing number of diseases, including inflammation, malignancy, autoimmunity and neurodegeneration. Apoptosis-related genes have been identified in most tissues and successful characterisation of such genes presents potential therapeutic targets. Many of today's medical conditions can be attributed directly or indirectly to the defects in the regulation of apoptosis that result in either cell accumulation, in which cell eradication is impaired, or cell loss, in which cell-suicide programme is inappropriately triggered. Identification of these genes and gene products has provided the foundation for a range of drug discovery programmes, in particular in the development of chemotherapeutic agents to cause apoptosis in otherwise "immortal" cancer cells.

1.3 Thesis aim and structure

In the three cases described above – P-gp and non-P-gp mediated MDR, and apoptosis – the cellular processes are characterised by changes in the ionic state of the cells, as well as changes in the physiology of the membrane. This thesis sets out to study these phenomena using a technique known as dielectrophoresis (DEP). DEP is an electrostatic phenomenon which has been increasingly used for cell analysis since its discovery in 1951 by Herbert Pohl. By studying the motion of cells when exposed to electric fields of different frequency, it is possible to determine the electrical properties of those cells, and

in combination with conventional cell biology techniques, to come to a new understanding of these cellular processes.

Although DEP has been used to study cancer cells in the past (Gascoyne et al, 1992; 1993; 1997; Cristofanilli et al, 2002; Wang et al, 2002), these studies have mainly concentrated on the cellular membrane rather than the cell and its components in entirety. This thesis aims to investigate the dielectric properties of the whole cell (and particularly the cytoplasm), as well as studying differences in P-gp mediated MDR with respect to drug sensitive cell lines (Chapter 3) and non-P-gp mediated MDR (Chapter 4), and to provide and clarify the principles of MDR by understanding the cellular physiology. DEP is also used as part of a novel approach to study the biophysical changes during different stages of apoptosis (Chapter 5). All of these results indicate that DEP can both reinforce and extend existing knowledge of key processes in MDR and cancer.

1.4. References

Alberts, B. Johnson, A. Lewis, J. et al. *Molecular Biology of the Cell*, 3rd edition (1994) Garland Publishing, Inc.

Cole, SPC. Bhardwaj, G. Gerlach, J.H. et al. Overexpression of a transporter gene in multidrug-resistant human lung cancer cell line (1992) *Science* **258** (5088): 1650-1654.

Cristofanilli, M. De Gasperis, G. Zhang, L. et al. Automated electrorotation to reveal dielectric variations related to HER-2/neu overexpression in MCF-7 sublines (2002) *Clinical Cancer Research,* **8**(2): 615- 619.

Dietel, M. What's new in cytostatic drug resistance and pathology (1991) *Pathology Research Practice*, **187**: 892-905.

Ferte, J. Analysis of the tangled relationships between P-glycoprotein-mediated multidrug resistance and the lipid phase of the cell membrane (2000) *European Journal of Biochemistry,* **267**(2): 277-294.

Fisher, G.A. Lum, B.L. Hausdorff, J. Sikic, B.I. Pharmacological considerations in the modulation of multidrug resistance (1996) *European Journal of Cancer,* **32**A(6): 1082-1088.

Ford, J.M. Experimental reversal of P-glycoprotein-mediated multidrug resistance by pharmacological chemosensitisers (1996) *European Journal of Cancer,* **32**A(6): 991- 1001.

Grant, C.E. Valdimarsson, G. Hipfner, D.R. et al. Overexpression of multidrug resistance-associated protein (MRP) increases resistance to natural product drugs (1994) *Cancer Research*, **54** (2): 357-361.

Gottesman, M.M. Fojo, T. Bates, S. Multidrug resistance in cancer: Role of ATP-dependent transporters (2002) *Nature Reviews Cancer*, **2**(1): 48- 58.

Higgins, C.F. Gottesman, M.M. Is the multidrug transporter a flippase (1992) *Trends in Biochemical Science*, **17**(1), 18-21.

Higgins, C.F. Linton, K.J. Structural biology - The xyz of ABC transporters (2001) *Science*, **293**(5536), 1782-1784.

Hughes, D. Mehmet, H. *Cell proliferation and apoptosis. Advanced methods* (2003) Bios Scientific Publishers Limited. Oxford.

Izquierdo, M.A, Vanderzee, A.G.J. Vermorken, J.B. et al. Drug resistance-associated marker LRP for prediction of response to chemotherapy and prognoses in advanced ovarian carcinoma (1995) *Journal of the National Cancer Institute* **87** (16): 1230-1237.

Jedlitschky G, Leier I, Buchholz U. et al. Transport of glutathione, glucuronate, and sulfate conjugates by the MRP gene-encoded conjugate export pump (1996) *Cancer Research*, **56** (5): 988-994.

Juliano, R.L. Ling, V. A surface glycoprotein modulating drug permeability in Chinese hamster ovary cell mutants (1976) *Biochimica et Biophysica Acta*, **255**: 152-162.

Kerr, J.F. Wyllie, A.H. Currie, A.R. Apoptosis: a basic biological phenomenon with wide-ranging implications in tissue kinetics (1972) *British Journal of Cancer*, **26**:239-257.

Krishna, R. Mayer, L.D. Multidrug resistance (MDR) in cancer. Mechanisms, reversal using modulators of MDR and the role of MDR modulators influencing the pharmacokinetics of anticancer drugs (2000) *European Journal of Pharmaceutical Sciences*, **11**(4): 265-283.

Litman, T. Druley, T.E. Stein, W.D. et al. From MDR to MXR: new understanding of multidrug resistance systems, their properties and clinical significance (2001) *Cellular and Molecular Life Sciences*, **58**(7): 931- 959.

Maliepaard, M. van Gastelen, M.A. de Jong, L.A. et al. Overexpression of the BCRP/MXR/ABCP Gene in a Topotecan-selected Ovarian Tumor Cell Line (1999) *Cancer Research*, **59**, 4559-4563.

Mistry, P. Stewart, A.J. Dangerfield, W. et al. In vitro and in vivo reversal of P-glycoprotein-mediated multidrug resistance by a novel potent modulator, XR9576 (2001) *Cancer Research,* **6**(1): 749- 758.

Pohl, H.A. The motion and precipitation of suspensoids in divergent electric fields (1951) *Journal of Applied Physics*, **22**(7): 869-871.

Rang, H. P. Dale, M.M. Ritter, J.M. *Pharmacology* (1995) Churchil Livingstone.

Roe, M. Folkes, A. Ashworth, P. et al. Reversal of P-glycoprotein mediated multidrug resistance by novel anthranilamide derivatives (1999) *Bioorganic & Medicinal Chemistry Letters,* **9**(4): 595- 600.

Rosenberg, M.F. Callaghan, R. Ford, R.C. et al. Structure of the multidrug resistance P-glycoprotein to 2.5 nm resolution determined by electron microscopy and image analysis (1997) *Journal of Biological Chemistry,* **272**(16): 10685- 10694.

Sanchenkov, A. Livak, D.A Cabot, M.C. Targeting ceramide metabolism - a strategy for overcoming drug resistance (2001) *Journal of the National Cancer Instiute,* **93**(5): 347- 357.

Schindler, M. Grabski, S. Hoff, E. et al. Defective pH regulation of acidic compartments in human breast cancer cells (MCF-7) is normalised in Adriamycin-resistant-resistant cells (MCF-7adr) (1996) *Biochemistry*, **35**: 2811-2817.

Scuetz, E. Strom, S. Promiscuous regulator of xenobiotic removal (2001) *Nature Medicine,* **7**(5): 536- 537.

Simon, S.M. Schindler, M. Cell biological mechanisms of multidrug resistance in tumors (1994) *Proceedings of the national Academy of the United States of America*, **91** (9): 3497-3504.

Slapak, C.A. Lecerf, J-M. Daniel, J.C. et al. Energy dependent accumulation of daunorubicin into subcellular compartments of human leukaemia cells and cytoplasts (1992) *The Journal of Biological Chemistry*, **267** (15): 10638-10644.

Sognier, M.A. Zhang, Y. Eberle, R.L. et al. Sequestration of doxorubicin in vesickes in a multidrug resistant cell line (LZ-100) 1994 *Biochemical Pharmacology*, **48** (2): 391-401.

Thomas, H. Coley, H.M. Overcoming multidrug resistance in cancer: an update on the clinical strategy of inhibiting P-glycoprotein (2003) *Cancer Control*, **10**(2): 159-165.

Wang, X.J. Becker, F.F. Gascoyne, P.R.C. Membrane dielectric changes indicate induced apoptosis in HL-60 cells more sensitively than surface phosphatidylserine expression or DNA fragmentation (2002) *Biochimica et Biophysica Acta*, **1564**(2): 412-420.

Warburg, O. On the origin of cancer cells (1956) *Science* **123**:309-14.

2. Dielectrophoresis

2.1. Introduction

AC- electrokinetics is the collective term used to describe a group of phenomena such as dielectrophoresis (DEP) and electrorotation (ROT). The motion of suspensoid particles resulting from polarisation forces produced by an inhomogenous electric field was first described and termed *dielectrophoresis* by Herbert Pohl (1950). He determined that this phenomenon was related to the related phenomenon of electrophoresis, in which suspended particles are moved by the action of an electrostatic field on the charged particles.

If a dielectric particle (such as a cell) is suspended in an electric field, it will polarise and acquire a dipole. The direction and magnitude of this induced dipole depends on the frequency and magnitude of the electric field and on the dielectric properties of the cell and the medium (Pohl, 1978). Historically, the use of non-uniform electric fields was suggested by Pohl to have dated back to the 19th century, when Lowden in 1891 patented an invention for the removal of metal particles from used lubricating oils. The DEP phenomenon was widely applied, later on, to the manipulation, separation and analysis of cellular and viral particles (Jones 1995, Zimmermann and Neil 1996, Hughes 2002).

Particles experiencing such forces can be made to exhibit a variety of motions including attraction to, and repulsion from, regions of high electric field (termed

positive and negative DEP respectively) by changing the frequency of the applied electric field. Pohl (1978) described how bio-particles such as bacteria, cells or viruses can be characterised by their dielectric properties, and since then dielectrophoresis can be used to distinguish between different types of bacteria (Markx et al, 1994a), to detect changes in cell cytoplasmic properties (Mahaworasilpa, 1994) and to detect whether cells are viable or non-viable (Ying et al, 1992; Falokun et al, 2003). The main factors influencing the dielectric properties of a bioparticle are the surface charge, the membrane capacitance and the conductivity of the cytoplasm. If drugs such as antibiotics change any of these factors, the dielectric properties of the cell change and can be detected (Johari et al, 2003); this change can then be used to distinguish between cells that are resistant or sensitive to a drug.

By exploiting the fact that different particles may experience forces acting in different directions when all other factors are the same, researchers have been able to use DEP to analyse and separate mixtures of cells on electrode arrays. For example, work has demonstrated that DEP can be used to examine the effect of drugs on cells, such as the effect of nystatin on erythrocytes (Gimsa et al. 1994) or the response of neutrophils to activation by chemotactic factors (Griffith and Cooper 1998). Since populations of particles may experience forces acting in different directions within specific frequency windows, separation has been demonstrated for mixtures of viable and non-viable yeast cells (Markx et al 1994b), and CD34+ cells from bone marrow (Stephens et al 1996), which can be separated from human blood. Other demonstrations of cell separation have been made in separating breast

cancer cells from blood, erythrocytes with and without malarial parasite infection, leukocytes, and different types of viruses in solution using this technique (Gascoyne et al 1997; Yang et al 1999; Morgan et al 1999), respectively.

DEP can be used to determine the dielectric properties of particles by examining the behaviour of particles across a broad frequency range. This typically involved the determination of a frequency where the dielectrophoretic force on a particle is zero, and hence determining the dielectric properties of the membrane (Burt et al, 1990) This method has been applied to studies of cellular responses to a broad range of toxicants (Ratanachoo et al, 2002), membrane changes during apoptosis (Wang et al, 2002), malarial infection (e.g. Gascoyne et al, 2002) and cancer cell transformation (Huang et al, 1996). Studies of the dielectrophoretic behaviour of cells over a broader frequency range have elicited information about both membrane and cytoplasm, and have been used to examine the effects of antibiotics on bacteria (Johari et al., 2003), the effects of copper sulphate on algae (Hübner et al, 2003). This potentially makes DEP a very valuable tool for screening applications.

In order to extract dielectric parameters from dielectrophoretic data, modelling techniques are used to find best-fit parameter for given sets of data indicating the time-dependent polarisibility of the particles. Analytical expressions have been derived for the dielectrophoretic behaviour of homogeneous spheres (eg Benguigui and Lin 1982). However, it is generally considered (Jones 1995) that the expansion of the equation linking the dielectrophoretic behaviour to the dielectric properties of

the particle is too complex to provide useful analytical expressions directly linking the dielectric properties of the cell to the observed dielectrophoretic behaviour. In general, the estimation of dielectric properties is performed by best-fit numerical analysis (Huang et al 1996) in order to determine the properties of the membrane and the cytoplasm to provide information of potential significance to biological scientists.

2.2. Theory

A polarisable particle suspended in a uniform electric field (as shown in Figure 2.1A) will experience no net movement, as the forces induced by the interaction between each of the dipolar charges and the electric field are equal and opposite; the cell will not move unless it carries a net charge. Even when there is a net charge, the particle will not undergo observable displacement unless the field frequency is equal to, or near, zero.

The interaction of the charges on each side of the dipole with the electric field generates a force. Coulomb's law states that a charge Q_1 generates an electric field E, and that this electric field induces a force on second charge Q_2 according to the following expression (equation 1):

$$\boldsymbol{E} = \frac{Q_1}{4\pi\varepsilon d^2}\boldsymbol{r}$$

$$\boldsymbol{F} = Q_2\boldsymbol{E} \qquad (1)$$

where d the distance between the charges, $\boldsymbol{r}$ is the unit vector directed from Q_1 to Q_2, and ε is the permittivity of the material surrounding Q_2.

If there is an electric field gradient across the cell, the magnitude of the forces on either side of the cell will be different. The cell will thus experience a net movement (Figure 2.1B), in the direction of increasing field strength.

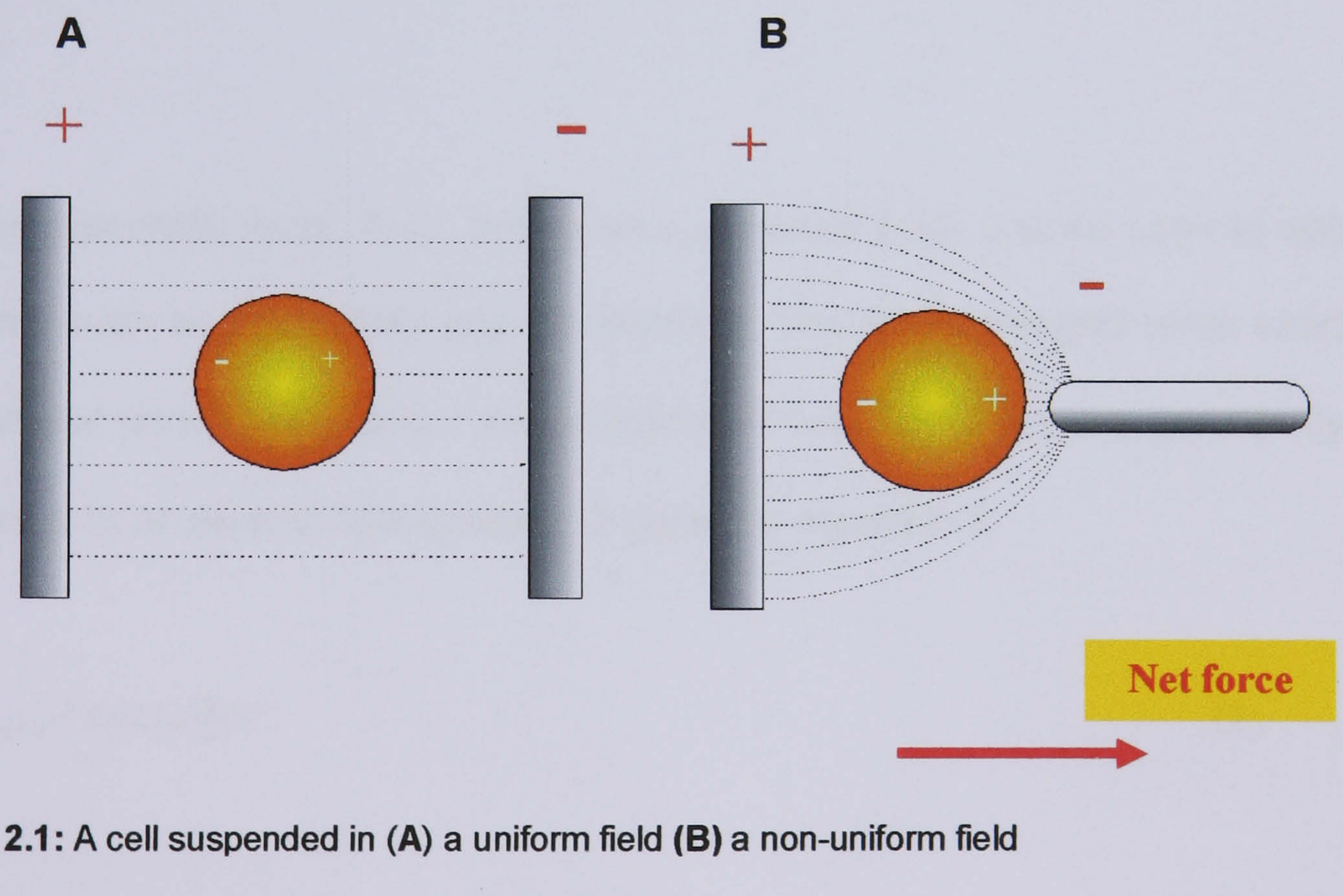

Figure 2.1: A cell suspended in (**A**) a uniform field **(B)** a non-uniform field

The particle will always move along the direction of greatest increasing electric field regardless of the field polarity; the dipole will re-orient itself with the applied polarity (AC or DC fields), and the force is always governed by the field gradient rather than the field orientation. This force is termed dielectrophoresis (DEP).

DEP can be further classified by direction (Jones, 1995). If the particle is more polarisable than the surrounding medium, it will experience a phenomenon called *positive DEP*, where cells are attracted to the electrodes. Its opposite effect, where cells are repelled from the electrodes, is called *negative DEP*. Whether a particle experiences positive or negative DEP is governed by its polarisibility relative to the suspending medium. It is the positive dielectrophoresis phenomenon that is used in this work.

The dielectrophoretic force, $\mathbf{F}_{DEP}$, acting on a spherical body can be used to obtain parameters such as permittivity and conductivity. The time-averaged force exerted on a spherical particle of radius r suspended in a medium of relative permittivity ε_r and exposed to an electric field gradient is given by equation 2:

$$\mathbf{F}_{\mathbf{DEP}} = 2\pi\varepsilon_0\varepsilon_r r^3 Re[K(\omega)]\nabla E^2 \qquad (2)$$

where ∇E^2 is the gradient of the strength of the applied electric field squared and Re [K(ω)] is the real part of the Clausius-Mossotti factor given by equation 3:

$$K(\omega)=\left(\frac{\varepsilon_p^* - \varepsilon_m^*}{\varepsilon_p^* + 2\varepsilon_m^*}\right) \tag{3}$$

where ε_p and ε_m are the complex permittivities of particle and medium respectively, given by equation 4:

$$\varepsilon_i^* = \varepsilon_i - j\frac{\sigma_i}{\omega} \tag{4}$$

where ε_i and σ_i refer to the (real) permittivity and conductivity of material *i*.

Characterisation of cells is made on the basis of physical phenomena occurring inside the cell, such as changes in conductivity (which reflects the ability to carry the electric charge) and permittivity (reflecting the ability to store the electric charge), for both cytoplasm and the membrane. Where the particle, rather than being homogeneous, consists of a shell surrounding a homogeneous core (as shown schematically in Figure 2.2, a more complex model is required). As described by Huang (1992), the smeared-out sphere approach can be used to determine the effective frequency dependent complex permittivity of multi-shelled particles. We can replace the complex permittivity with an effective value combining the properties of the shell and the core, thus:

$$\varepsilon_{1eff}^{*} = \varepsilon_{2}^{*} \frac{\left(\frac{r_2}{r_1}\right)^3 + 2\frac{\varepsilon_1^{*} - \varepsilon_2^{*}}{\varepsilon_1^{*} + 2\varepsilon_2^{*}}}{\left(\frac{r_2}{r_1}\right)^3 - \frac{\varepsilon_1^{*} - \varepsilon_2^{*}}{\varepsilon_1^{*} + 2\varepsilon_2^{*}}} \qquad (5)$$

where subscripts 1 and 2 correspond to the core and shell, and r_1 and r_2 are the radii from the centre of the sphere to the inside and outside of the membrane, so that the Clausius-Mossotti factor for the ensemble is given by equation 6:

$$K(\omega) = \frac{\varepsilon_{1eff}^{*} - \varepsilon_3^{*}}{\varepsilon_{1eff}^{*} + 2\varepsilon_3^{*}} \qquad (6)$$

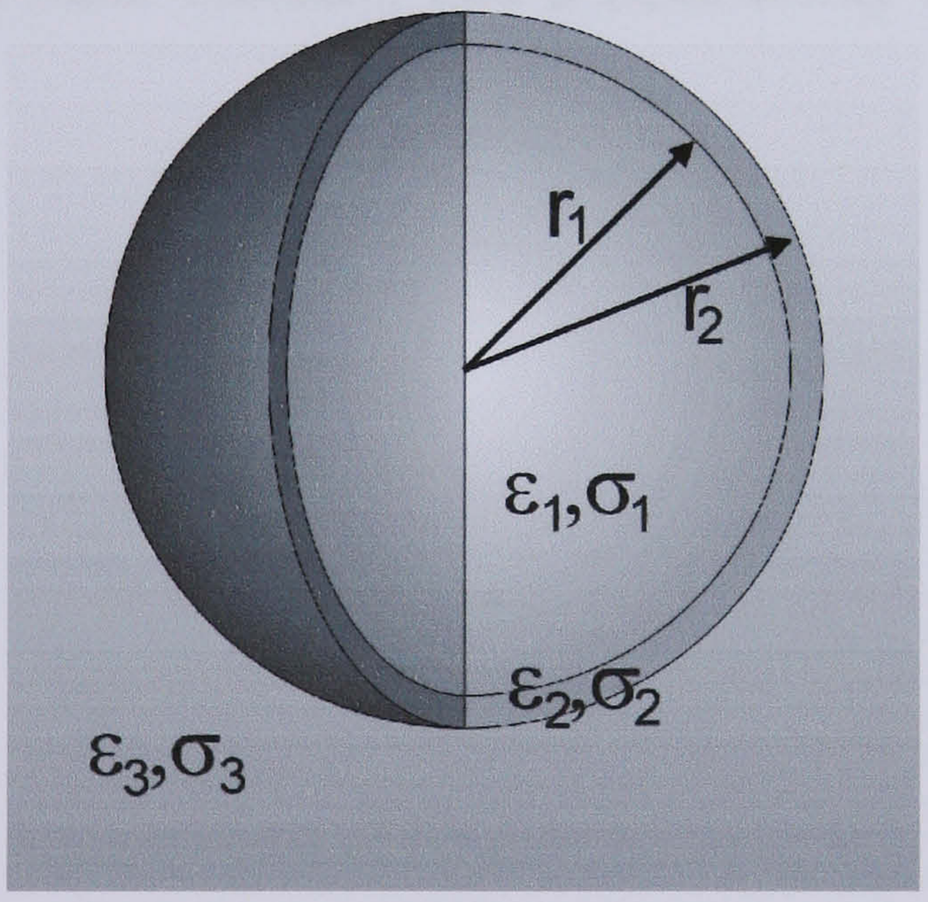

Figure 2.2: A schematic of a single shell model, showing the shell surrounding a core, and suspended in a dielectric medium. The inner and outer radii of the membrane have values r_1 and r_2

Where the subscript 3 refers to the suspending medium. If the full expression for $Re[K(\omega)]$ is expressed analytically, it is sufficiently complex to render direct mathematical analysis hopelessly complicated (Jones, 1995); instead, researchers have used numerical methods to determine dielectric properties by analysis of dielectrophoretic spectra. Where analysis of dielectrophoretic data have been analysed (e.g. Gascoyne et al., 1997) by simplifying the solution using assumptions and by examining a number of crossover spectra as a function of medium conductivity. However, such methods are limited, particularly where the sample of cells precludes the repeating of sample analysis or where multiple populations are present.

A given sphere, where the shell is of relatively low conductivity compared to the inner compartment and outer medium, has a polarisibility spectrum of the type is shown in Figure 2.3.

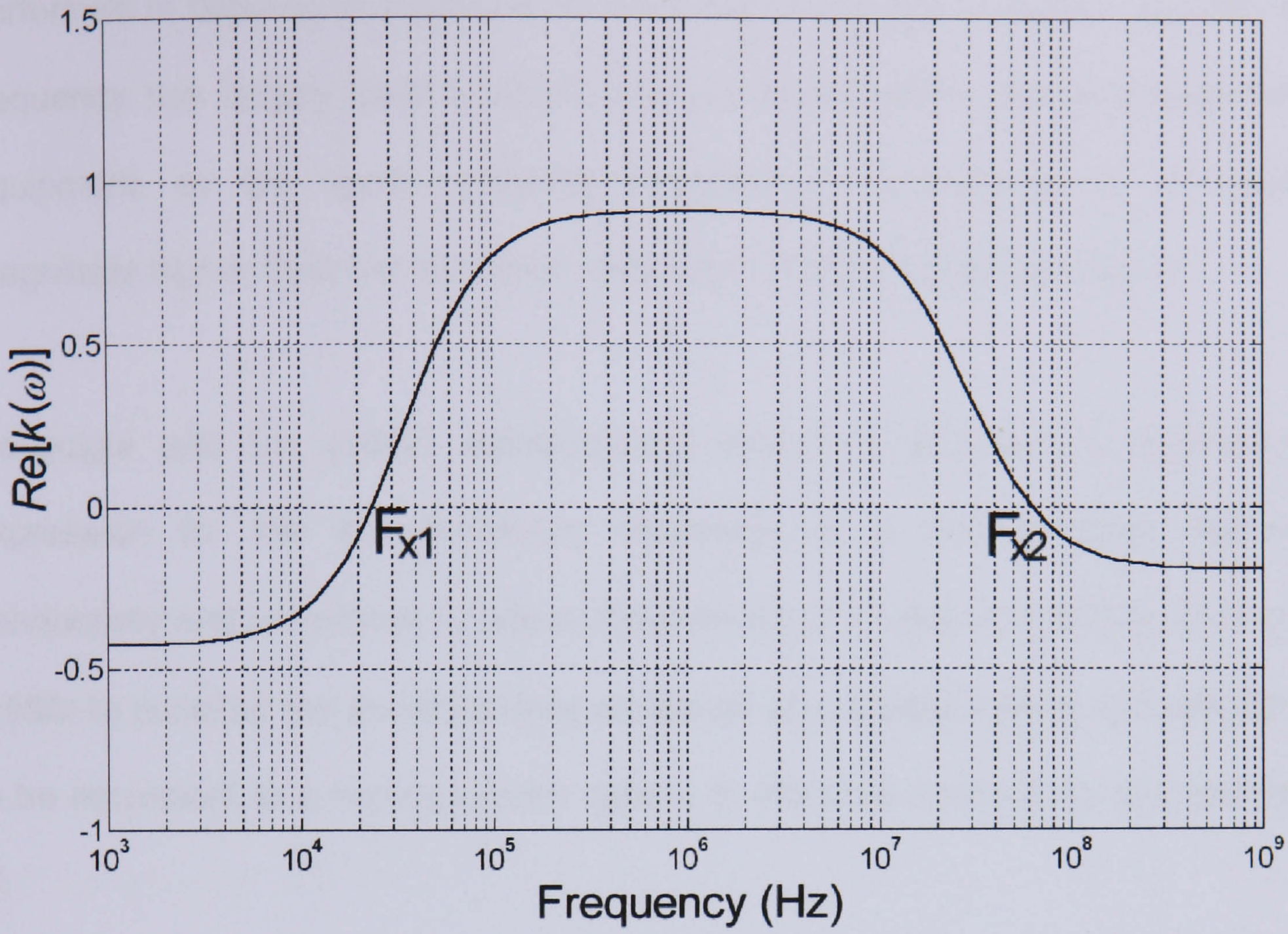

Figure 2.3:. A typical spectrum showing the relative polarisibility (Re[K(ω)]) of a single-shelled particle as a function of frequency. Note the three plateaus at low frequency (negative DEP), intermediate frequencies (positive DEP) and high frequency (negative DEP). The transit between these plateaus takes approximately 1 decade; the lower and upper crossover frequencies, where Re[K(ω)]=0, are indicated by F_{x1} and F_{x2} respectively.

This displays two characteristic dispersions, one rising at lower frequency and one falling at higher frequency. The frequency where the polarizibility crosses from negative to positive for a homogenous sphere allows the direct determination of the properties of the sphere from equation (3) by equating it to zero; however, for a shelled sphere the expression is much more complicated. Some work has been

performed in deriving expressions for the lower crossover frequency, but the upper frequency has largely been ignored because of limitations with signal generation equipment, as the upper crossover frequency is typically up to an order of magnitude higher than the maximum frequency of most signal generators.

Benguigui and Lin (1982) demonstrated that it is possible to determine an expression for the low frequency crossover of a homogeneous sphere of conductivity and permittivity ε_p and σ_p respectively; this was extended by Huang et al (1996) to consider the low-frequency crossover of a shelled sphere by considering it to be equivalent to a homogeneous sphere of effective conductivity and permittivity of:

$$\left.\begin{aligned}\varepsilon_p &= \varepsilon_2\left(\frac{r2}{r2-r1}\right)\\ \sigma_p &= \sigma_2\left(\frac{r2}{r2-r1}\right)\end{aligned}\right\} \tag{7}$$

Using this approximation, Huang and co-workers produced an expression for the low-frequency crossover F_{x1}:

$$F_{x1} = \frac{1}{2\pi}\sqrt{\frac{2\sigma_3^2 - A\sigma_2\sigma_3 - A^2\sigma_{23}^2}{A^2\varepsilon_2^2 - A\varepsilon_2\varepsilon_3 - 2\varepsilon_3^2}} \tag{8}$$

Where $A=\left(\frac{r_2}{r_2-r_1}\right)$; that is, the ratio of the radius of the cell to the thickness of the membrane.

At low frequencies (reviewed by Pethig, 1991), the total current comprises a surface current around the cell, plus a bulk membrane current, both having radial and tangential components. The overall conductivity of the particle has an additional term given by:

$$\sigma_p = \sigma_{pbulk} + \frac{2K_s}{r} \tag{9}$$

Where σ_{pbulk} is the bulk conductivity of the cell membrane, K_s is the surface conductance and r is the cell radius.

It is known that for the majority of cells, the thickness of the membrane is considerably smaller than the radius of the cell; that is, the ratio $a=\left(\frac{r_2}{r_1}\right)^3$ has a value very near 1. If we make the approximation a=1, we find that the high-frequency crossover frequency F_{x2} is given by the following:

$$F_{x2} = \frac{1}{2\pi}\sqrt{\frac{\sigma_1^2 - \sigma_1\sigma_3 - 2\sigma_3^2}{2\varepsilon_3^2 - \varepsilon_1\varepsilon_3 - \varepsilon_1^2}} \tag{10}$$

Numerical studies of the output of the full expression indicate that this approximation holds for the upper crossover frequency for a wide range of electrical values provided a<1.15 (approx), corresponding to a ratio of cell radius to membrane thickness of 20:1. Within this limit, which represents all cases of biological cells, equation (10) holds. The only case where the equation does not

work is where no upper crossover exists, which happens when $\varepsilon_1 > \varepsilon_3$ (meaning the real part of the Clausius-Mossotti factor remains positive for all frequencies above F_{x1}) or $\sigma_1 < \sigma_3$ (meaning the real part of the Clausius-Mossotti factor never has a value greater than zero). The former is a highly unlikely event in biology, and the latter can be controlled by the use of low-conductivity media. Provided these conditions are not met, ε_1 and σ_3 have very little effect on F_{x2}. Since the upper crossover frequency is independent of size, largely independent (in biological cells) of cytoplasmic permittivity or membrane properties, and of the remaining variables those relating to the medium can be precisely defined, F_{x2} provides a direct measurement of the cytoplasmic conductivity.

This result is significant for determining the upper dispersion characteristics. Although the actual crossover frequency is often too high to be observed with conventional function generators, the behaviour of the dielectric dispersion – taking approximately one decade to transit between stable plateaux of $Re[K(\omega)]$ – means that the frequency at which $Re[K(\omega)]$ begins to decline is *also* dependent only on σ_1. This can be extended to multiple populations, as described in Chapter 5; the presence of multiple upwards- or downwards- pointing dispersions can be related to the presence of multiple populations, where the downwards- pointing dispersions (with increasing frequency) points to populations categorised solely by their cytoplasmic conductivities.

2.3. DEP for biological characterisation

The first application of DEP to living cells was described by Pohl and Hawk (1966), where they described the first means of physically separating live and dead cells. Since then, DEP and related phenomena have been shown to be useful in a variety of biological systems, including algae (Hübner et al, 2003), bacteria (Markx et al, 1994), yeasts (Huang et al, 1992) and mammalian white blood cells (Yang et al, 1999) and red blood cells (Gimsa et al, 1996). The use of DEP in treating aqueous suspensions of cells or organelles is generally restricted to using *alternating* electric (AC) fields rather than *static* fields as applied to electrophoresis, which is a major point of difference in the two techniques (Pohl, 1978); this is because in AC fields the average displacement due to the electrophoretic force component to zero.

Without a model of the behaviour of complex bioparticles such as cells, Pohl (1978) interpreted positive DEP behaviour in the light of known biophysical properties of cells. Working on the assumption that positive DEP was driven entirely by a particle having greater permittivity than the medium, he described how water is a high polar material, and as such will be pulled strongly toward the region of highest field intensity by the nonuniform field. If the cell was to move to the region of highest field intensity, it must therefore exhibit an even higher specific polarisibility. Pohl described a number of ways the cellular system can attain this high polarisibility. First, the cell itself is largely water, second, there are dissolved intracellular regions of numerous polar molecules-proteins, sugars, DNA and RNA, all of which can contribute to polarisation. Third, there are structured regions that can act as

capacitative regions, e.g. lipid membranes across which electrolytes can act to produce charge distributions. Fourth, there are structured areas in the surface where ionic double layers can produce very large polarisations. As frequency increases, the conductivity of membrane and cytoplasm also make important contributions. Since that time, it has been shown that Maxwell-Wagner interfacial polarisation is the dominant source of dipolar polarisation, meaning that conductivity and surface charge can also play a significant role in determining polarisibility (e.g. see Hughes, 2002 for explanation).

The first successful experiments reported of the use of DEP to collect living cells were by Pohl and Hawk (1966). The authors used very simple equipment -a voltage supply, a pair of small, bare wire (pin), plate electrodes and a microscope. They showed that yeast (*S. cerevisiae*) could be made to collect at a reliable rate in the region of highest field intensity. Other yeast work was carried out using different configurations, such as the pin-pin design shown in the schematic diagram (Figure 2.3) below, and used in this thesis.

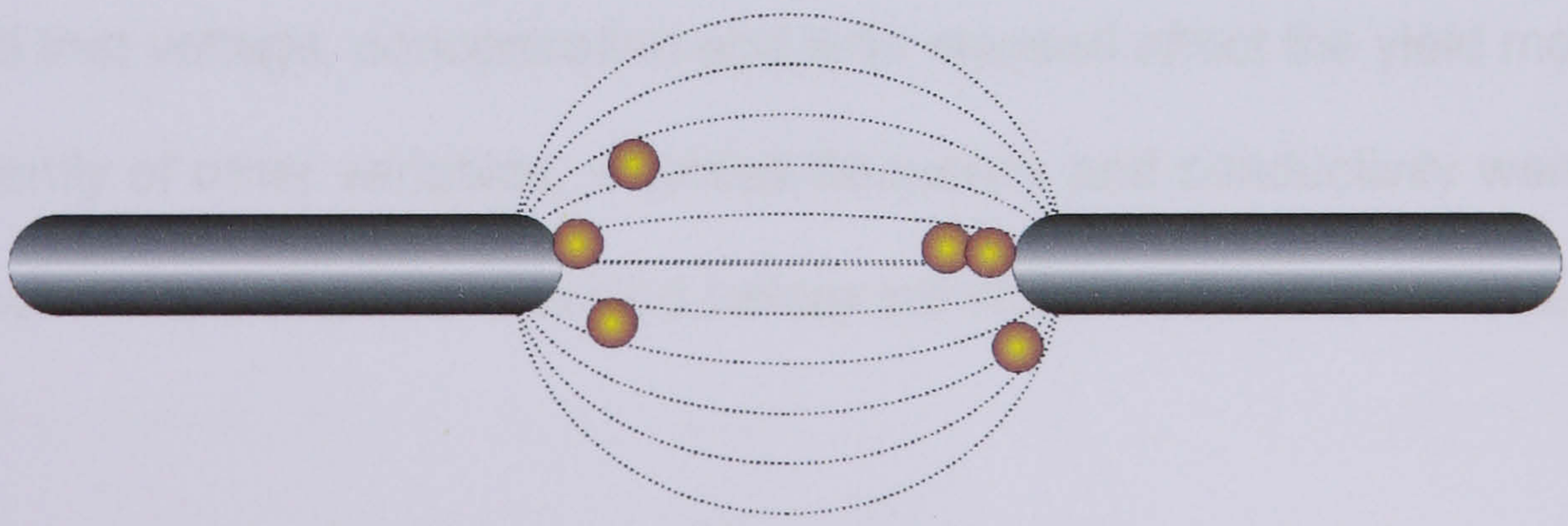

Figure 2.3: A schematic diagram of the pin-pin electrode configuration

In the early period of DEP study, no adequate model existed for explaining frequency-dependent DEP behaviour of complex bioparticles, so empirical studies were performed using DEP and yeast cells by varying the experimental conditions and observing the effect on the number of cells collected. This was measured as the average length of the pearl chain groups of cells attached to the electrodes after a particular time of collection. From this, the dielctrophoresis collection rate (DCR) was obtained, defined as the yield per unit time. The units of yield were divisions of the reticule of a microscope eyepiece (1 division corresponding to an object length of 10.3 μm). Physical parameters varied included voltage, cell concentration and frequency and conductivity (Pohl, 1978). The response of the cells was found to be approximately linear with that of voltage, but at much higher voltages, the yield was reduced. This reduction was suggested to be primarily due to the 'stirring' effect (now called electro-thermal flow), which results from the application of intense fields in free liquids. When the stirring is moderate it brings in more cells close to the pins where they can be more readily collected by the strong field gradient on the pins. At higher voltages, this effect becomes so strong that the flow becomes turbulent and prevents cells from reaching the electrodes, hence reducing the yield. The yield was also found to be linear with the cell concentration. The overall results (Pohl, 1978) concluded that voltage, concentration and time elapsed affect the yield more or less independently of other variables, whereas frequency and conductivity were strongly coupled, where one must be specified before the effect of the other can be given.

Other experiments with yeast cells involved investigating the effects of external agents on collection of cells. The biological parameters investigated included colony age, heat treatment, exposure to UV radiation and treatment with herbicides. Pohl and Hawk (1966) noticed that the organisms were greatly affected by heat, and demonstrated that heat-killed (or autoclaved) yeast cells could be physically separated from the living by DEP. DEP yield of yeast cells, that had been irradiated with UV light, has been studied. After treating the cells at a wavelength that was believed to have inflicted nuclear damage, DEP results showed that selective UV treatment did not affect the polarisation responses of cells. DEP has also been exploited in the study of herbicides to determine the effectiveness of the herbicides tested (as reviewed in Pohl, 1978).

To examine the effect of ageing yeast colonies (*S. cerevisae*), samples from different incubation periods were compared by Pohl and Crane (1971) using DEP over a range of frequencies (10^2 -10^7 Hz). When relatively high solution conductivity was used, the very old cells had a slightly higher yield at low frequencies, and a slightly lower yield at high frequencies. The younger cells differed from the older cells by exhibiting no collection at 100 Hz.

Further early DEP studies included comparing canine blood platelets, or thrombocytes from normal male and female dogs, and their Factor VIII deficient counterparts (reviewed in Phol, 1978). The yield DEP spectra were compared, and moderate differences in the polarisiblity of normal and various haemophilic type

blood platelets were observed, and bacteria such as *flavobacterium*, and *E. coli*, *P. aeruginosa*, *B. megaterium* and *B. cereus* (reviewed in Pohl, 1978).

In the 1980s, DEP research concentrated primarily on two aspects; the search for a model capable of accurately predicting DEP response, and further exploitation of the technique for biological applications. One such application was the use of DEP to bring cells together for electrofusion (reviewed in Zimmermann and Neil, 1996). Other applications, pursued largely by Dimitrov and colleagues saw DEP applied to characterisation of a range of cell types myelomas, hybridomas and lymphocytes B (Stoicheva and Dimitrov, 1986a), red blood cells (Tsoneva and Dimitrov, 1986), and white blood cells (Stoicheva and Dimitrov, 1986b), among others. During this period, the discovery of electrorotation by Arnold and Zimmermann (1982a) allowed a second electrokinetic method of cell analysis; this was applied for the measurement of membrane capacitance of single mesophyll cells in avena-sativa (oats), and the rotation of a single cell in a rotating field (Arnold and Zimmermann 1982a,b). Subsequent work used ROT to determine the dielectric properties of shelled spheres such as cells using theory developed by Fuhr and others (reviewed in Arnold and Zimmermann, 1988).

In the 1990s DEP research expanded dramatically due to a number of factors. First, the *"smeared-out"* multi-shell model (originally developed by Hanai et al, 1960), then by Irimajiri et al (1979) and later applied by Huang et al. (1992), supplanted earlier methods of determination of electrical properties, allowing DEP and ROT data to be interpreted more readily. For example, Chan et al (1997) used

multi-shell models to describe the electrokinetic behaviour of liposomes, and they demonstrated that the information provided by DEP and ROT yielded values of dielectric parameters of liposome-like particles. Second, application of microengineering to the production of microelectrodes allows easy and direct observation of cell DEP in any lab. Finally, the growth of the "lab on a chip" movement brought an increase in interest in microengineered analysis and separation devices, particularly those with potential commercial applications.

Positive and negative DEP were first demonstrated on microelectrodes in 1992 by Pethig et al and Gascoyne et al. The former group used yeast cells to show that collection arising from both positive and negative DEP was facilitated using the castellated electrode geometry, and the two forms of collection differed significantly as functions of the frequency of the applied non-uniform electric field and of the conductivity of the suspending medium. The latter group (Gascoyne et al, 1992) used positive and negative DEP to characterise normal, leukaemic and differentiation-induced leukaemic mouse erythrocytes as a function of frequency in the range 5×10^2-10^5 Hz, which were shown to be significantly different. The group also demonstrated that by choosing the suitable frequency and cell suspension medium, DEP could be used to separate these cells.

DEP was also used as a characterisation technique where the dielectric properties were used to provide the basis of subsequent separation work. For example, the effective electrical conductivity values for Gram-positive and Gram-negative bacteria

were determined in the frequency range (10 kHz- 100 kHz) (Markx et al, 1994a), where this information enabled experimental conditions to be selected to separate different microorganism species using DEP.

Another example where DEP and ROT were used in combination was that by Huang et al (1996), as the two techniques were used to determine the dielectric properties of a clone of normal rat kidney cells, which exhibited a transformed phenotype at 33°C and a non-transformed phenotype at 39°C. DEP measurements of the crossover frequency (at which cells experienced zero force) as a function of the suspension medium revealed that, in response to a temperature shift from 33°C to 39°C for 24 hours, a significant decrease was observed in the specific membrane capacitance and conductance. ROT analyses demonstrated a similar reduction in the membrane capacitance but showed insignificant changes in the internal conductivity. The changes observed in the membrane dielectric properties and the membrane specific capacitance was correlated with cell membrane surface or morphology complexity, as confirmed by scanning electron microscopy. Other studies have considered the assessment of biocide action on bacterial biofilms (Zhou et al, 1995), for the detection of toxic chemicals.

The use of DEP towards the mid and late 1990s showed an increased interest in the microbiology field. Quin et al (1996) investigated this technology for the rapid analysis of ozonated *Cryptosporidium parvum* oocysts, where two key frequencies were used for DEP collection (100 kHz and 10 MHz) to compare the effects of ozonation at various dosages. A consistent pattern was suggested between

increasing the ozone dose and a decrease in oocyte internal conductivity, as supported using a multi-shell mathematical modelling of spheres. The use of DEP as part of microbial analysis included characterisation of microbes in water (Betts and Brown, 1999), where the cell collection spectra were determined and used as the basis for distinguishing different cell types. This analytical application was then suggested as a method of separation in microbiology. Water quality testing and healthcare in general have provided ideas for exploiting DEP. One study (Dalton et al, 2001) investigated the electrical properties of two waterborne protozoan parasites, *Giardia muris* and *Cyclospora cayetanesis*, with the potential use of the technique as a rapid and a precise assay for the determination of parasite viability. A more recent study (Hübner et al, 2003) suggested the potential use of DEP as a low-cost and a rapid method of testing water quality, as the authors used DEP for the dielectrophoretic measurements of fresh water algae *Selenastrum capricornutum* in the presence of different copper sulphate concentrations.

One limitation of DEP for automated study is the requirement to observe cell motion. In the late 1990s, Suehiro et al (1999) described a new technique that realises the estimation of biological cell concentration in an aqueous medium. The group used a dielectrophoretic impedance measurement (DEPIM) method between two electrodes, and used positive DEP to capture cells on an interdigitated electrode system in pearl-chain formation. By monitoring the variations in the electrical impedance, cell populations were analysed quantitavely according to theoretical model of cell collection process, where a suspension of *E. coli* could accurately be assayed in about 10 minutes at $10^5/cm^{-3}$ concentration. In a more recent literature

source, Suehiro et al (2003) proposed a newer method to improve DEPIM sensitivity using an electropermeabilisation technique, which was applied after using DEP to trap cells in order to release intracellular ions. When high AC fields were applied across the trapped bacteria, an increase in conductance was observed, which was suggested to be due to electropermeabilisation.

Since DEP allows the determination of drug action, it has potential for routine testing of the effects of drugs for pharmaceutical applications. A recent study (Johari et al, 2003) described the application of DEP, to determine drug resistance by studying the dielectric parameters of *Staphylococcus epidermidis*. The results indicated a strong similarity between the dielectric properties of sensitive and resistant strains in the absence of antibiotic treatment, whereas there was a significant difference between the sensitive and resistant strains after treatment.

Owing to the fact that DEP allows the non-invasive study of cells, to the obvious applications were in the analysis of human cells for potential medical applications. A number of approaches have been taken. One of which was the challenge of using DEP for the production of small and low cost automated devices for assessing parasite concentrations with potential drug sensitivity studies and diagnosis of malaria (Gascoyne et al, 2002). The other and most common approach was that of studying cancer, and is discussed in more detail later.

Since DEP is most readily applied to suspended cells, the majority of work has been performed on blood cells. To this end, studies have been performed on the most

abundant cells in the blood, including erythrocytes (Minerick et al, 2003), lymphocytes (Ermolina et al, 2000), leukocytes (Yang et al, 1999) and platelets (Neu et al, 2002). Furthermore, Chan and co-workers (2000) conducted a study of circulating trophoblast cells, which detach from the placental lining and enter the circulation during pregnancy, as a potential means of isolating and testing foetal DNA.

2.4. Cancer studies using DEP

Since cancer is a major cause of morbidity (as discussed in the previous chapter), it is the subject of extensive research across many disciplines. Although a broad spectrum of treatments have been developed, the determination of the prognosis and early detection is important; this is where DEP has potential applications. AC-electrokinetic techniques have been amongst the methods used to investigate cancer cells by ways of characterising them relative to their non-cancerous counterparts. Changes in the dielectric properties could potentially be used to separate cancer cells from blood. In this section, we will review how DEP and AC-electrokinetics have been used to characterise cancer cells, assess their behaviour before and after treatment, and to form the basis of techniques to separate cancerous from non-cancerous cells. The cellular biophysical properties can reflect cellular states such as differentiation and viability (Hu et al, 1990; Burt et al, 1990), and DEP-based manipulation of tumour cells have formed part of the lab-on-a-chip based devices in cancer research (reviewed by Gambari et al, 2003).

2.4.1. Characterisation of cancer cells

The use of DEP for characterisation of cancer cells dates back to the 1980s, where it was used to characterise human malignant melanocytes (Mischel et al, 1983), myeloma and, hybridoma cells and lymphocytes (Stoicheva and Dimitrov, 1986a). The most recent application at time of writing was that of Cristofanilli et al (2002), where automated ROT was used to examine dielectric variations related to HER-2/neu overexpression in breast cancer cell sublines (MCF-7). The study evaluated the behaviour of MCF-7/neo and p185(neu) transfectants (MCF/HER2-11 and MCF/HER2-18) to investigate whether differences in HER-2/neu expression were associated with differences in dielectric properties. Western blots were used to assess the overexpression and the specific membrane capacitance was measured. The results suggested that ROT was sufficiently sensitive to detect variations in the dielectric properties in breast cancer cell lines overexpressing p185(neu), with the mean specific membrane capacitance being significantly different in MCF/neo from the other transfected sublines (MCF/HER2-11 and MCF/HER2-18). These differences were suggested to be related to the morphological alterations determined by HER-2/ *neu* overexpression.

Many characterisation experiments have involved examining changes caused by treatment with different agents to assess the effect of the agent on these dielectric properties of cancer cells. An example of this was performed by Burt et al (1990) and co-workers, who used DEP to study the membrane changes accompanying the induced differentiation of Friend murine erythroleukaemia cell lines (DS19 and R1)

following treatment with hexamethylene bisacetamide (HMBA) and dimethyl sulfoxide (DMSO). These are agents that induce terminal differentiation in DS19, but not in R1. The authors found that the membrane capacitance of DS19 was decreased by 30%, and the membrane conductivity to fall by a factor of five after treating DS19. No response was seen by R1 after treatment. They also found that the theoretical model was useful for comparing differences in the data, but also reported several significant discrepancies between predications and the experimental data observed, and suggested the discrepancies to be accounted by factors such as, surface charge effects and intracellular compartments. The same erythropoetic differentiation agent (HMBA) was later used (Wang et al, 1994) to investigate alterations in the plasma membrane of DS19 using ROT. Scanning and transmission electron microscopy revealed that the high membrane capacitance obtained for DS19 before treatment reflected the large area of plasma membrane associated with complex surface morphology, such as the presence of microvilli. Furthermore, ROT demonstrated that treatment with HMBA for 3 days resulted in a fall in the membrane capacitance, which correlated with a reduction in the density of microvilli. This work demonstrated that cells exposed to 72 hour of differentiation had an enhanced resilience relative to their untreated counterparts, and the authors suggested that this evidences the early stages of development of the membrane skeleton which becomes fully developed in mature erythrocytes. They highlighted the value of ROT as a non-invasive method for the characterisation of viable leukaemic cells and their responses to stimuli, and showed that membrane capacitance reflects membrane morphology.

A more recent study where the same principle, of using DEP to characterise the dielectric property changes following treatment with an agent, include the study by Wang et al (2002). DEP was suggested as a more sensitive technique to indicate membrane dielectric changes, in HL-60 induced apoptosis (programmed cell death), than the conventional flow cytometric analysis of surface phosphatidylserine expression or DNA fragmentation. The membrane capacitance was measured following 1 to 4 hours of incubations with genistein (GEN) - an apoptosis inducing agent. DEP was used in conjunction with annexin v assay, and the results showed a decrease in the membrane capacitance as the incubation period with GEN increased to 4 hours. Furthermore, the results were suggested to indicate that it might be possible to correlate changes in cell dielectric properties with very early stages of apoptosis and cell DEP characteristics as early and sensitive prognostic markers of apoptosis. The authors pointed to the applicability of DEP-based technology to rapidly detect, separate and quantify normal, apoptotic and necrotic cells from cell mixtures. Another study (Ratanachoo et al, 2002) employed DEP for the detection of cellular responses to toxicants. Paraquat, styrene oxide (SO), N-nitrosos-N-methylurea (NMU) and puromycin were used and chosen because of their different mechanisms of action, namely membrane free radical attack, simultaneous membrane and nucleic acid attack, nucleic acid alkylation and protein synthesis inhibition, respectively. For all treatments, membrane capacitance of HL60- cells decreased. The DEP responses correlated sensitively with alterations in cell surface morphology, especially microvilli and blebs, which were also observed by scanning electron microscopy. The study pointed to the DEP-based method being more sensitive to agents that had a direct action on the membrane than those

agents for which membrane alterations were secondary. Direct detection of DEP responses were found to be 15 and 30 minutes after exposure to agents that directly damaged membrane and those acted on the cell intracellular targets.

Huang et al (1995) used ROT measurements to study the cytoplasmic dielectric properties of DS19 cells following HMBA treatment. After treatment, the DS19 cells exhibited a slight increment in the average interior permittivity and a decrement in the interior conductivity. Of significance was the average permittivity of cell interiors, which was larger than that of pure water (75 ε_0). Using numerical simulations, the nuclear dielectric parameters were looked at to investigate the effects of nuclei on ROT spectra of intact cells, and the analysis subsequently considered other intracellular organelles such as mitochondria. The authors concluded the large permittivity observed did not result from cell nuclei or mitochondria, and instead may have arisen from the combined effects of cytoplasmic organelles. Finally, in order to assess whether DEP affects the cells exposed to nonuniform fields, Wang and Gascoyne (1999) used dielectrophoretic manipulations to investigate DS19 (murine erythroleukaemia). It was found that hydrogen peroxide was produced when sugar-containing media were exposed to fields outside the typical field strengths in AC-electrokinetics. The AC typical fields used for the dielectrophoretic manipulation and sorting of cells do not damage DS19 cells.

2.4.2. Separation of cancer cells

The use of DEP as a separation technique in a cancer setting goes back to the early 1990s. Gascoyne et al (1992) demonstrated the first use of DEP as a separation technique for cancer cells. The dielectrophoretic characteristics of normal, leukaemic and differentiation-induced leukaemic mouse erythrocytes were measured as a function of frequency and were shown to be significantly different, by selecting the appropriate frequency they were able to demonstrate positive and negative DEP of healthy and Friend murine erythroleukaemic cells. Since then, the majority of separators have been flow separators, either separating by flowing cells across an electrode array and trapping by positive DEP, or by using field-flow fractionation (FFF) (Markx et al 1997), where cells are repelled and are sorted according to the height they are repelled to (and hence the speed at which they flow). These two schemes are shown in Figure 2.4.

The most common form of flow separation is that of using positive and negative DEP. In 1995, the first work on separation of human cancer cells was published using this method. At the time, a considerable biomedical and clinical interest in isolating cell subpopulation of bone marrow (BM) and peripheral blood stem cell collections (PBSC) emerged. These collections contain haemopoietic stem cells required for bone marrow reconstitution. The CD34+ antigen was used as a marker to identify haemopoietic precursor cells, which were strongly expressed in the primitive cells, but lost in differentiated cells. The limitation of detecting this antigen is that it is expressed on 1-4% of BM and PBSC. DEP investigations were carried

out during this time period to study the dielectrophoretic separation and enrichment of CD34+ subpopulation from BM and PBSC (e.g. Talary et al, 1995). The results indicated that maximum enrichment of stem cells (of 4.9 fold) occurred at a frequency of around 5 kHz. A follow-up CD34+ enrichment study (Stephens et al, 1996) used DEP for isolating CD34+ cell populations from leukaemic patients undergoing peripheral blood stem cell harvests. The study pointed to the limitations of the conventional techniques that rely on the use of antibodies specific to the surface marker CD34+ as being expensive and time consuming, and therefore used DEP as a tool to separate CD34+ cells, as it does not rely on cell-specific markers. The results indicated that a maximum enrichment was obtained in the region of 10-20 kHz.

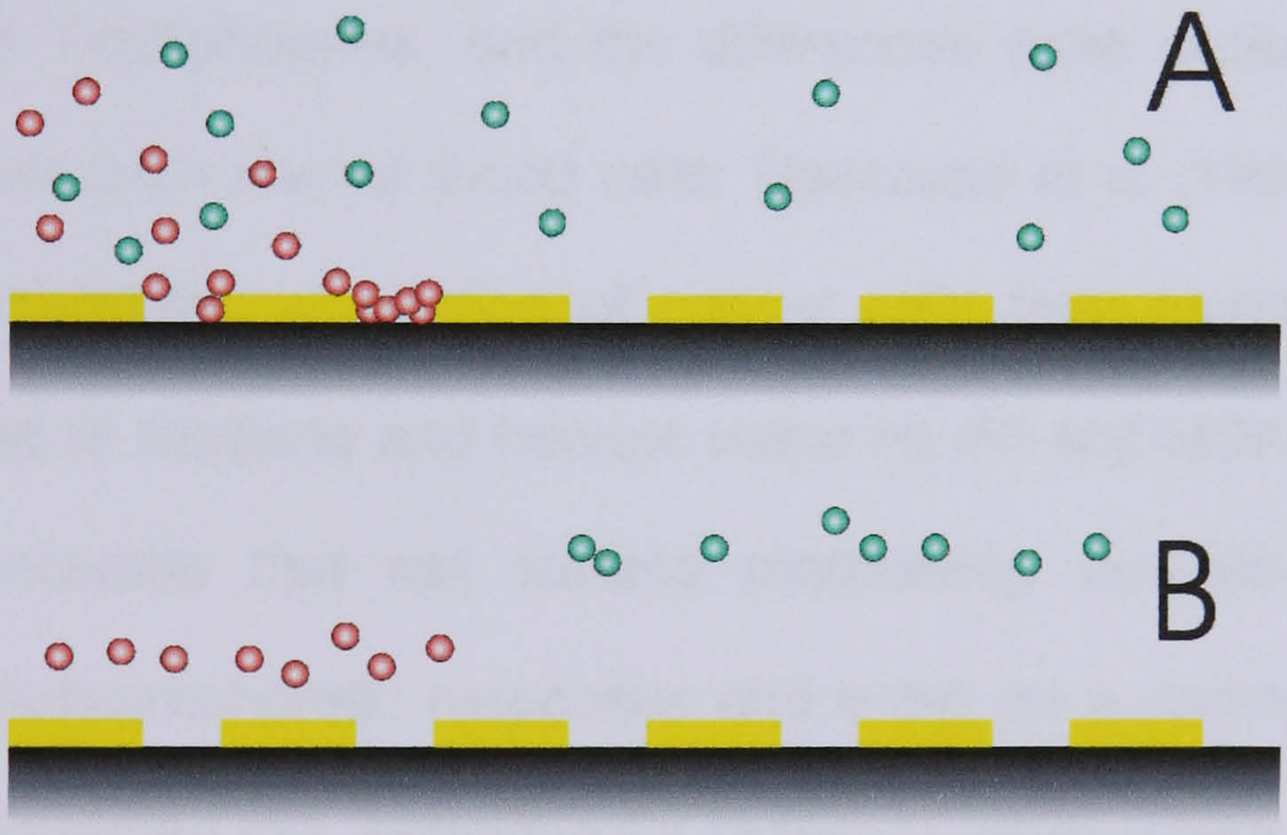

Figure 2.4: Two common forms of DEP flow separation. (A) When particles from different populations flow across an electrode, conditions can be chosen for one population to be trapped on the electrodes (shown red) whilst the other (green) experiences negative DEP and is flushed out. (B) In DEP-FFF, both populations are repelled by negative DEP, but by different amounts; this causes them to travel at different heights above the electrodes, and hence at different speeds. Particle flow in both figures is from left to right.

The research team which has advanced the field of DEP separation for cancer diagnosis is that of Becker, Gascoyne and co-workers (1994), who used a flow cell and castellated electrode array (which they termed a "dielectric affinity column"), usually in conjunction with electrorotation for cell analysis. Interdigitated microelectrode arrays were used to retain human promyelocytic leukaemic cells (HL-60) from blood collected from venipunctures in a ratio of 3:2. HL-60 cells could subsequently be released by removal of the dielectrophoretic field and collected, while normal blood cells were eluted from the electrode chamber. This work on separation of cancer cells from blood was further explored by the same group (Becker et al 1995) to demonstrate that the dielectric properties of metastatic human breast cancer cell line MDA-231 were significantly different from those of erythrocytes and T-lymphocytes, and the differences were exploited to separate breast cancer cells from normal blood cells. Gascoyne et al (1997) continued the work on dielectrophoretic separation of cancer cells from blood. The 'dielectric column' was used to separate and harvest viable HL-60 and MDA-231 from whole blood. They concluded that cell surface morphology coupled with cell size, dominated cell dielectrophoretic responses and acted as a sorting criterion. They have also recommended this technique for research areas where cell modification (such as that by stain or antibodies) may compromise the results, or where specific markers or antibodies might not be available. Furthermore, since the parameters by which cells are identified in current sorting and characterisation technologies, such as fluorescence- activated sorting, affinity column and centrifugal techniques play little or no role in AC- electrokinetics, they suggested the dielectrophoretic affinity

column approach might be applied as an adjunct to the conventional methods to yield an overall improved discrimination.

The use of FFF for cancer studies has also been pursued by Gascoyne and co-workers. One example, used to separate cancer cells from stem cells, was performed by Huang et al (1999) by exploiting a combination of fluid flow and DEP. DEP-field flow-fractionation (DEP-FFF) was used to purge human breast cancer MDA-435 cells from haemopoietic $CD34^+$ stem cells. A chamber with an array of interdigitated microelectrodes was used to generate DEP forces that levitated the cell mixture in a fluid flow profile. The $CD34^+$ cells were levitated higher and were carried faster by the fluid flow, earlier than the MDA-435. Using this set up as well as on-line flow cytometry, efficient separation of the cell mixture was observed in less than 12 minutes, with $CD34^+$ cell fractions being more than 99% pure. The authors suggested the potential usefulness of DEP-FFF in biomedical cell separation problems, including microfluid-scale-based diagnosis and providing a preparative-scale purification of cell subpopulations.

Other groups are exploring new methods of cell separation for cancer applications. For example, a novel use of cell levitation was investigated later by a different group (Altomere et al, 2003), where they described the use of an innovative printed circuit board (PCB) device to generate DEP-based. This was used to create software-controlled "cages" that can be moved to any place inside the microchamber, and entrap cells according to their dielectrophoretic properties. Different tumour cell lines were used, including Jurkat (T-lymphoid), erythroleukaemic (HEL) and melanoma

(Colo38). The electrode array was suggested to form the basis for a lab on a chip, performing cell separation the basis of DEP levitation and movement of different tumour cells under different DEP conditions.

2.5. Conclusion

Dielectrophoretic methods have been studied for over four decades, and extensively so from the 1990s. It has employed a wide range of applications, and in different fields and hosts, such as plants, bacteria and viruses, as well as different mammalian systems, in particular those including samples of human origin. DEP has been used to move, trap, sort and separate, and analyse cells on the basis of characterising cells under different conditions, be it change of environment or drug treatment, the general aim has always involved obtaining a better understanding as to how cells or particles behave under certain conditions. Investigations like these have led the potential applications of DEP in areas like pharmacology, microbiology, oncology and some of which have made their way to commercial technology with many filed patents based on electrode design or a novel application. The most promising of all is the new merge of this technique, whether alone or in combination with others, into lab-on-a-chip systems.

2.6. References

Altomare, L. Borgatti, M. Medoro, G. et al. Levitation and movement of human tumour cells using a printed circuit board device based on software controlled dielectrophoresis (2003) *Biotechnology and Bioengineering*, **82**(4): 474-479.

Arnold, W.M. Zimmermann, U. Rotation of an isolated cell in a rotating field (1982a) *Naturwissenschaften*, **69**(6): 297-298.

Arnold, W.M. Zimmermann, U. Rotating field induced rotation and measurement of the membrane capacitance of single mesophyll cells of *Avena-Sativa* (1982b) *Zeitschrift fur Naturforschung-c- A Jjournal of Biosciences*, **37**(10): 908-915.

Arnold, W.M. Zimmermann, U. Electrorotation: development of a technique for dielectric measurements on individual cells and particles (1988) *Journal of Electrostatics*, **21**: 151-191.

Becker, F.F. Wang, X.B. Huang, Y. et al. the removal of human leukaemia cells from blood using interdigitated microelectrodes (1994) *Journal of Applied Physics D*, **27**: 2659-2662.

Becker, F.F Wang, X.B. Huang, Y. et al. Separation of human breast cancer cells from blood by differential dielectric affinity (1995) *Proceedings of the National Academy of Sciences of the United States of America*, **92**(3): 860-864.

Benguigui, L. Lin, I.J. More about the dielectrophoretic force (1982) *Journal of Applied Physics*, **53**(2): 1141-1143.

Betts, W.B. Brown, A.P. Dielectrophoretic analysis of microbes in water (1999) *Journal of Applied Microbiology*, **85**: 201S-213S.

Burt, J.P.H. Pethig, R. gascoyne, P.R.C. et al. Dielectrophoretic characterisation of friend murine erythroleukaemic cells as a function of induced differentiation (1990) *Biochimica et Biophysica Acta*, **1034**(1): 93-101.

Chan, K.L. Gascoyne, P.R.C. Becker, F.F. et al. Electrorotation of liposomes: verification of dielectric multi-shell model for cells (1997) *Biochimica et Biophysica Acta*, **1349**(2): 182-196.

Chan, K.L. Morgan, H. Morgan, E. et al. Measurements of the dielectric properties of peripheral blood mononuclear cells and trophoblast cells using AC-electrokinetic techniques (2000) *Biochimica et Biophysica Acta*, **1500**(3):313-322.

Cristofanilli, M. De Gasperis, G. Zhang, L.S. et al. Automated electrorotation to reveal dielectric variations related to HER-2/neu overexpression in MCF-7 sublines (2002) *Clinical Cancer Research*, **8**(2): 615-619.

Dalton, C. Goater, A.D. Drysdale, J. et al. Parasite viability by electrorotation (2001) *Colloids and Surfaces A-Physicochemical and Engineering Aspects*, **195** (1-3): 263-268.

Ermolina, I. Polevaya, Y. Feldman, Y. Analysis of dielectric spectra of eukaryotic cells by computer modelling (2000) *European Biophysics Journal with Biophysics Letters*, **29**(2): 141-145.

Falokun, C.D. Mavituna, F. Markx, G.H. AC electrokinetic characterisation and separation of cells with high and low embrygenic potential in suspension cultures of carrot (Daucus carota) 2003, *Plant Cell Tissue and Organ Culture*, **75**(3): 261-272.

Gambari, R. Borgatti, M. Altomere, L. et al. Applications to cancer research of "lab-on-a-chip" devices based on dielectrophoresis (DEP) (2003) *Technology in Cancer Research and Treatment*, **2**(1): 31-40.

Gascoyne, PR.C. Huang, Y. Pethig, R. et al. Dielectrophoretic separation of mammalian cells studied by computerised image analysis (1992) *Measurement Science and Technology*, **3**(5): 439-445.

Gascoyne, P.R.C. Wang, X.B. Huang, Y. et al. Dielectrophoretic separation of cancer cells from blood (1997) *IEEE Transactions on Industry Applications*, **33**(3): 670-678.

Gascoyne, P. Mahidol, C. Ruchirawat, M. et al. Microsample preparation by dielectrophoresis: isolation of malaria (2002) *Lab On a Chip*, **2**(2): 70-75.

Gimsa, J. Schnelle, T. Zechel, G. et al. Dielectric spectroscopy of human erythrocytes investigations under the influence of nystatin (1994) *Biophysical Journal*, **66**(4): 1244-1253.

Gimsa J. Muller T. Schnelle, T. et al.. Dielectric spectroscopy of single human erythrocytes at physiological ionic strength: Dispersion of the cytoplasm (1996) *Biophysical Journal*, **71**(1): 495-506.

Griffith, A.W. Cooper, J.M. Single-cell measurements of human neutrophil activation using electrorotation (1998) *Analytical Chemistry*, **70**(13): 2607-2612.

Hanai, T. Theory of the dielectric dispersion due to the interfacial polarisation and its application to emulsion (1960) *Kolloid Z*, 171:23-31.

Huang, Y. Hölzel, R. Pethig, R. et al. Differences in the CA electrodynamics of viable and non-viable yeast cells determined through combined dielectrophoresis and electrorotaion studies (1992) *Physics in Medicine and Biology*, **37**(7):1499-1517.

Huang, Y. Wang, X.B. Hölzel, R. et al. Electrorotational studies of the cytoplasmic dielectric properties of Friend murine erythroleukaemia cells (1995) *Physics in Medicine and Biology*, **40**(11): 1789-1806.

Huang, Y. Wang, X.B. Becker, F.F. et al. Membrane changes associated with the temperature sensitive P85(gag-mos)-dependent transformation of rat kidney cells as determined by dielectrophoresis and electrorotation (1996) *Biochimica et Biophysica Acta*, **1282**(1): 76-84.

Huang, Y. yang, J. Wang, X.B. et al. The removal of human breast cancer cells from haemopoetic CD34+ stem cells by dielectrophoretic field flow fractionation (1999) *Journal of Hematotherapy & Stem Cell Research*, **8**(5): 481-490.

Hübner, Y. Hoettges, K.F. Hughes, M.P. Water quality test based on dielectrophoretic measurements of fresh water algae Selenastrum capricornutum (2003) *Journal of Environmental Monitoring*, **5** (6): 861-864.

Irimajiri, A. Hanai, T. Inouye, V.A. Dielectric theory of "multi-stratified shell" model with its application to lymphoma cell. (1979) *Journal of Theoretical Biology*, **78**: 251-269.

Hu, X. Arnold, W.M. Zimmermann, U. Alterations in the electrical properties of lymphocyte T and lymphocyte B membranes induced by mitogenic stimulation-activation monitored by electrorotation of single cells (1990) *Biochimica et Biophysica Acta*, **1021**(2): 191-200.

Huang, Y. Hölzel, R. Pethig, R. et al. Differences in the AC electrodynamics of viable and nonviable yeast cells determined through combined dielectrophoresis and electrorotation studies (1992) *Physics in Medicine and Biology* **37**(7): 1499-1517.

Hughes, M.P. Nanoelectromechanics in Engineering and Biology (2002), CRC press, Boca Raton.

Johari, J. Hübner, Y. Hull, J.C. et al. Dielectrophoretic assay of bacterial resistance to antibiotics (2003) *Physics in Medicine and Biology*, **48**: N193-N198.

Jones, T.B. Electromechanics of particles (1995), cambridge University Press, Cambridge.

Mahaworasilpa, T.L. Coster, H.G.L. George, E.P. Forces on biological cells due to applied alternating (AC) electric fields.1. Dielectrophoresis (1994) *Biochimica et Biophysica Acta*, **1193** (1): 118-126.

Markx, G.H. Huang, Y. Zhou, X.F. et al. Dielectrophoretic characterisation of microorganisms (1994a) *Microbiology*, **140**: 585-591.

Markx, G.H. Talary, M.S. Pethig, R. Separation of viable and non viable yeast using dielectrophoresis (1994b) *Journal of Biotechnology*, **32**(1): 29-37.

Markx, G.H. Rousselet, J. Pethig, R. DEP-FFF: Field-flow fractionation using non-uniform electric fields (1997) *Journal of Liquid chromatography & Related Technologies*, **20**(16-17): 2857-2872.

Minerick, A.R. Zhou, R.H. Takhistov, P. et al. Manipulation and characterisation of red blood cells with alternating current fields in microdevices (2003) *Electrophoresis*, **24**(21): 3703-3717.

Mischel, M. Rouge, F. Lamprecht, I. et al. Dielectrophoresis of malignant human melanocytes (1983) *Archives of Dermatological Research*, **275**(3): 141-143.

Morgan, H. Hughes, M.P. Green, N.G. Separation of submicron bioparticles by dielectrophoresis (1999) *Biophysical Journal*, **77**(1): 516-525.

Neu, B. Georgieva, R. Meiselman, H.J. et al. Alpha- and beta-dispersion of fixed platelets: comparison with a structure-based theoretical approach (2002) *Colloids and Surfaces A-Physicochemical and engineering aspects*, **197**(1-3): 27-35.

Pethig, R. Biological Electrostatics: Dielectrophoresis and Electrorotation (1991) *Institute of Physics Conference Series*, **118**: 13-26.

Pethig, R. Huang, Y. Wang, X-B. et al. Positive and negative dielectrophoretic collection of colloidal particles using interdigitated castellated microelectrodes (1992) *Journal of Physics D: Applied Physics*, **24**: 881-888.

Pohl, H.A. The motion and precipitation of suspenoids in divergent electric fields (1950) Journal of Applied Physics, 22(7): 869-871.

Pohl, H.A. Hawk, I. Separation of living and dead cells by dielectrophoresis (1966) *Science*, **152**: 647-649.

Pohl, H.A. Crane, J.A. Dielectrophoresis of cells (1971) *Biophysical Journal*, **11**: 711-727.

Pohl, H.A. Dielectrophoresis (1978), Cambridge University Press, Cambridge.

Quinn, C.M. Archer, G.P. Betts, W.B. et al. Dose dependent dielectrophoretic response of *Cryptosporidium* oocysts treated with ozone (1996) *Letters in Applied Microbiology*, **22**: 224-228.

Ratanachoo, K. Gascoyne, P.R.C. Ruchirawat, M. Detection of cellular responses to toxicants by dielectrophoresis (2002) *Biochimica et Biophysica Acta*, **1564**(2): 449-458.

Stephens, M. Talary, M.S. Pethig, R. et al. The dielectrophoresis enrichment of CD34(+) cells from peripheral blood stem cell harvests (1996) *Bone Marrow Transplantation*, **18**(4): 777-782.

Stoicheva, N.G. Dimitrov, D.S. Dielectrophoresis of myeloma cells, hybridomas and lymphocytes-B (1986a) *Dokladi na Bolgarskata Akademiya na Naukite*, **39**(2): 105-107.

Stoicheva, N. Dimitrov, D.S. Dielectrophoresis of single protoplasts, chloroplasts and lymphocytes in axisymmetrical fields (1986b) *Biophysical Journal*, **49**(2): A92-A92, part 2.

Suheiro, J. Yatsunami, R. Hamada, R. et al. Quantitative estimation of biological cell concentration suspended in aqueous medium by using dielectrophoretic impedance measurement method (1999) *Journal of Physics D: Applied Physics*, **32**: 2814-2820.

Suheiro, J. Shutou, M. Hatano, T. et al. High sensitive detection of biological cells using dielectrophoretic impedance measurement method combined with electropermeabilisation (2003) *Sensors and Actuators B-Chemical*, **96**(1-2): 144-151.

Talary, M.S. Mills, K.I. Hoy, T. et al. Dielectrophoretic separation and enrichment of CD34+ cell subpopulation from bone marrow and peripheral blood stem cells (1995) *Medical & Biological Engineering & Computing*, **33**(2): 235-237.

Tsoneva, I.C. Zhelev, D.V. Dimitrov, D.S. et al. Red-blood-cell dielectrophoresis in axisymmetrical fields (1986) *Cell Biophysics*, **8**(2): 89-101.

Wang, X.B. Huang, Y. Gascoyne, P.R.C et al. Changes in friend murine erythroleukaemia cell membranes during induced differentiation determined by electrorotation (1994) *Biochimica et Biophysica Acta*, **1193**(2): 330-344.

Wang, X.J. Yang, J. Gascoyne, P.R.C. Role of peroxide in AC electrical field exposure effects on Friend murine erythroleukemia cells during dielectrophoretic manipulations (1999) *Biochimica et Biophysica*, **1426** (1): 53-68.

Wang, X.J. Becker, F.F. Gascoyne, P.R.C. Membrane dielectric changes indicate induced apoptosis in HL-60 cells more sensitively than surface phosphatidylserine expression or DNA fragmentation (2002) *Biochimica et Biophysica Acta*, **1564**(2): 412-420.

Yang, J. Huang, Y. Wang, X. et al. Dielectric properties of human leukocyte subpopulations determined by electrorotation as a cell separation criterion (1999) *Biophysical Journal*, **76**: 3307-3314.

Zhou, X.F. Markx, G.H. Pethig, R. et al. Differentiation of viable and nonviable bacterial biofilms using electrorotation (1995) *Biochimica et Biophysica Acta*, **1245** (1): 85-93.

Zimmermann, U. Neil, G.A. Electromanipulation of cells (1996), CRC Press, Boca Raton.

3. Dielectrophoretic assessment of drug sensitive and resistant cancer cells

3.1. Introduction

During the lifetime of a cell, a number of and transport mechanisms are involved in regulating metabolism. These mechanisms include passive modes such as diffusion and facilitated diffusion, and active transport modes requiring energy expenditure. These are illustrated briefly in Figure 3.1.

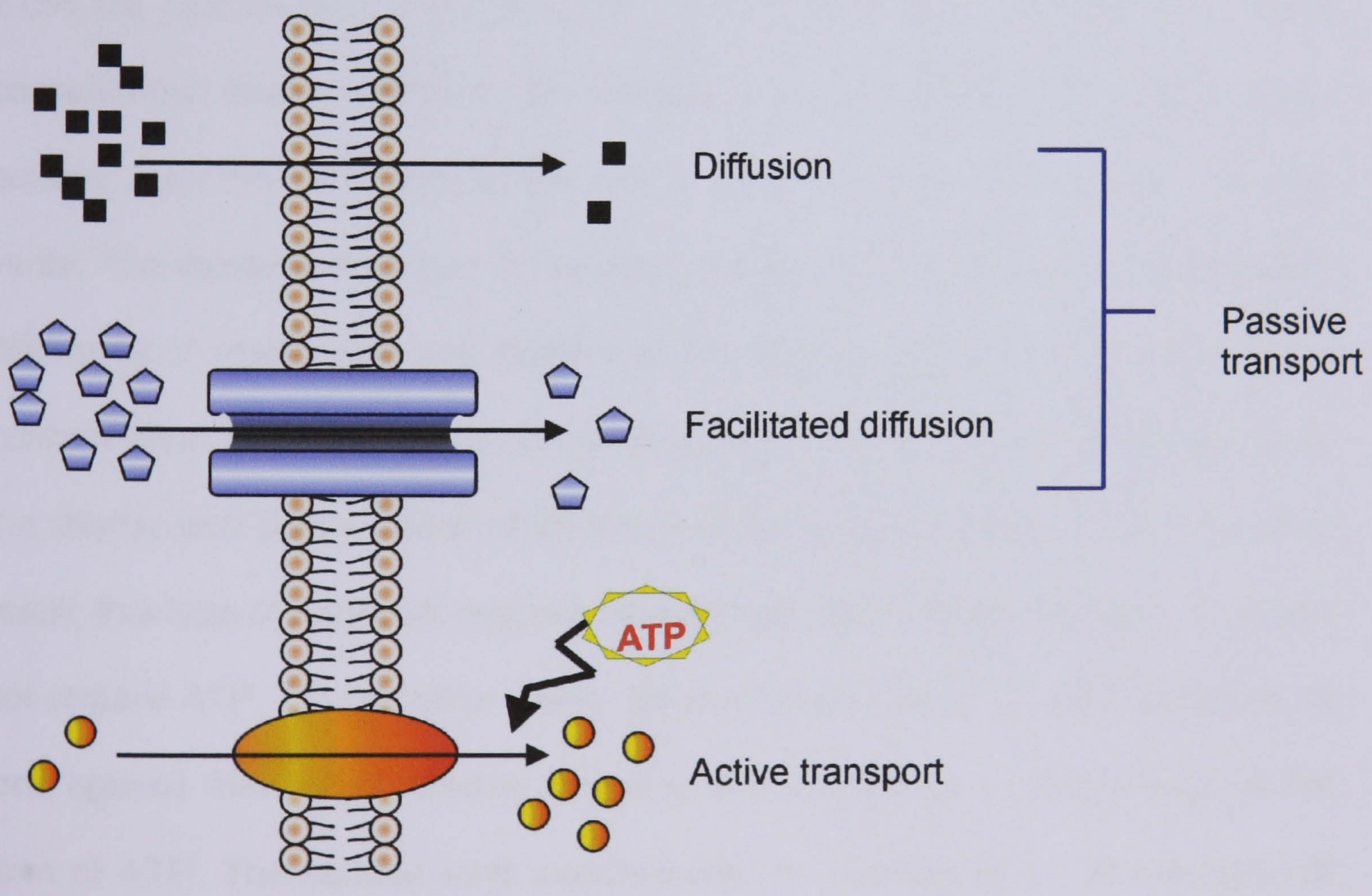

Figure 3.1: A schematic showing ion transport mechanisms across a membrane. Small non-polar molecules can diffuse across the membrane (top); if the rate of transport by diffusion is insufficient, it can be assisted by transport proteins (middle). Finally, if the cell requires transport against a diffusion gradient, a pump is required (bottom).

The internal concentration of different species of ions and molecules are maintained in their correct numbers by these processes and membranes, as they regulate the passage of all substances moving in and out of the cell and between membrane-bound interior compartments, such as those at the vesicular level. As part of this maintenance, substances constantly move in both directions across the cellular membranes. Substances such as metabolites and raw materials enter the cell from the outside, while cell waste material moves in the opposite direction and is expelled from the cell.

Ions constantly flow in both directions and between the different compartments in the cell interior. The two primary mechanisms that underlie the ionic transport in a cell are *passive* and *active transport*. The former simply depends on the ionic concentration inside relative to the outside of the cell; if it is more concentrated outside, then the movement of the ions will be from outside to inside, and *vice versa*. The movement of ions in this type of transport relies on the concentration difference of inside of a cell relative to the outside; movement is driven by a *concentration gradient*. The passive transport of ions is therefore influenced by the charge and concentration differences on either side of the membrane. As a result, this type of transport requires no expenditure of cellular energy, i.e. it does not require ATP. On the other hand, active transport involves the movement of ions against their concentration gradients and therefore requires energy in the form of ATP. The cellular ionic concentration is maintained by coordination of both passive and active transport proteins. This is to ensure that the ionic concentration inside the cell remains at the required levels for cellular functions.

3.1.1. Ion transport mechanisms

There are many mechanisms by which ions are transported across the membrane. In order to understand the mechanisms which contribute to the ionic strength - and hence cytoplasmic conductivity - it is necessary to review the primary transport mechanisms of the principal ionic species present in the cytosol. These ions include sodium, potassium, hydrogen, calcium, chloride and magnesium. The major ionic compositions inside and outside of a typical mammalian eukaryotic cell are shown in the Figure 3.2.

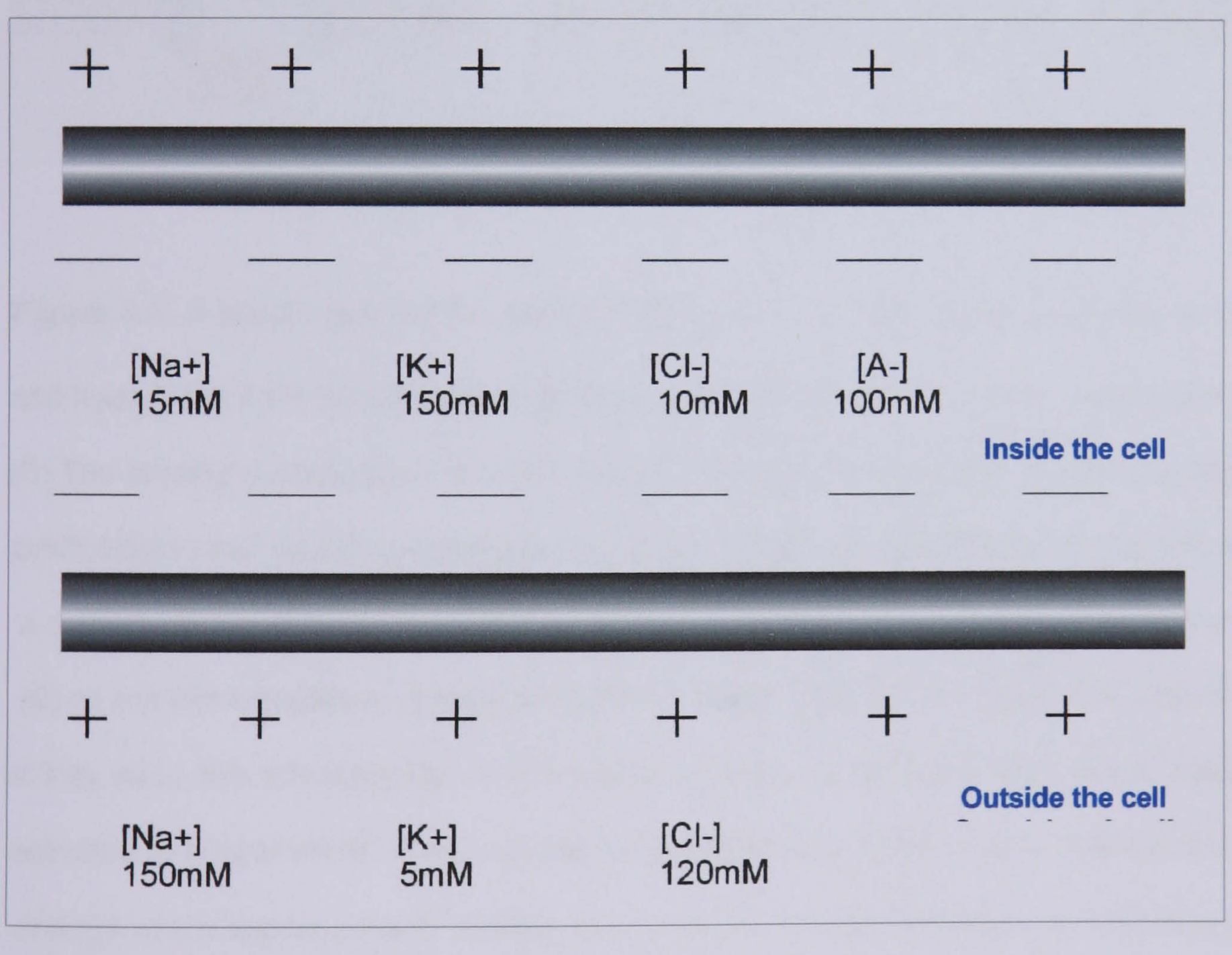

Figure 3.2: the principal ionic composition of a typical mammalian cell, with more K^+

Sodium (Na^+) is pushed outward by the sodium/potassium (Na^+/K^+) pump, which operates by pumping 3 Na^+ out of the cell for every 2 K^+ pumped in (the mechanism of which is shown in Figure 3.3).

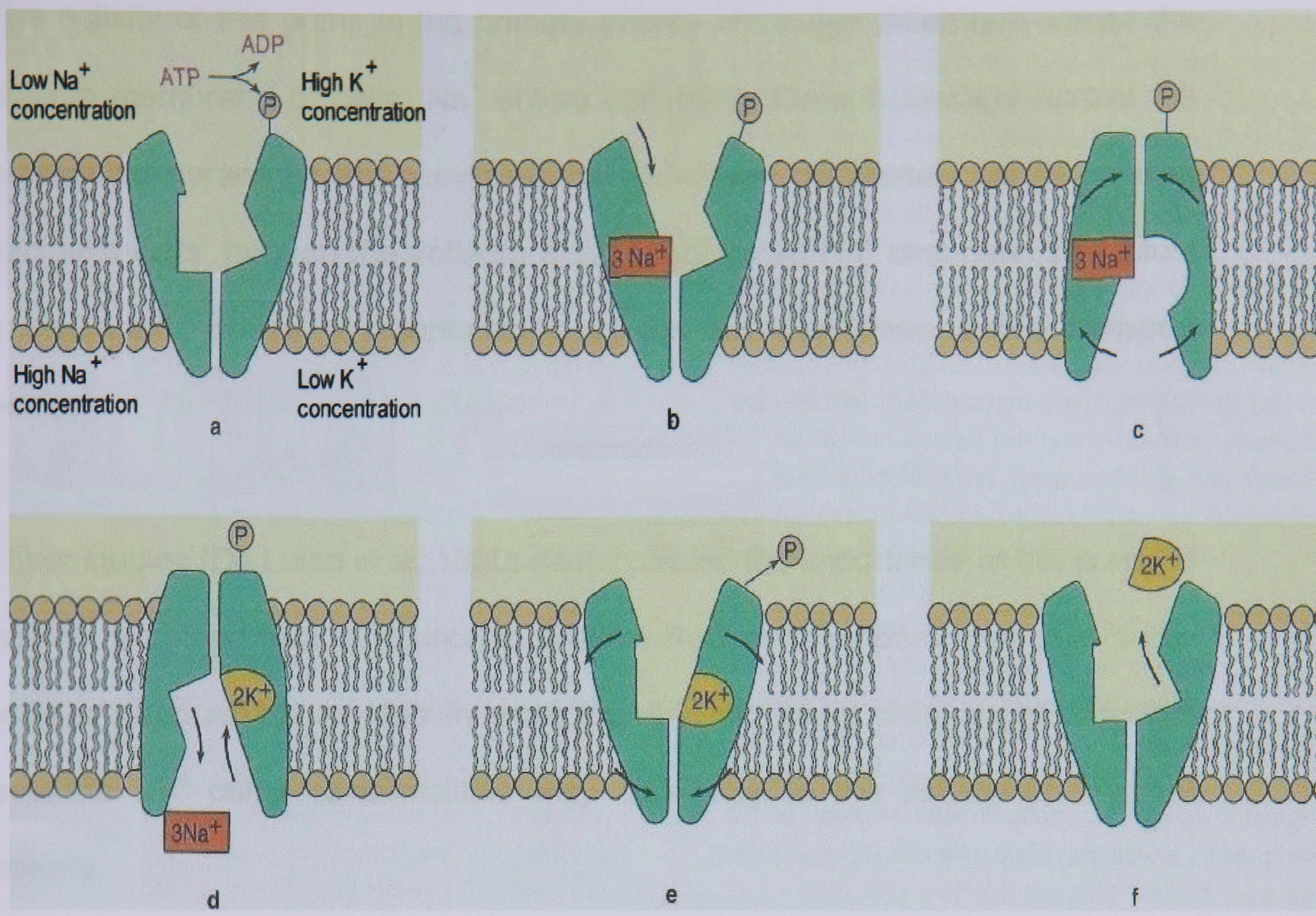

Figure 3.3: A mechanism for the operation of Na^+/K^+ - ATPase pump. In **(a)** the pump binds and hydrolyses ATP, the phosphate group is transferred from ATP to the transporter protein. **(b)** The binding of phosphate converts the Na^+ binding site to its high affinity state and will avidly bind to Na^+ on the cytoplasmic side of the membrane. **(c)** The binding of Na^+ triggers a conformational change that exposes the Na^+ binding to the medium outside of the cell. **(d)** As the conformational change becomes complete, the Na^+ binding site is altered to the low affinity state, this releasing Na^+ to the outside medium. At the same time, the K^+ binding site is activated to bind to the K^+ in the outside medium with high affinity. **(e)** K^+ induces a conformational change which exposes the K^+ binding site to the cell interior and releases the phosphate group. At the same time, the K^+ binding site is converted to low affinity state and K^+ is released to the cell interior. **(f)** Completion of this step returns the transporter to the initial state, ready to repeat the cycle. The transporter works by having 3 Na^+ moved to the outside and two K^+ to the inside of the cell for each turn of the cycle. (Picture taken from Wolfe, 1993).

The activity of this pump is the primary source of voltage difference across the plasma membrane of cells. Na^+ enters constantly through leakage across the plasma membrane by the activity of the Na^+-driven cotransport pumps, and in excitable cells, through the voltage- and ligand- gated Na^+ channels. The usual inward traffic of Na^+ is counteracted by the Na^+/K^+-ATPase active transport pump.

Other studies (De Luise et al, 1980) demonstrated the importance of this pump in human red blood cells in relation to obesity. Reduced numbers of sodium pump units and reduced pump activity were found in red blood cells, suggesting that possible Na^+ pump abnormalities may contribute to the pathophysiology of obesity.

The flow of K^+ into a cell is usually controlled by the activity of the Na^+/K^+-ATPase and by indirect active transport. In order to maintain a high inside/low outside gradient (as shown in the Figure 3.3), the outward movement of K^+ along this concentration gradient occurs passively through slow leakage across the plasma membrane and through the activity of voltage- and ligand-gated K^+ channels, which occur in both excitable and non-excitable cells. The internal loss of K^+ is usually counteracted, again, by the Na^+/K^+ - ATPase pump (Wolfe, 1993)

Hydrogen ions (H^+) are pushed out of the cytoplasm by the activity of the indirect active transporter that exchanges Na^+ outside for H^+ inside. This transporter is sometimes abbreviated to NHE. It functions to counteract for the constant production of surplus H^+ by metabolic reactions. NHE are integral proteins found

in the membranes of all eukaryotic cells (Aharonovitz et al, 2001). NHE (isoform 6) has been found in the recycling endosomes of cells (Brett et al, 2002). This exchanger operates by actively co-transporting anions, including Cl^-, $(PO_4)^{3-}$ and $(SO_4)^{2-}$ into cells for the exchange of Na^+ (Wolfe, 1993). It therefore helps to regulate the internal pH of the cytoplasm inside the cell. The other mechanism which controls the cytoplasmic pH is the removal of H^+ by the V-type active transport pumps. This mechanism works in collaboration with the cellular trafficking system (Figure 3.4A), as the pumps push the H^+ ions from the cytoplasm into vesicles such as the Golgi complex (and the trans-Golgi network, TGN), secretory vesicles and lysosomes. The activity of the V-type pumps simultaneously lowers the pH of the internal contents of these organelles and raises the pH of the surrounding cytoplasm. The increased acidity of the vesicles is critical to their functions in storage, in recycling during endocytosis and in the activation of the enzymes held by the vesicles (Wolfe, 1993). The cytoplasmic pH in most normal cells lies between 7.2-7.6; the pH of the nucleus ranges between 7.5-7.8, being around 0.3 pH units more alkaline than the cytoplasm (Seksek and Bolard, 1996; Altan et al, 1998). The cell cytoplasm also contains slightly more acidic organelles and vesicles, such as the Golgi, early endosomes and late endosomes (also called prelysosomal compartment). The pH ranges between 6.2-6.4 in the Golgi, 6.0-6.5 in the early endosomes, 5.2-5.8 in the late endosomes, 5.8 in the secretory vesicles and 4.8-5.2 in the lysosomes (Seksek et al, 1995, Kim et al, 1996 and Schindler et al, 1996). Figure 3.4B shows an example of the pH values in different compartments of breast cells.

Calcium (Ca^{2+}) ions are removed from the cytoplasm by the activity of Ca^{2+} - ATPase pumps in the plasma membrane and in the vesicles of the endoplasmic reticulum (ER). The mitochondria can take up and store large amounts of Ca^{2+} by the formation of the inorganic calcium deposits in the mitochondrial matrix. The resultant Ca^{2+} gradient, which is high in the cell exterior, in the ER and in the mitochondria, but low in the cytoplasm, controls a range of cellular mechanisms. The low Ca^{2+} is maintained by the pumps that remove the ions from the cytoplasm. Sudden influxes of Ca^{2+}, which could be triggered by a variety of systems, set the control mechanisms. Entry of the Ca^{2+} could either be through the voltage- or ligand gated channels, and contributes to the generation of electrical impulses in nerve cells (Wolfe, 1993).

Magnesium (Mg^{2+}) is another important ion mainly involved in the function of enzymes, as it is an essential cofactor. It can also play an important role in the regulation of membrane transporters such as Ca^{2+} active transport pumps. Mg^{2+} has been suggested (Wolfe, 1993) to steadily and slowly leak out into most cell types from relatively high concentrations in the extracellular medium. Free cytoplasmic concentrations of Mg^{2+} are kept relatively low, through binding to cellular molecules such as ATP and RNA, and by the antiport system that is driven by the high outside/low inside Na^{+} gradient. As Na^{+} moves inward, the antiport pumps Mg^{2+} outward.

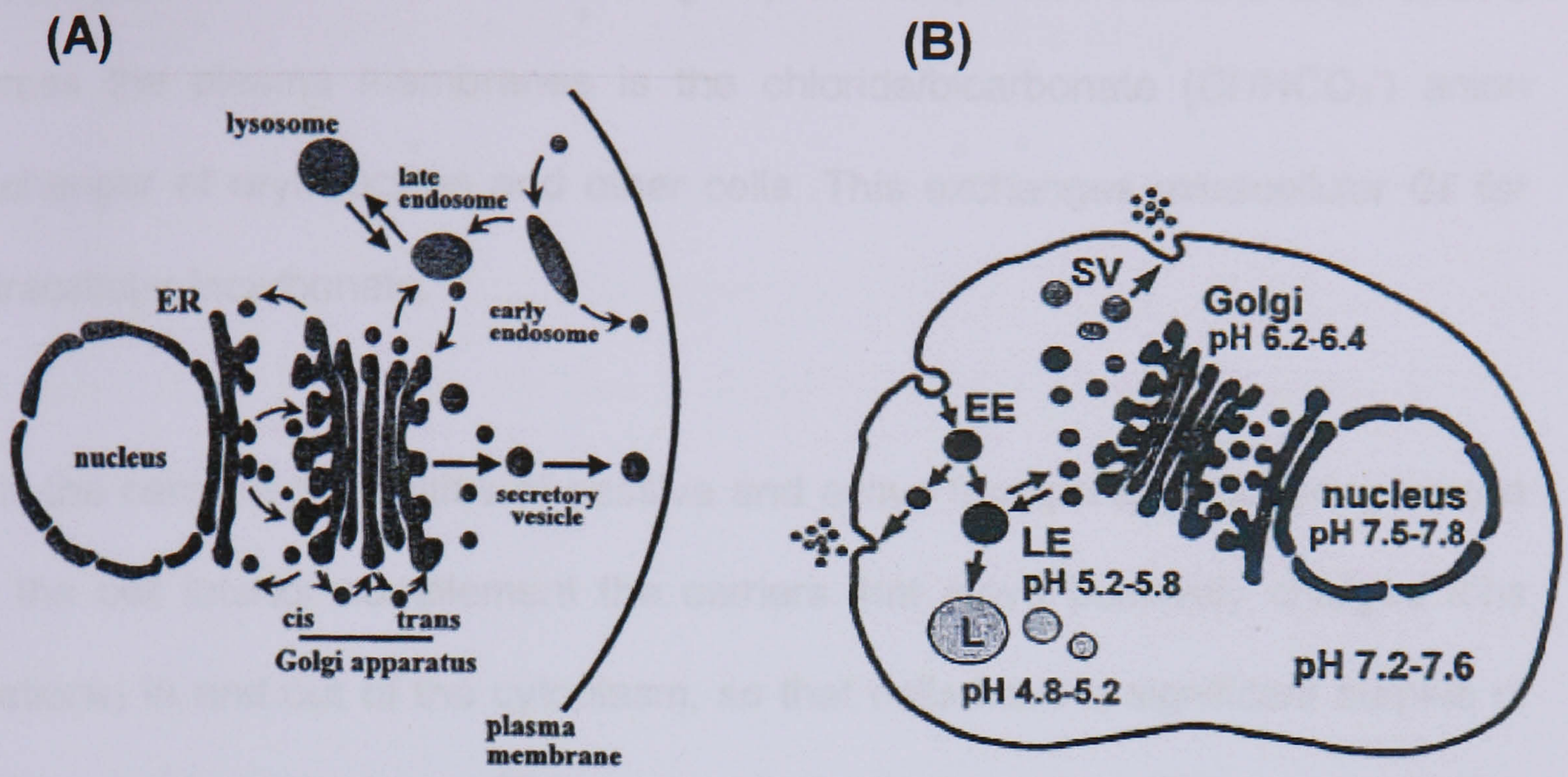

Figure 3.4: **(A)** A diagram showing a summary of the major membrane trafficking routes within the cell. The newly synthesised protein leaves the endoplasmic reticulum (ER) for post-transcriptional processing in the Golgi apparatus. The proteins are then transferred either to secretory vesicles or the pre-lysosomal compartments (called late endosomes). Proteins that are taken form the cell surface undergo a peripheral sorting in the early endosomes and part of the material is carried back to the cell surface. In other cases, the material is recycled and carried to the interior of the cell in transport vesicles to the pre-lysosomal compartments, where it mixes with lysosomal enzymes from Golgi to form lysosomes. Since the volume of the membrane remains constant, endocytosis is balanced by the outward flow of protein-containing vesicles. **(B)** The pH values of different intracellular compartments in normal breast cells. (Altenberg et al, 1993, Seksek et al, 1995, Kim et al, 1996, Schindler et al, 1996, Seksek and Bolard, 1996, Altan et al, 1998 and Belhoussine, 1999 and as reviewed by Larsen, 2000). (L= lysosomes, LE= late endosome (or early lysosome), EE= early endosome, SV= secretory vesicles).

On the other hand, negatively charged ions (anions) can enter the cells by either passive diffusion or active transport. In cells, facilitated diffusion transporters can permit entry of anions, such as chloride (Cl^-), phosphate $(PO_4)^{3-}$ and sulphate $(SO_4)^{2-}$. The same anions can also be actively pumped into cells by Na^+ - driven

cotransport. Another member of the group of transporters that exchange anions across the plasma membranes is the chloride/bicarbonate (Cl^-/HCO_3^-) anion exchanger of erythrocytes and other cells. This exchanges extracellular Cl^- for intracellular bicarbonate.

It is the combined activities of passive and active transporters delivering anions to the cell interior complement the carriers that move positively charged ions (cations) in and out of the cytoplasm, so that cells have a significant surplus of anions in the cytoplasm. This unequal distribution of positive and negative charges produces the charge or voltage difference characteristic of living cells, in which the interior of the cell is negative relative to the exterior. This potential difference is referred to as membrane potential.

The work of active transporters in maintaining cellular ion concentration at the appropriate level has a significant contribution to the total energy expenditure in the cell. As much as 20% of the heat used to maintain body temperature is generated by the transformation of chemical energy to heat as the active transporters move ions across the plasma membrane. The greatest consumer of these active transporters is the Na^+/K^+ -ATPase pump, which reflects its importance in controlling the osmotic balance and setting up the Na^+ gradient used for cotransport (Wolfe, 1993).

3.1.2. Multidrug resistance and cellular ions and trafficking

Multidrug resistance (MDR) is always multifactorial, but one or more than one mechanism can be present in one tumour cell. The mechanism of resistance, as reviewed in chapter 2 of this thesis, may be associated with decreased drug accumulation (decreased drug uptake and/or increased drug efflux) and altered intracellular drug distribution, or possibly due to the expression of the ABC transporters, (also known as *ABCC* gene family, including P-gp, MRP and LRP,) (Dano, 1973; Juliano and Ling, 1976; Cole et al, 1992; Scheper et al, 1993; Gottesman and Pastan, 1988). This new nomenclature was developed by the Human Gene Nomenclature Committee (HUGO) in 1999. The ABCC family comprise other members such as sulfonylurea receptors (SUR) and the cystic fibrosis transmembrane conductance regulator (CFTR). Subsequent cloning characterised another transporter, the canalicular multispecific organic anion transporter (cMOAT) from rat (Ishikawa et al, 2000).

The mechanism related to altered intracellular drug distribution is of main concern (as reviewed by Larsen et al 2000). Most anticancer drugs target the nucleus or DNA, so that sequestration of the drug in cytoplasmic organelles such as the trans-Golgi network (TGN), the recycling endosomes and lysosomes causes a decrease in drug target interaction and a decrease in cytotoxicity, even if the total intercellular drug concentration remains unchanged. Larsen and co-workers (2000) suggested that altered intracellular drug distribution is closely related to drug accumulation, making it difficult to separate the two processes, which seem to be the most common mechanisms of resistance in tumour cells.

- The other common modification in MDR cells is alkalisation of the intracellular pH. It has been reported (Roepe et al, 1993; Altenberg et al 1993; Seksek et al, 1995; Kim et al, 1996; Seksek and Bolard, 1996; Altan et al 1998; Belhoussine et al 1999) that many drug resistant tumour cell lines show alterations in intracellular pH relative to the parent cell lines. Changes in internal pH gradients are associated with changes in drug distribution and sensitivity to anticancer agents. Figure 3.5A and B below show the differences in pH values that may occur in drug sensitive and drug resistant breast cancer cells, as an example.

It has been noted that the intracellular pH was altered in tumour cells, such that the cytoplasm became more acidic, while the vesicular pH became more alkaline. The result was a greatly decreased intracellular pH gradient relative to parental cells. This defect was correlated with disruption in the function and organisation of the trans-Golgi network (TGN) (Altenberg et al, 1993, Schindler et al, 1996, Altan et al, 1998, Belhoussine et al, 1999). Treatment of doxorubicin resistant cells with ionophores that disrupt the acidification of the vesicles, lead to the re-sensitisation of the resistant cancer cell line, strongly suggesting a direct association between the intracellular pH gradient and drug resistance (Schindler et al, 1996, Altan et al, 1998).

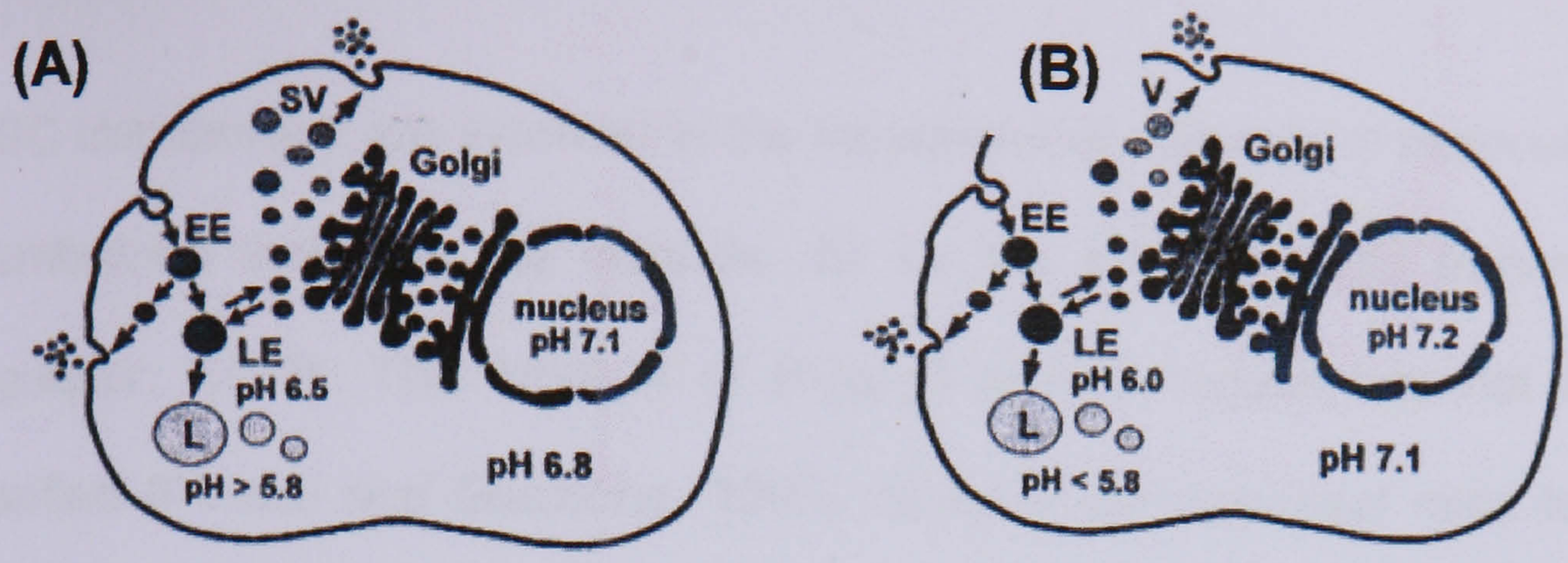

Figure 3.5: The pH values of different intracellular compartments of the parental drug sensitive (A) and MDR (B) breast cancer cells. (Altenberg et al, 1993; Seksek et al, 1995; Kim et al, 1996; Schindler et al, 1996; Seksek and Bolard, 1996; Altan et al, 1998; Belhoussine, 1999 and as reviewed by Larsen, 2000). (L= lysosomes, LE= late endosome (or early lysosome), EE= early endosome, SV= secretory vesicles).

It has been documented that the intracellular pH of mammalian cells was mainly regulated by Na^+/ H^+ exchange and HCO_3^-dependent transport mechanisms. In addition, the vacuolar type H^+ ATPase may have been expressed in some tumour cells (Martinez-Zaguilan et al 1993). An interesting study has shown that at least one subunit of the vacuolar proton ATPase was over-expressed in cells over-expressing P-gp. The results suggested an involvement of this ATPase in the drug efflux from resistant cells (Marquardt and Center, 1991). Over-expression of certain ABC transporters can be accompanied by increases in certain ion channels. MRP over-expression accompanied increases in both K^+ and volume-regulated Cl^- channel currents (Jirsch et al, 1993). On the other hand, P-gp has been proposed to function as a Cl^- channel (Valverde et al, 1992), while another study reported that P-gp was, rather, a channel regulator (Hardy, et al, 1995). This implies that the ABC transporters may participate in ion regulation, thereby modulating vesicular transport, as described by Larsen et al (2000).

ABC transporters are involved in the movement of a variety of molecules across membranes including the chloride, Cl^- by the cystic fibrosis transmembrane regulator, CFTR. The function of P-gp in normal tissues has not been fully clarified (Pinedo and Giaccone, 1995). Studies with knockout mice lacking the *mdr1a* gene (that codes for P-gp) demonstrated the importance of this protein in the blood-brain barrier and drug disposition (Schinkel et al, 1994).

3.1.3. P-gp and multidrug resistance

Multidrug resistance (MDR) is the simultaneous resistance of tumour cells to different natural anticancer drugs that have no common structure or function. Several mechanisms contribute to the MDR phenotype, a common correlate of MDR is the over-expression of an ATP driven membrane protein, P-gp (Figure 3.6), as reviewed by Thomas and Coley (2003).

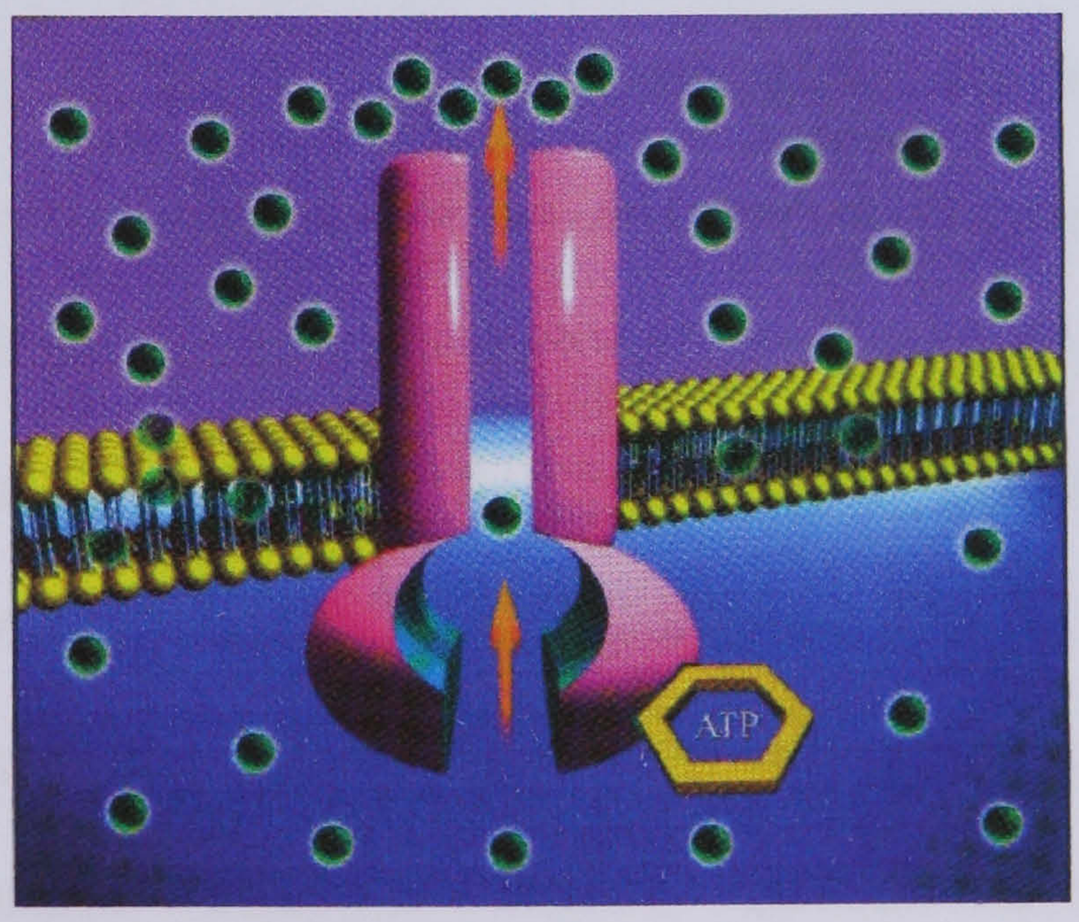

Figure 3.6: The function of P-gp in MDR. The hydrolysis of the bound ATP molecule activates the efflux pump to drive the cytotoxic drug outside the cell. (Reprinted from Thomas and Coley, 2003).

For the last two decades, P-gp inhibition has been studied as a way of reversing MDR. As a result, agents such as verapamil and cyclosporin were identified in the 1980s (reviewed in Krishna and Mayer, 2000). These affect the function of P-gp as a transporter, hence the name 'modulators' or 'chemosensitisers'. These agents have produced some disappointing results when used at clinically relevant doses in human subjects. Many of the first generation modulators identified were substrates for P-gp and were competitors with the anticancer agents for efflux by P-gp. Thus, high serum concentrations were required to produce adequate intracellular concentration to exert the desired modulatory effect, based on *in vitro* studies. In addition, many of those agents were not only substrates for P-gp, but to other transporter and enzyme systems, resulting in unpredictable pharmacokinetic interactions in the presence of anticancer drugs (reviewed in Krishna and Mayer, 2000). To overcome these limitations, several analogues of these early modulators were developed with the aim of having less toxicity and more potency. These were classed as *second-generation* MDR modulators and further developed into the *third-generation* modulators that are being studied in current clinical trials. An example of the former is valspodar (PSC833), a non-immunosuppressive derivative of cyclosporin D, which inhibits P-gp and with 10-20 fold greater activity than cyclosporin A (Teboekhorst et al. 1992; Twentyman and Bleehen, 1991). This second- generation modulator is also a substrate for cytochrome P450 isoenzyme 3A4. As a result of this, competition took place (Figure 3.7) between the anticancer agent and modulator for phase I metabolic reactions. Hence, clinical trials highlighted the consequential unpredictable pharmacokinetic interactions produced. When PSC833 is used with paclitaxel (Taxol), it inhibits the cytochrome P450 3A4

mediated metabolism of Taxol causing an increase in serum concentrations, thus putting patients at risk of over-exposure (Bates et al. 2001; Fischer et al. 1998).

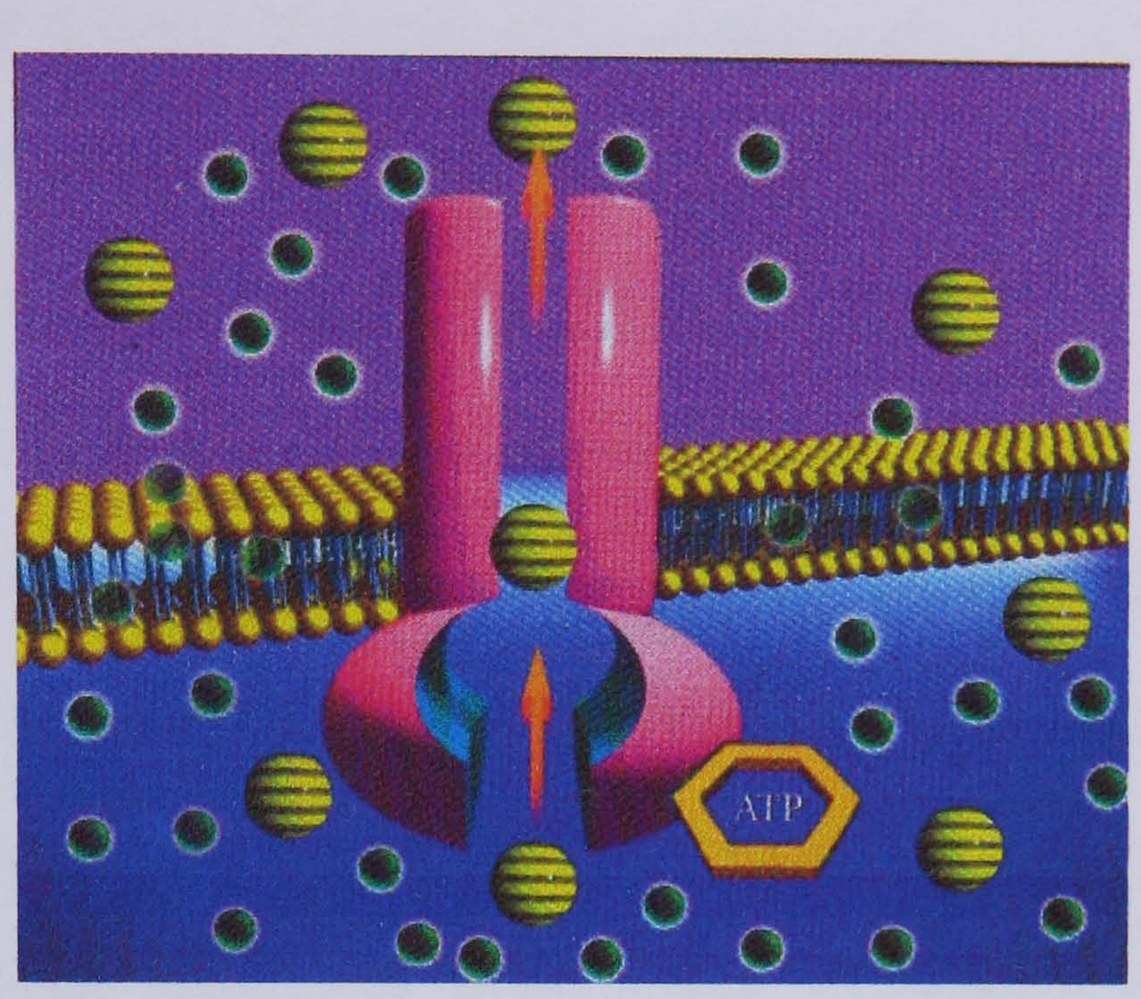

Figure 3.7: First and second generation modulators undergo competitive inhibition. The modulators compete as substrates with the cytotoxic agents for transport by the pump. This would limit the efflux of the cytotoxic agent, increasing its intracellular accumulation. (Reprinted from Thomas and Coley, 2003).

In order to counteract this, the common response by clinical researchers is to reduce the dose of the anticancer agent. However, this may still result in under- or over-dosing, as the pharmacokinetic interactions between the second-generation modulators and anticancer drugs are unpredictable and cannot be determined in advance (Gottesman et al. 2002; Fischer et al. 1998). The non-specificity of these second- generation modulators to P-gp, such as that of PSC833 affecting MRP1 (Krishna and Mayer, 2000; Yanagisawa et al; 1999; Rowinsky et al. 1998) may cause adverse effects of anticancer drugs. For example, BCRP (breast cancer resistant protein, another example of an ABC

transporter) is a functional regulator of the haemopoetic stem cells, and inhibition of it may contribute to neutropaenia (Dantzig et al, 1999).

Generally, the unpredictability of these second generation P-gp modulators on cytochrome P450 3A4-mediated drug metabolism has made it difficult to establish a safe but effective dose of the anticancer drug. Hence, this represents a major limitation in the use of second-generation modulators in treatment of MDR. In addition to inhibiting P-gp, second-generation modulators can act as substrates for other transporters within the ABC family. Inhibition of these can leave other normal cells and tissues less capable of protecting themselves against cytotoxic agents, especially when many of these transporters have important roles in eliminating xenobiotics such as those in the kidney, liver and gastrointestinal tract (Krishna and Mayer, 2000; Thomas and Coley, 2003) .

ABC transporters are also involved in the regulation of the permeability of the central nervous system (blood-brain barrier), testes and placenta, thus protecting these systems from being exposed to the cytotoxic agents circulating in the blood. First- and second-generation modulators act by competitive inhibition of P-gp; as a result, the modulator and the anticancer drug would compete for transport by the P-gp pump, which in turn limits the efflux of the drug and thus causes an increase in its intracellular accumulation. To overcome the limitations of the second-generation modulators, *third-generation* modulators were developed to specifically inhibit P-gp potently. These were developed by studying the structure-activity relationships, and act by *non-competitive* inhibition of the P-gp pump (Figure 3.8). Some of these may bind with high affinity to the

pump but are not substrates themselves (e.g. tariquidar, or also known as XR9576). The binding then causes a conformational change in the protein and prevents ATP hydrolysis, which inhibits the transport of the anticancer drug outside the cell. This results in an increase in the intracellular level of the drug (Thomas and Coley, 2003).

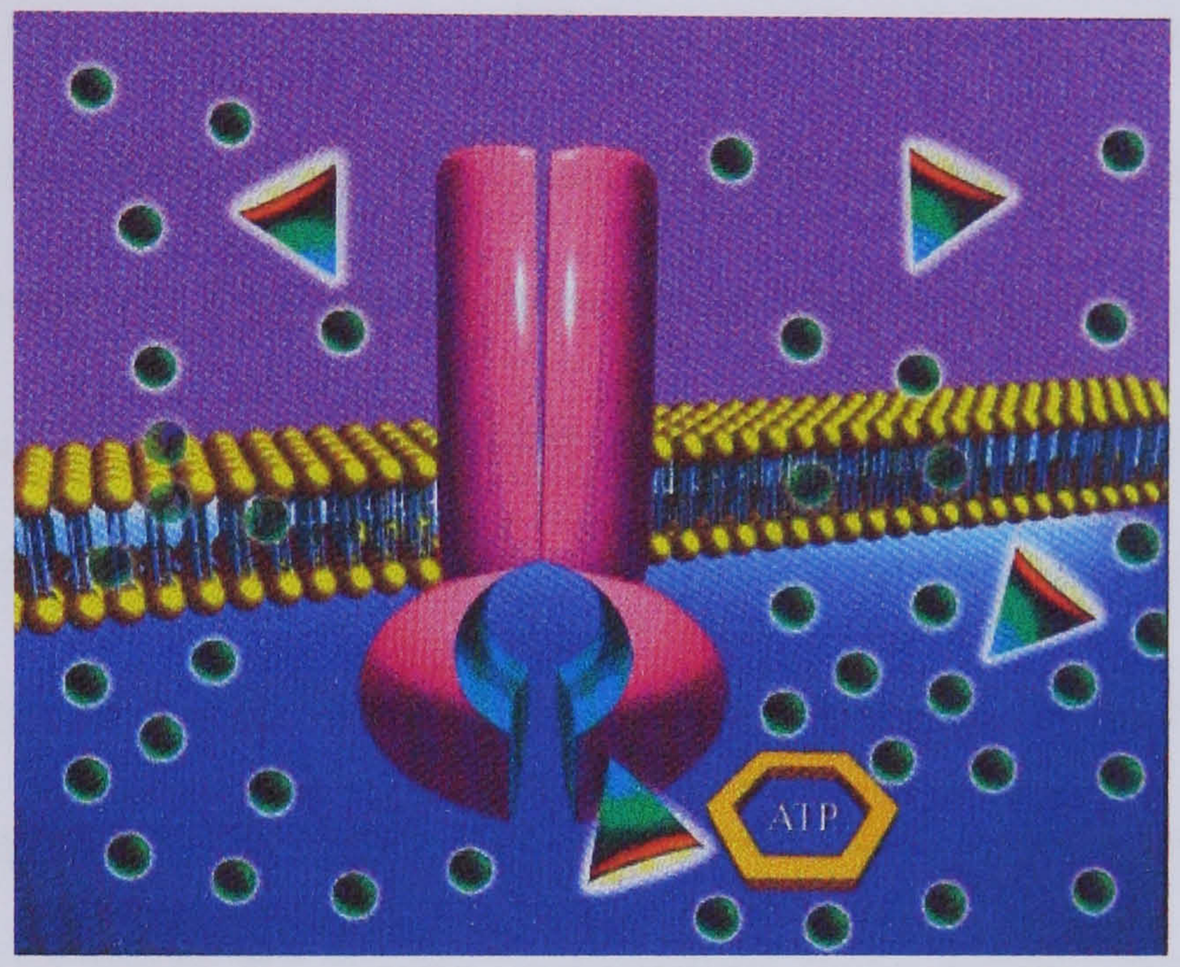

Figure 3.8: Non-competitive inhibition of P-gp. Third generation modulators, such XR9576 operate in this manner, as it binds to the pump with high affinity, but it is not a substrate. The binding causes a conformational change in the protein, hence preventing ATP hydrolysis and the transport of the cytotoxic agent to the outside. The drug would therefore accumulate inside the cell. (Reprinted from Thomas and Coley, 2003).

Furthermore, these agents do not affect cytochrome P450 3A4 and have not been tested for other ABC transporters, but their specificity to the P-gp pump minimises the possibility. An example of a third generation modulator that is currently in clinical development is an anthrylamide derivative, called tarquidar (XR9576), which is P-gp specific (Roe et al, 1999), but has recently been shown to affect another type of the ABC transporter called *breast cancer resistant*

protein (BCRP) (Robey et al, 2004). The inhibitory effect of XR9576 on P-gp exceeds those of first- and second- generation modulators with respect to potency and duration of action. In an *in vitro* study, P-gp transport remained blocked for more than 22 hours after XR9576 had been removed from the culture medium (Mistry et al, 2001). XR9576 specifically and non-competitively binds to the P-gp pump with an affinity that greatly exceeds that of the substrates (Van Zuylen. et al, 2000). It is not clear whether the binding of XR9576 on P-gp is to the ATP binding site, but it inhibits ATPase activity of P-gp. It has been proposed that there are multiple drug interaction sites on P-gp that are functionally classified as transport. The multiple-binding sites model suggest that XR9576 binding can prevent substrate binding, alter ATP hydrolytic ability pf P-gp or a combination of these two possibilities (Martin et al, 1999). Pharmacokinetic studies in healthy subjects show that single doses of XR9576 up to 2 mg/kg taken intravenously, or 750 mg orally, are well tolerated and provide complete P-gp inhibition for at least 24 hours, according to a study using rhodamine 123 accumulation in $CD56^{+}$ lymphocytes (Stewart et al, 2000). XR9576 showed no effect on the pharmacokinetics of Taxol or doxorubicin when it was administered to patients with solid tumours (Thomas and Coley, 2003; Abraham et al, 2001; Thomas et al, 2001; Ferry et al, 2001). XR9576 is currently in phase III clinical trials.

Many studies have shown that MDR can be reversed after the use of substrate analogues or MDR modulators. However, our understanding of MDR modulation is incomplete. A previous study (Vayuvegula et al, 1988) used the membrane potential sensitive dye DIOC5 to compare the membrane potential of drug sensitive and MDR cancer cell lines before and after treatment with the modulators verapamil and cyclosporin A (CsA). The MDR cell lines (the murine P388 leukaemia-Adriamycin resistant and human acute lymphatic leukaemia-vincristine resistant) were reported to have a lower membrane potential compared with their corresponding drug sensitive parental cell lines. Incubation of the MDR cell lines with CsA or verapamil appeared to indicate the restoration of membrane potentials to that of the parent cell lines. They suggested that alteration of membrane potentials was one of the mechanisms responsible for MDR in malignancy and showed that it was corrected after using modulators.

The aim of this chapter is to investigate the dielectric differences between drug sensitive and resistant cancer cells, and to relate these to the mechanisms by which resistance is conferred to these cells relative to their parent lines. Furthermore, DEP has also been employed to elucidate the mechanism of action, by means of examining the differences in dielectric properties, which in turn can reflect membrane potentials between drug sensitive and MDR cancer cells before and after treatment with the modulator XR9576. Our results have shown marked differences between the drug resistant and their sensitive parental lines, with significant changes in the cytoplasm of these cells. Also, the results have cast doubt on the earlier observation by Vayuvegula et al (1988) and instead support a later study (Gollapudi and Gupta, 1992) in suggesting that

DIOC5 is a substrate for the ABC transporter. The results showed that the process of MDR modulation is not associated with changes in the electrical properties of cancer cells. Moreover, the results demonstrate that using the flow cytometric method alone may produce artefactual results with MDR cells. In combination with dielectrophoresis, the results show the role of MDR modulators in preventing drug efflux in MDR cells, indicating that using flow cytometry to reveal membrane potential is flawed.

3.2. Materials and methods

3.2.1. Chemicals and reagents

Taxol was obtained as a pharmacy preparation (Bristol Myers Squibb, Nottingham, UK) and further dissolved in 0.9% NaCl solution to give a 1mM stock solution and sterilized by filtering through a 0.2 micron filtration membrane. Doxorubicin (Sigma Aldrich, Poole, UK) and XR9576 (was kindly provided by Xenova Ltd, Slough, UK), both were dissolved in dimethyl sulfoxide (DMSO) (Roe et al, 1999), and stored frozen as stock solutions, which were thawed prior to use.

3.2.2. Cell culture

Human chronic myelogenous leukaemia (K562), its doxorubicin (formerly known as Adriamycin) resistant counterpart (K562AR), human promyelocytic leukaemia (HL60) and its doxorubicin resistant counterpart (HL60AR) were grown in 20 mM HEPES modified RPMI-1640 medium supplemented with 10% heat-inactivated foetal calf serum (FCS), (Invitrogen, Paisley, UK), 2 mM L- glutamine and 100

units/ mL penicillin-streptomycin. All cell culture reagents were obtained from Sigma Aldrich (Poole, UK), unless stated otherwise. The cells were grown under standard cell culture conditions at 37°C. K562AR and HL60AR resistance were maintained in the presence of 100nM and 50nM doxorubicin, respectively. The human breast cancer (MCF-7) parent cell line, its Taxol and doxorubicin resistant counterparts (MCF-7TaxR and MCF-7DoxR, respectively) were grown in similar conditions as that of K562, K562AR, HL60 and HL60AR, using 20 mm HEPES modified Dulbecco's Modified Eagle Medium (DMEM) medium (Sigma, Poole, UK), with supplements as before. MCF- 7TaxR was maintained in the presence of 6 nM Taxol, and MCF-7DoxR was maintained in the presence of 100 nM doxorubicin. The parent cell lines were obtained from The European Collection of Cell Culture, Porton Down, Salisbury, UK (ECACC), but MCF-7TaxR and MCF-7DoxR cell lines were developed by Dr. Helen Coley at the University of Surrey, and hence they were novel in-house models.

Human ovarian resistant tumour cell line (T8) was kindly provided by Professor Jan Schellens from the Netherlands Cancer Institute, Amsterdam, and was resistant to topotecan. These cells were used as BCRP overexpressing cells and were grown using the same reagents and conditions as that for MCF-7, and the resistance was maintained at 950 nM topotecan.

3.2.3. Confirmation of MDR phenotype

3.2.3.1. Chemosensitivity testing

The colorimetric assay using MTT (3-(4,5-Dimethylthiazol-2-yl)-2,5-diphenyltetrazolium bromide) was used to titrate cell viability following drug treatment, as described by Mosmann (1983). Briefly, K562 and K562AR were measured at a density of 1×10^5 cells/mL in 20mM HEPES-modified in RPMI-1640. Densities of the order 10^4 cells/mL were used for MCF-7, MCF-7TaxR and MCF-7DoxR, as they exhibit a higher exponential growth, and were measured in DMEM. The media contained 10% FCS and 100 units/mL penicillin-streptomycin. Cells were then dispensed into 96-well plates in volumes of 200 μL and left to equilibrate for 24 hours at 37°C and 5% CO_2. Freshly thawed drug solution (doxorubicin or Taxol, depending on the cell line) was diluted in 20mM HEPES-modified RPMI-1640 (or DMEM, depending on the cell line) containing 10%FCS and added in a volume of 50 μL in increasing concentrations. Control wells containing cell suspension were supplemented with a similar volume of culture medium only. Following 72-hour incubation, cultured cells were treated with 20 μL of 5mg/mL MTT in PBS (Sigma Aldrich, UK). After four hours of incubation, the plates containing the leukaemia lines in suspension were centrifuged at 200 ×g and the medium was removed, as breast cancer cells are adherent. Tetrazolium crystals were dissolved in 200 μL of DMSO. Absorbance was read at 540nm using an automated ELISA plate reader. The same procedure was followed using doxorubicin in the case of MCF-7 and MCF-7DoxR, and Taxol in the case of MCF-7 and MCF-7TaxR. The chemosensitiser

XR9576 (Xenova Ltd, Slough, UK.) was added at a 100 nM final concentration (Martin et al, 1999) to half of the wells on each plate, so as to ensure that cells were exposed to both the drug and the chemosensitiser, while cells in the second half were exposed to the drug alone. The results were expressed as IC_{50}, i.e. the concentration of cytotoxic drug that reduces cell viability by 50% relative to the control (untreated cells).

3.2.3.2. Western Immuno-blotting

Crude cell membrane preparations were made using hypotonic lysis buffer containing 1mM PMSF (phenylmethylsulfonyl fluoride, a protease inhibitor), 1mM $NaVO_4$, apoprotinin and leupeptin, 150 mM NaCl, in 10 mM Tris buffer (pH 7.4) (Helena Biosciences, Sunderland, UK). The cells were left to lyse for 30 minutes, sonicated and then centrifuged for 10 minutes at 450 ×g, followed by a further centrifugation (Centrikon-T2060) of 60,000 ×g at 4°C. The final pellet was resuspended in lysis buffer containing 0.2% SDS. The protein content of the lysates was determined using a modified Bradford protein assay (Bio-Rad Laboratories, Hemel Hempstead, UK).

50 μg of membrane protein was loaded onto a 10% acrylamide SDS and resolved by SDS-PAGE. The presence of P-gp was detected with anti-P-gp rabbit polyclonal antibody, H241. In order to assess the presence of BCRP, the mouse BCRP monoclonal antibody was used (both antibodies were purchased from Santa Cruz Biotechnology Inc, Autogen Bioclear, Wiltshire, UK). Visualisation was carried out using HRP conjugated secondary antibody with

chemiluminescence (Pierce, Perbio Science UK Ltd, Cheshire, UK). The expression of P-gp was demonstrated by visualising a band of 170kDa in molecular weight, and a band of 70kDa for BCRP.

3.2.4. Cell preparation

3.2.4.1. DEP experiments

The drug resistant and sensitive cells were centrifuged at room temperature at 190 ×g for 5 minutes. The pellets were washed and resuspended in isotonic medium consisting of 8.5% (w/v) sucrose plus 0.3% (w/v) dextrose buffer (Gascoyne et al. 1997). The medium conductivity was adjusted to 2.5 mS/m using PBS and the final conductivity, before use, was verified with a conductivity meter (RS components Ltd, London, UK). The final cell population was counted using a haemocytometer and adjusted to approximately $3x10^5$ cells/ mL (±15%) for DEP measurements. In order to reduce the effect of variation in cell number in each sample, the experiments were repeated many times (generally 4-6) with different populations, which were summed prior to modelling.

The same procedure as that mentioned above was followed for K562, K562AR, MCF-7 and MCF-7TaxR, only now the XR9576 modulator was used. Drug resistant (K562AR and MCF-7TaxR) and their parental cell lines, before and after incubation in 100nM XR9576 for 30 minutes at 37 °C with XR9576), were centrifuged at room temperature at 190 ×g for 5 minutes. As before, the pellets

were washed and resuspended in isotonic medium consisting of 8.5% (w/v) sucrose plus 0.3% (w/v) dextrose buffer (Gascoyne et al. 1997). The medium conductivity was adjusted to 2.5 mS/m using PBS and the final conductivity, before use, was verified with a conductivity meter (RS components Ltd, London, UK). The final cell population was counted using a haemocytometer and adjusted to approximately $3x10^5$ cells/ ml (±15%) for DEP measurements.

As shown in Figure 3.9, the DEP system consisted of a signal generator, a light microscope and the dielectrophoresis chamber in which the cell suspension was placed. The dielectrophoretic forces were generated by two needle-shaped electrodes, pointing towards each other, with opposing tips spaced approximately 100 μm apart in a glass petri dish. The needles were formed by cutting a thin stainless steel rod at a shallow angle, such that cell collection occurred along the sharpened edge. These edges were placed face-down on the bottom of the chamber to ensure that cell collection always occurred within the field of focus of the microscope. The cell suspension was added to the electrodes by micropipette.

The electrodes were energised by a Thurlby Thandar (Huntingdon, UK) signal generator in the range 10 kHz to 20 MHz at an applied voltage of 20 V (peak-peak). Recordings were taken by exciting the electrodes for 1 minute and counting the collected cells using a hand held tally counter, as described by Pohl (1978). The cell density was sufficiently low for the cell population to be disperse enough for cell-cell interactions (pearl-chaining) not to significantly affect the

results. Similarly, the cells were counted at arrival to the electrode edge to ensure accuracy.

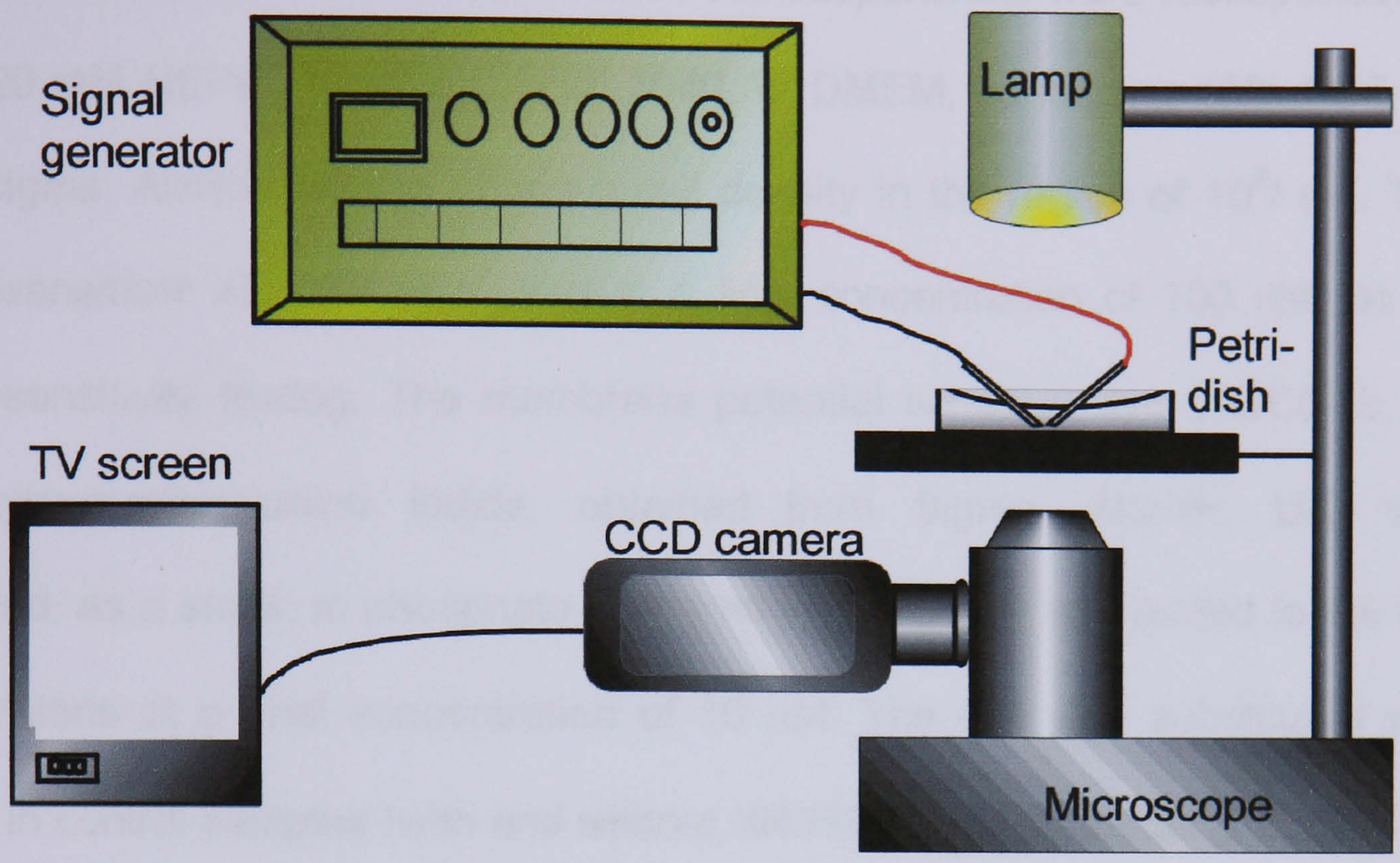

Figure 3.9 : A schematic diagram of DEP arrangement.

The inter-electrode gaps was chosen to be sufficiently large, and the time over which the experiment was performed ensured that the volume over which cells were attracted to the electrodes was sufficiently large for variations in the local electric field gradient due to cell collection to have a minimal effect on the behaviour of the cell collection process. Measurements were taken at five frequencies per decade, between 1 kHz and 20 MHz. Experiments were observed using a Zeiss inverted microscope and CCD camera. The dielectric parameters for each cell line, and in the absence or presence of XR9576 were obtained by fitting the measurement spectra to the single shell model (Irimajiri et al, 1979).

3.2.4.2. Flow cytometry

K562, K562AR, MCF-7 and MCF-7TaxR cell suspensions were resuspended in fresh 20 mM HEPES-modified RPMI-1640, or DMEM, containing 10% FCS (all from Sigma, Aldrich, UK) to obtain a cell density in the region of 10^6/ mL. The chemosensitiser XR9576 was used at a final concentration of 100 nM, as for chemosensitivity testing. The membrane potential sensitive dye DIOC5 (3, 3′-Dipentyloxacarbocyanine iodide, obtained from Sigma, Aldrich, UK) was prepared, as a stock, in phosphate- buffered saline (PBS) and added to the cell suspensions at a final concentration of 10 μM. The dye was substituted with media in control samples (with and without XR9576). After incubating at 37°C for 30 minutes (with and without XR9576), membrane potentials were recorded using a FACS analyser (Becton Dickinson, Oxford, UK). Resting membrane potentials from drug sensitive cells were set on the fluorescence scale by adjusting the laser using the FL 1-PMT (525 nm) green fluorescence setting on the analyser. The cells were gated on volume *versus* scatter for uniform size distribution. The membrane potentials were compared according to the intensity of green fluorescence emitted (assigned by the parameter of geometric mean, GM, values). Thus, an increased membrane potential (hyperpolarisation) is indicated by a higher fluorescence intensity (i.e. a higher GM value), with the reverse (hypopolarisation) being seen for lower membrane potentials.

3.3. Results

3.3.1. MDR confirmation using MTT chemosensitivity testing

Tables 3.1 and 3.2 show the IC_{50} values (the concentration of the drug that reduces the number of cells by 50% relative to control, untreated cells) for doxorubicin and taxol, respectively. As illustrated in Table 3.1, the IC_{50} value for K562 and K562AR were 0.58 μM (± 0.28) and 8.13 μM (± 1.18) respectively, indicating an increase in resistance of 14-fold. The values also show no significant inter-assay variation, as the standard deviation values, for each IC_{50}, were relatively low. MCF-7DoxR was shown (Table 3.1) to be resistant to doxorubicin, relative to the parental cell line, MCF-7, as it showed 5-fold resistance. Table 3.2 shows the IC50 values obtained for MCF-7 and MCF-7TaxR after treating with Taxol. The resistance phenotype was evident in MCF-7TaxR relative to the parent MCF-7, as the resistance fold was 15 (Table 3.2).

Cell Line	Average IC_{50} with Doxorubicin μM (± SD)	Resistance fold
K562	0.58 (0.28)	
K562AR	8.13 (1.18)	**14**
MCF-7DoxR	2.60 (0.50)	**5**
MCF-7	0.51 (0.03)	

Table 3.1: The doxorubicin IC_{50} values for the doxorubicin sensitive and resistant cell lines (n=4)

Cell Line	Average IC_{50} with Taxol nM (± SD)	Resistance fold
MCF-7	4.5 (1.10)	
MCF-7TaxR	77.7 (2.12)	**15**

Table 3.2 The Taxol IC_{50} values of the Taxol sensitive and resistant cell lines (n=4)

3.3.2. MDR confirmation using Western immunoblotting

3.3.2.1 P-gp expression

In addition to the MTT assay discussed earlier, the Western immunoblot (Figure 3.10) visualisation has revealed the expression of the MDR protein, P-gp. The blot showed the expression of P-gp in the MDR cell line (K562AR), but was absent in the parental (K562) cells. The same blot shows a more intense band, indicating a greater degree of expression of P-gp, in the resistant breast cancer cell line (MCF-7TaxR). On the other hand, MCF-7DoxR showed no expression of P-gp. The human myeloid leukaemic cell lines (HL60) and its doxorubicin counterpart (HL60AR) were used as negative controls for P-gp, as HL60AR expresses another MDR protein known as the multidrug resistance associated protein (MRP) of 190 kDa in molecular weight.

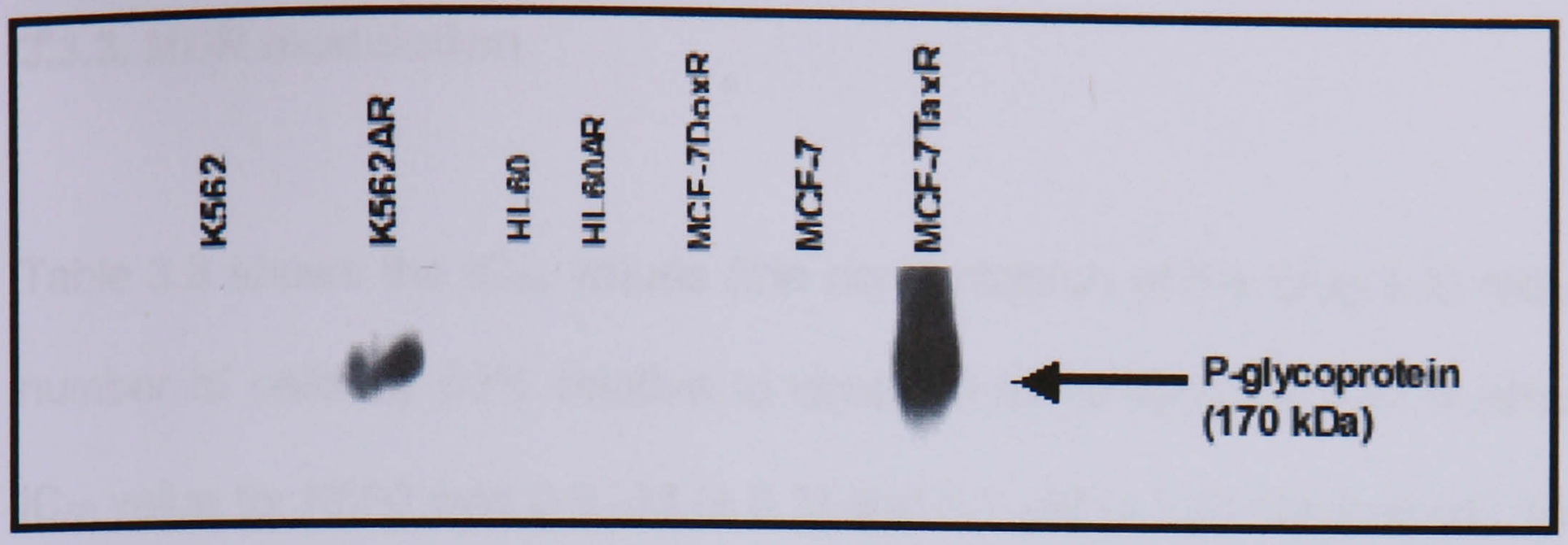

Figure 3.10: A Western blot showing the expression of P-gp in different cell lines. The expression of the protein is indicated by the arrow pointing to its molecular weight (170kDa)

3.3.2.2. Breast cancer resistant protein (BCRP) expression

MCF-7DoxR lacked the expression of P-gp, but was found to be positive in expressing another ABC transporter protein, known as *breast cancer resistant protein*, BCRP (Figure 3.11). The same band intensity was seen in both MCF-7 and MCF-7DoxR, indicating the same level of BCRP expression in both cell lines. T8 was used as a positive control that overexpresses BCRP.

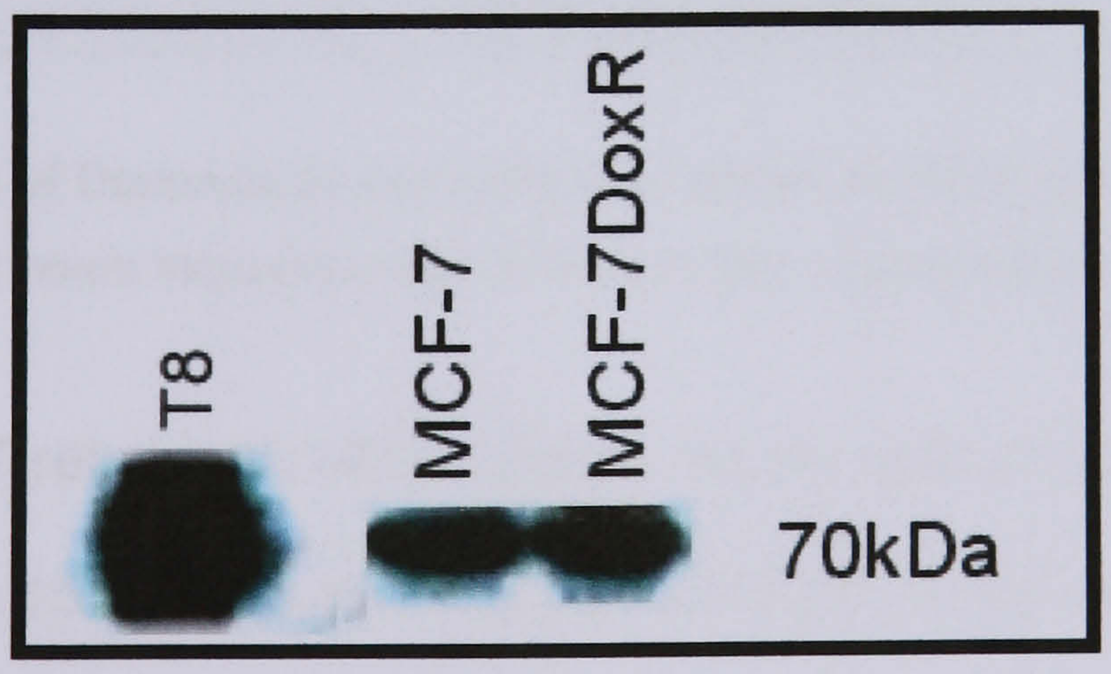

Figure 3.11: A Western blot showing the expression of BCRP in different cell lines. Positive expression was evident by a band shown at 70kDa in molecular weight. T8 was a positive control that overexpresses BCRP.

3.3.3. MDR modulation

Table 3.3 shows the IC_{50} values (the concentration of the drug that reduces the number of cells by 50% relative to controls) for doxorubicin. As illustrated, the IC_{50} value for K562 was 0.6 μM (± 0.3) and 8.1 μM (± 1.2) respectively, indicating resistance of 14-fold. The treatment of K562AR cells with doxorubicin in combination with the modulator XR9576 reduced the IC_{50} value to resemble that of the parent cell line (0.5 μM ±0.1 and 0.6 μM ±0.3, respectively), indicative of resistance reversal.

Cell Line	Average IC_{50} with Doxorubicin μM (± SD)	Average IC_{50} with Doxorubicin and XR9576 μM (± SD)	Resistance fold
K562	0.6 (0.3)	0.4 (0.1)	
K562AR	8.1 (1.2)	0.5 (0.1)	14

Table 3.3: MTT results of Doxorubicin and XR9576 (100nM) for K562 and K562AR summarising the IC_{50} values after 72 hours incubation and of at least three experiments.

The IC_{50} for MCF-7 relative to MCF-7TaxR can be seen in Table 3.4, where the resistance fold was 15, thus confirming the resistance phenotype of MCF-7TaxR. XR9576 modulation reversed the resistance, as demonstrated by the drop in IC_{50} following treatment.

Cell Line	Average IC_{50} With Taxol nM (± SD)	Average IC_{50} with Taxol and XR9576 nM (± SD)	Resistance fold
MCF-7	4.5 (1.1)	5.3 (0.6)	
MCF-7TaxR	77.7 (14.1)	7.8 (2.4)	**15**

Table 3.4: MTT results of Doxorubicin and XR9576 (100nM) for MCF-7 and MCF-TaxR, summarising the IC_{50} values after 72 hours incubation and of at least three experiments.

3.3.4. DEP experiments

3.3.4.1. Drug sensitive versus drug resistant cancer cells

The data points are the average of at least 5 experiments. For each experiment, the number of cells collected was noted after applying an electric field for 1 minute exposure to each frequency, using a range of frequencies between 5 kHz-20MHz, at 5 frequencies per decade. Parameters such as conductivity and permittivity of both membrane (represented as specific membrane capacitance) and the cytoplasm were obtained using the Classius-Mossotti equation based modelling, where the dielectric parameters were estimated using a single shell dielectric model (Huang et al. 1992). From Table 3.5 and Figure 3.12, it can be seen that K562 and K562AR began collecting above 10^4 Hz in frequency.

However, the collection rate showed a decline above 2-3 MHz for K562, unlike K562AR where the decline began at 8-10MHz.

	Cytoplasm		Membrane	
	σ (S/m)	ε	K_s (nS)	C_{spec} (mF/m^2)
K562	0.23 (0.21- 0.24)	40- 80	0.008	3.9 (3.3-3.6)
K562AR	0.50 (0.48- 0.51)	40- 80	0.008	3.5 (2.9-4.1)

Table 3.5: DEP parameters for K562 and K562AR (radius= 4.3 μm for both cell lines)

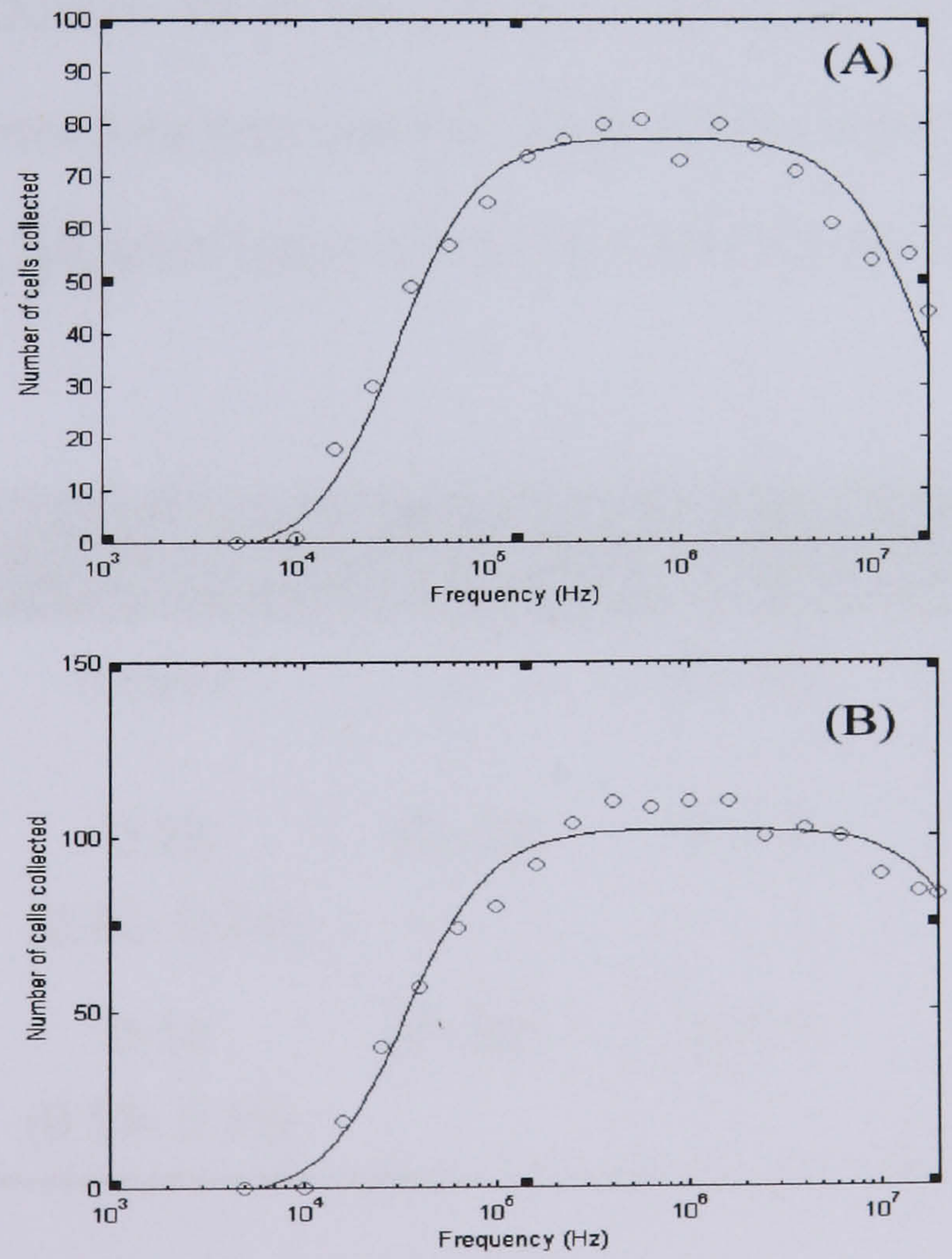

Figure 3.12: DEP best fit models for K562 (A) and K562AR (B)

Table 3.5 shows the parameters calculated for the cytoplasm and membrane. The calculation was based on obtaining the best fit to experimental data. The best fit was found by scaling the polarisability by an arbitrary factor to match the curve to the measured data, and then altering the permittivity and conductivity of the membrane and cytoplasm until a best match was found. K562 had a significantly lower cytoplasmic conductivity than K562AR (0.23 and 0.50 S/m, respectively), indicating a lower ionic strength, in the drug sensitive K562 in comparison to the resistant counterpart, K562AR. Also, there were no significant changes in the membrane morphology as the specific membrane capacitance values were not significantly different in the two cell lines. The numbers in brackets, in the table indicate the ranges, between which, the curve would still best fit the data. Outside those ranges, the curves would no longer best fit the data. The same procedure was used to obtain similar measurements for MCF-7, MCF-TaxR (Table 3.6 and Figure 3.13) and MCF-7DoxR (Table 3.7 and Figure 3.14).

	Cytoplasm		Membrane	
	σ (S/m)	ε	K_s (nS)	C_{spec} (mF/m^2)
MCF-7	0.23 (0.22- 0.24)	40- 80	0.010	6.0 (5.5-6.6)
MCF-7TaxR	0.14 (0.13- 0.15)	40- 80	0.010	8.3 (8.2-8.9)

Table 3.6: DEP parameters for MCF-7 (radius= 9.3 μm) and MCF-7TaxR (radius= 9.6 μm)

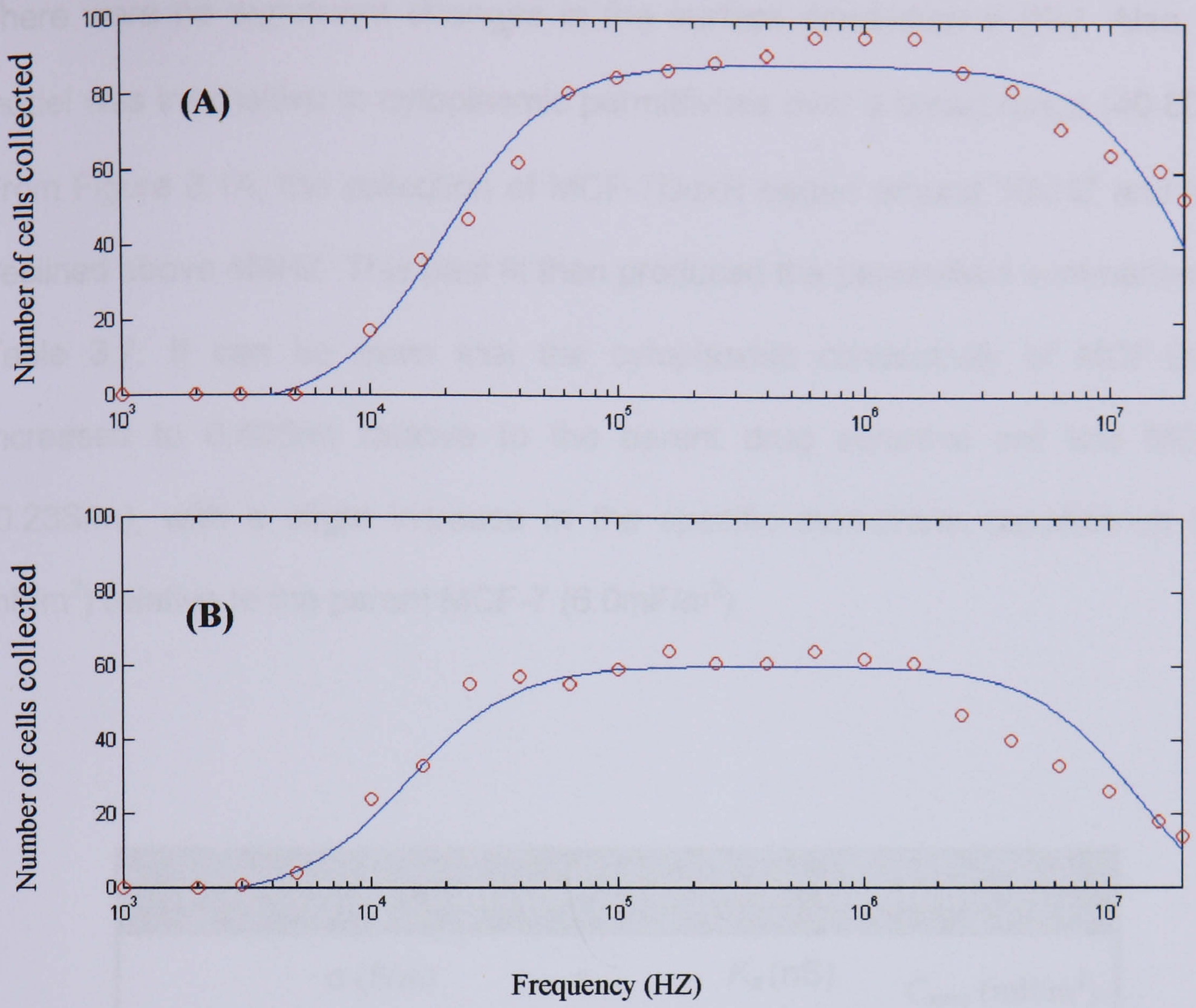

Figure 3.13: DEP best fit models for MCF-7 (A) and MCF-7TaxR (B)

From Figure 3.13, the collection of MCF-7 started around 10kHZ, while that of MCF-7TaxR started around 5kHZ. The collection of MCF-7 decreased above 6MHz, while that of MCF-TaxR decreased around 250kHZ. The parameters obtained from these fits are summarised in Table 3.6. MCF-7 had a higher cytoplasmic conductivity relative to its MDR counterpart, MCF-7TaxR (0.23 and 0.14 S/m, respectively). This implies a lower ionic content in the cytoplasm of the drug sensitive breast cancer cell line than that of MCF-7TaxR. Also, the results highlighted noticeable differences in the membrane morphology, as the specific membrane capacitance increased from 6.0 mF/m^2, in MCF-7, to 8.3 mF/m^2 in MCF-7TaxR.

There were no significant changes in the surface conductance (Ks). Also, the model was insensitive to cytoplasmic permittivites over a broad range (40-80 ε_0. From Figure 3.14, the collection of MCF-7DoxR began around 10kHZ and later declined above 4MHZ. This best fit then produced the parameters summarised in Table 3.7. It can be seen that the cytoplasmic conductivity of MCF-DoxR increased to 0.40S/m relative to the parent drug sensitive cell line MCF-7 (0.23S/m), with a slight increase in the specific membrane capacitance (6.4 mF/m^2) relative to the parent MCF-7 ($6.0mF/m^2$).

	Cytoplasm		Membrane	
	σ (S/m)	ε	K_s (nS)	C_{spec} (mF/m^2)
MCF-7	0.23 (0.22-0.24)	40-80	0.011	6.0 (5.5-6.6)
MCF-DoxR	0.40 (0.38-0.41)	40-80	0.01	6.4 (5.8-7.1)

Table 3.7: DEP parameters for MCF-7 (radius= 9.3 μm) and MCF-7DoxR (radius= 9.6 μm)

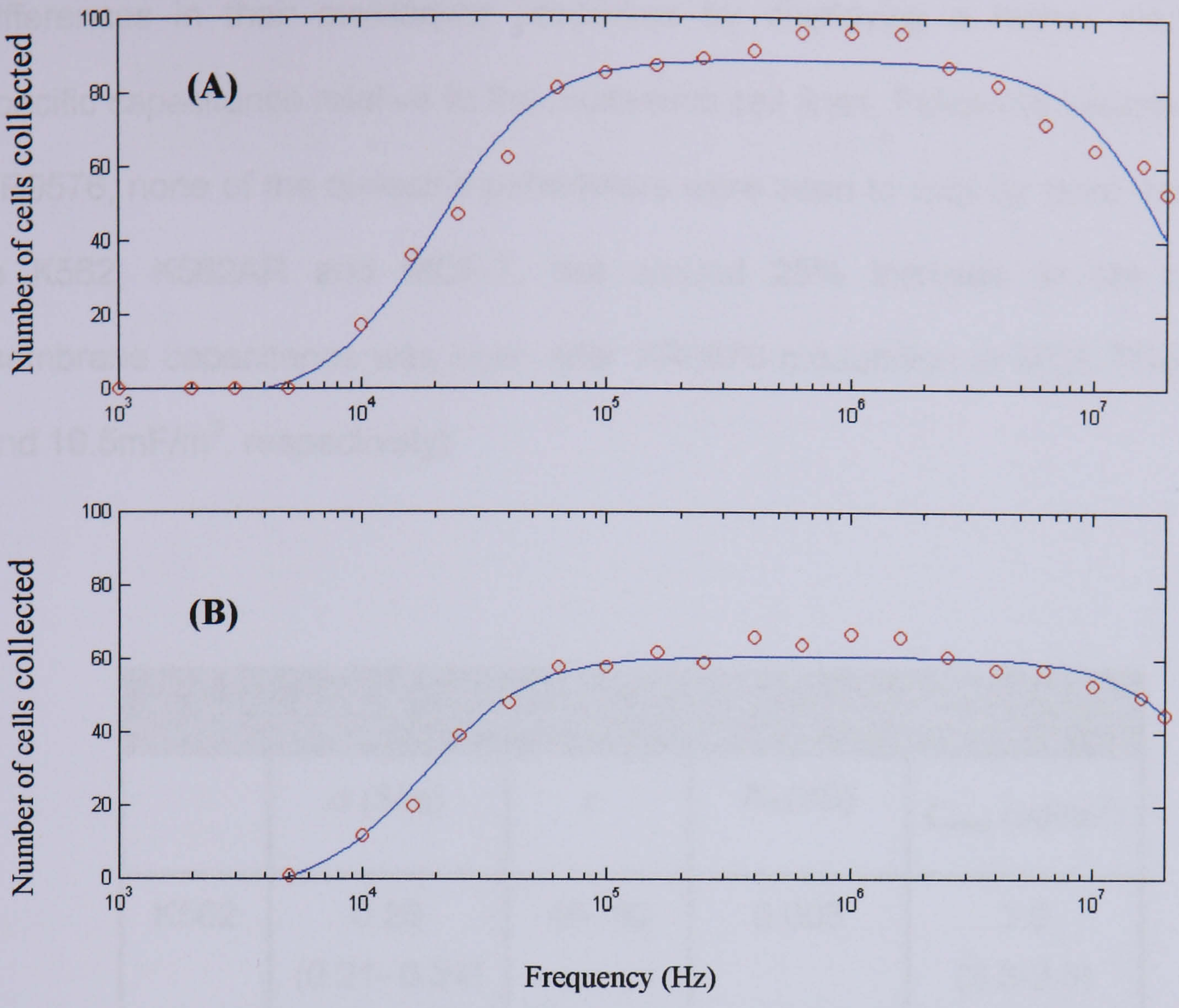

Figure 3.14: DEP best fit models for MCF-7 (A) and MCF-7DoxR (B)

3.3.4.2. MDR modulation

The results of modelling are summarised in Table 3.8 for K562 and K562AR, before and after modulation with XR9576, and Table 3.9 for MCF-7 and MCF-TaxR, before and after modulation. K562 had a lower cytoplasmic conductivity relative to K562AR (0.23 and 0.50 S/m, respectively), while MCF-7 had a higher cytoplasmic conductivity relative to its MDR counterpart, MCF-7TaxR (0.23 and 0.14 S/m, respectively). Comparison of the membrane specific capacitance of MCF-7TaxR relative to MCF-7 reveals that the former is greater significantly (8.3 and 6.0mF/m^2, respectively). Overall, the breast cancer cell lines exhibited

differences in their membrane properties by displaying a higher membrane specific capacitance relative to the leukaemic cell lines. Following treatment with XR9576, none of the dielectric parameters were seen to vary by more than 15% in K562, K562AR and MCF-7, but around 25% increase in the specific membrane capacitance was seen after XR9576 modulation in MCF-7TaxR (8.3 and 10.5mF/m^2, respectively).

	Cytoplasm		Membrane	
	σ (S/m)	ε	K_s (nS)	C_{spec} (mF/m^2)
K562	0.23 (0.21- 0.24)	40- 80	0.008	3.9 (3.3-3.6)
K562AR	0.50 (0.48- 0.51)	40- 80	0.008	3.5 (2.9-4.1)
K562+ XR9576	0.20 (0.19- 0.21)	40- 80	0.008	3.9 (3.3-3.6)
K562AR + XR9576	0.55 (0.51- 0.58)	40- 80	0.008	3.5 (2.9-4.1)

Table 3.8: A summary of the DEP results showing the electrical parameters of both the cytoplasm and the membrane of K562 (radius= 4.3 μm) and K562AR (radius= 4.3 μm) before and after modulation with XR9576 (σ=. Conductivity, ε=. permittivity, K_s = surface conductance, C_{spec} = specific capacitance)

	Cytoplasm		Membrane	
	σ (S/m)	ε	K_s (nS)	C_{spec} (mF/m^2)
MCF-7	0.23 (0.22- 0.24)	40- 80	0.010	6.0 (5.5-6.6)
MCF-7TaxR	0.14 (0.13- 0.15)	40- 80	0.010	8.3 (8.2-8.9)
MCF-7+ XR9576	0.26 (0.25- 0.27)	40- 80	0.011	6.0 (5.5-6.6)
MCF-7TaxR+ XR9576	0.14 (0.13- 0.15)	40- 80	0.010	10.5 (9.9-11.1)

Table 3.9: A summary of the DEP results showing the electrical parameters of both the cytoplasm and the membrane of MCF-7 (radius= 9.3 μm) and MCF-7TaxR (radius= 9.6 μm) before and after modulation with XR9576 (σ=. Conductivity, ε=. permittivity, K_s = surface conductance, C_{spec} = specific capacitance)

3.3.5. Flow cytometry

Membrane potentials of drug sensitive and resistant cancer cells were assessed after 30 minutes exposure to the dye. The results for K562, K562AR, MCF-7 and MCF7TaxR before and after modulation are shown in Figures 3.15 and 3.16, respectively. These are representatives of many experiments and they all have shown similar patterns. Control drug sensitive and resistant cancer cells before and after treatment exhibited negligible fluorescence before using DIOC5. The green fluorescence intensity emitted by the dye, as shown in Figure 3.15, was markedly decreased in K562AR (GM value = 36) relative to the K562 parental cell line (GM value = 124).

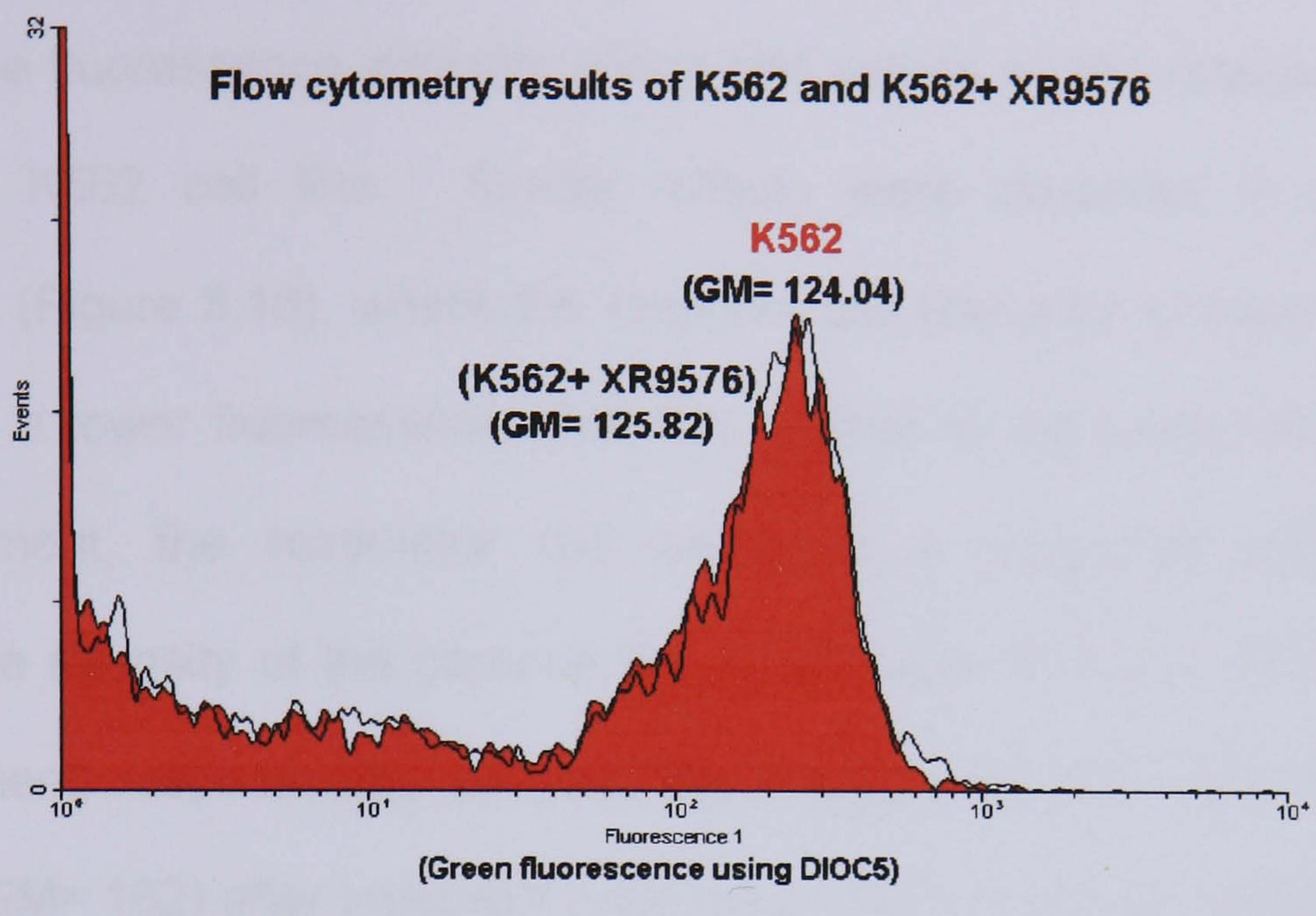

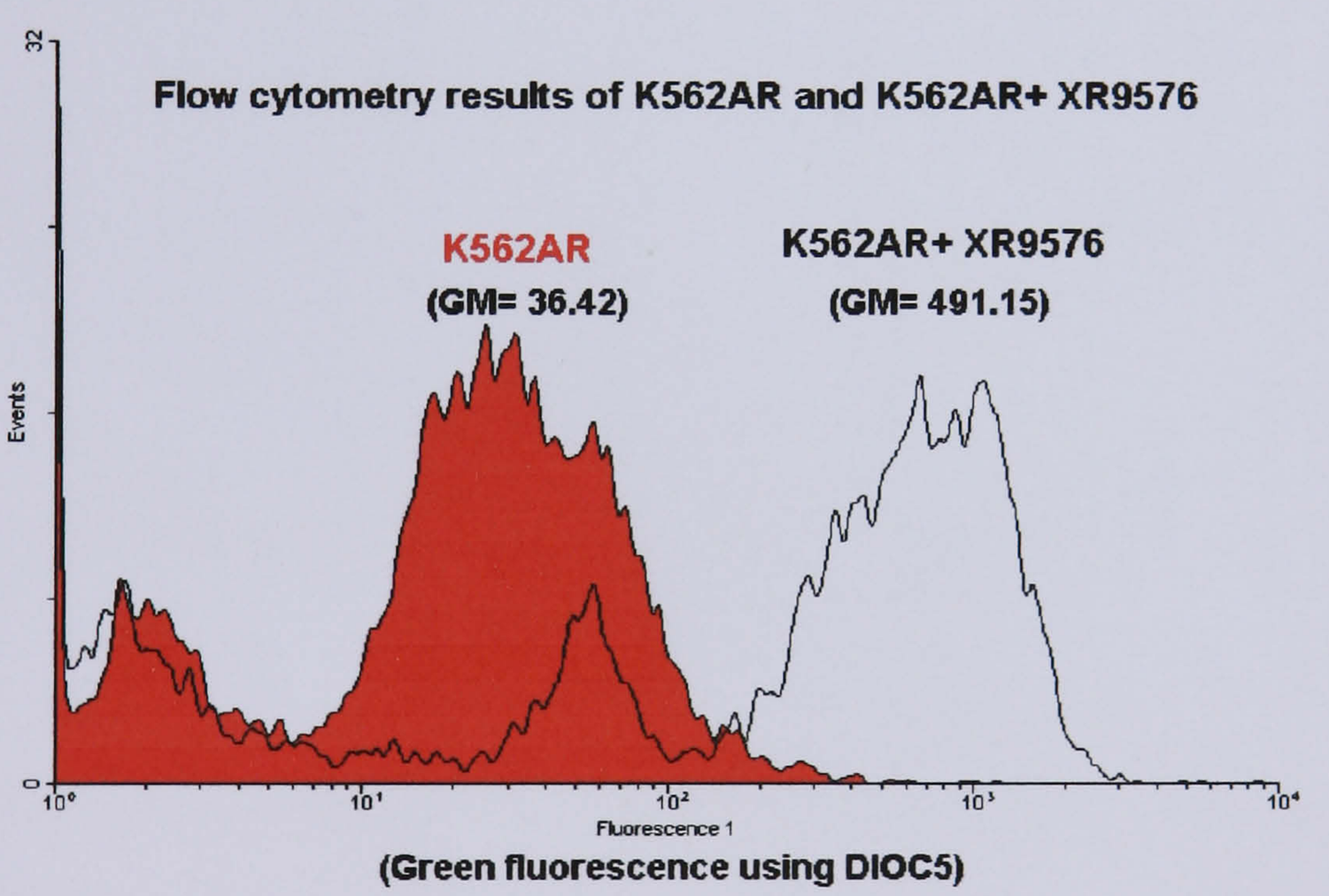

Figure 3.15: Flow cytometry data for K562 and K562AR before and after modulation with XR9576

The modulator XR9576 did not have a significant effect on the green fluorescence intensity in K562, with GM values unchanged following treatment with XR9576 (126). However, the use of XR9576 with K562AR had a striking effect on the fluorescence intensity giving GM values of 491 relative to 124 for the parent K562 cell line. Similar effects were observed in MCF7 and MCF7TaxR (Figure 3.16), where the resistant cell line prior to treatment, MCF-7TaxR had a lower fluorescence (GM=84) relative to the parent MCF-7 (243). After treatment, the modulator did not have a significant effect on the fluorescence intensity of the parental line (GM values 243 and 272 before and after treatment, respectively), whereas the intensity for MCF-7TaxR increased markedly (GM= 162) after treatment relative to (GM= 84, before treatment).

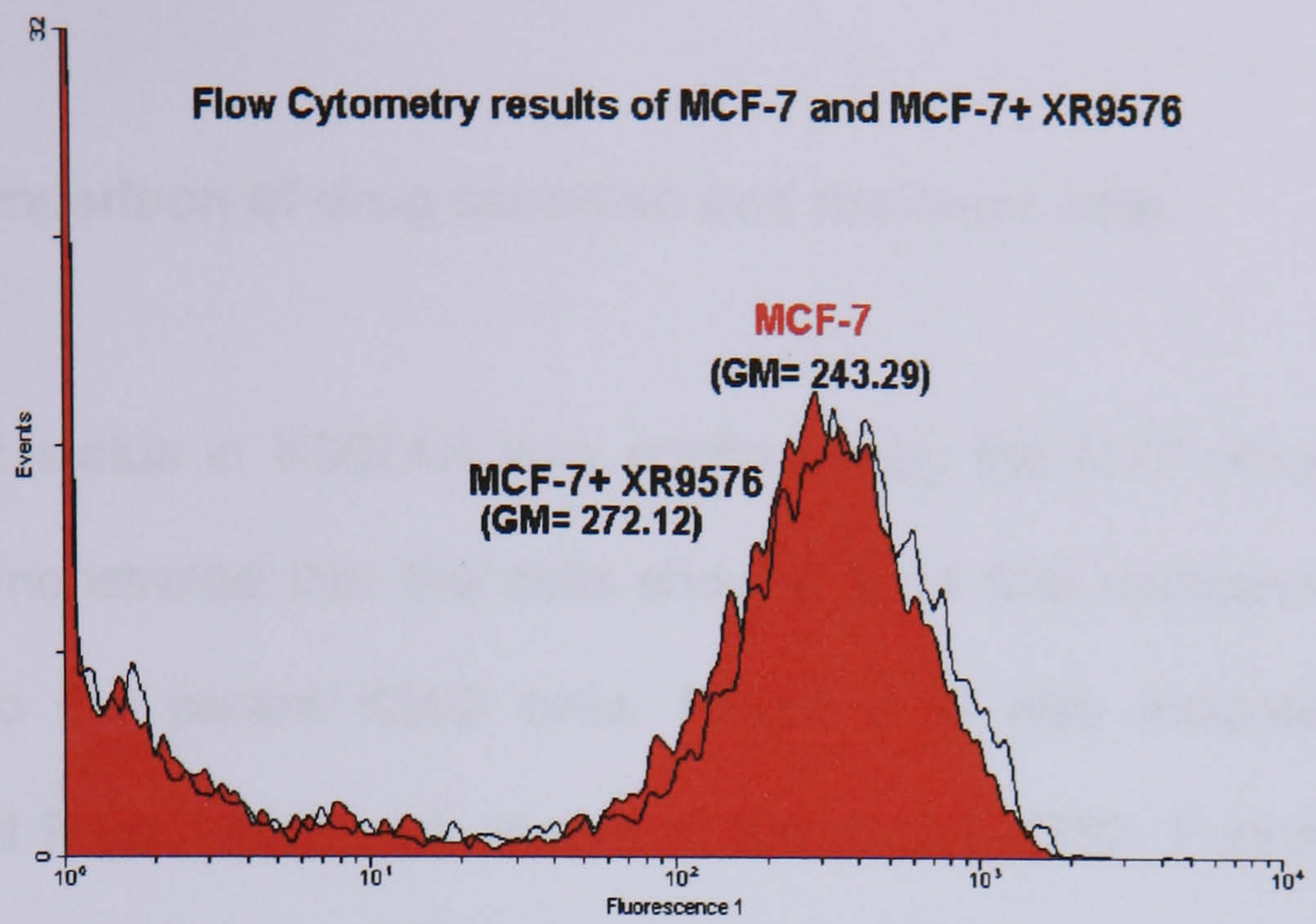

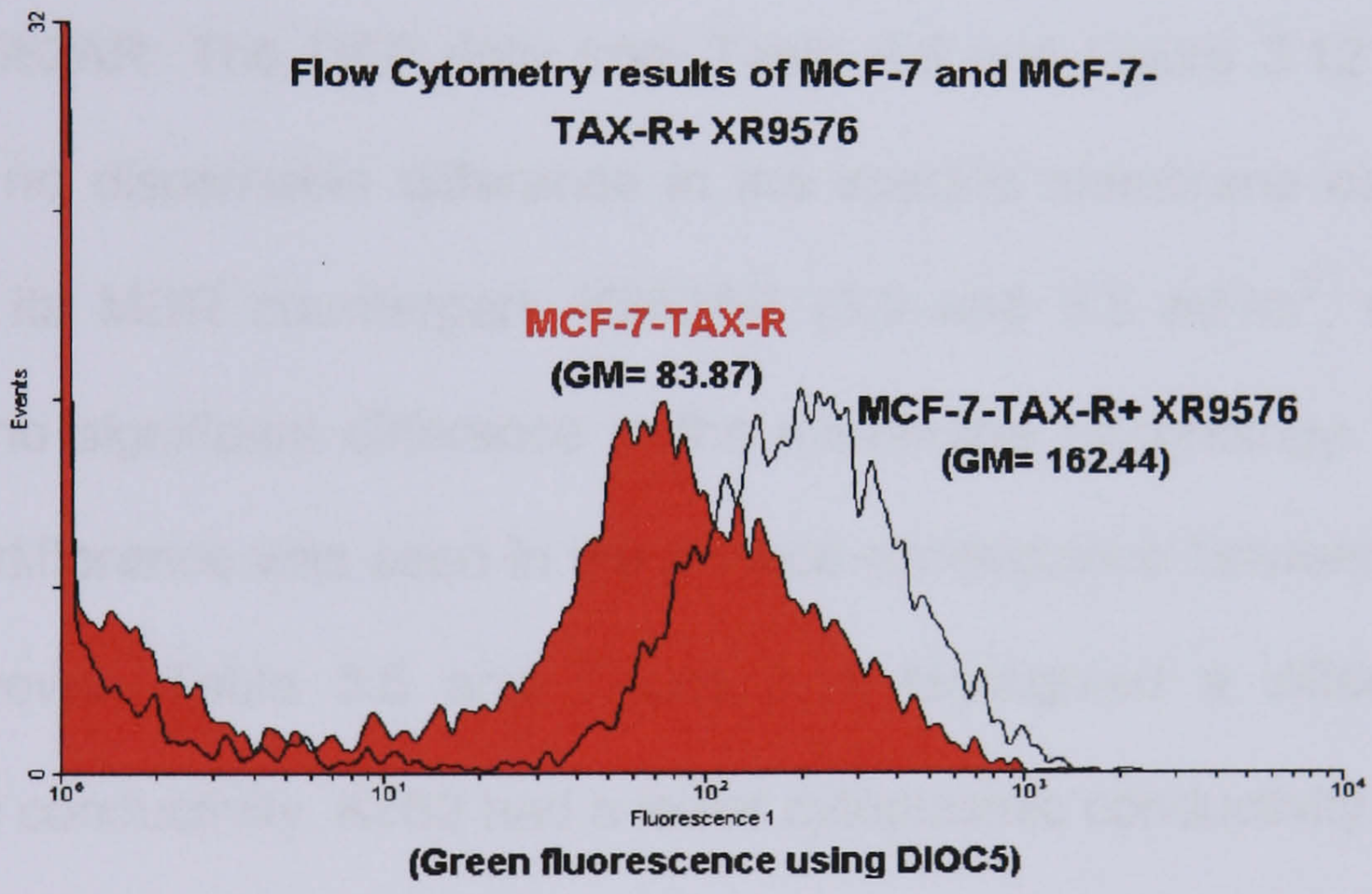

Figure 3.16: Flow cytometry data for MCF-7 and MCF-7TaxR before and after modulation with XR9576

3.4. Discussion

3.4.1. Comparison of drug sensitive and resistant cells

The MDR status in K562AR was confirmed by the MTT results in Table 3.1, which demonstrated that the cells showed a 14 fold resistance to doxorubicin relative to the parent K562 cells. Figure 3.10 also indicated that K562AR expressed P-gp, which was absent in the parent K562. Furthermore, the MTT results in Table 3.3 demonstrated MDR reversal after using the P-gp specific modulator XR9576. These results point to P-gp being the sole contributor to MDR in K562AR. The DEP data from Table 3.5 and Figure 3.12 showed that there was no discernable difference in the specific membrane capacitance of K562 and its MDR counterpart, K562AR (3.9 and 3.5 mF/m^2, respectively), indicating no significant difference in the membrane morphology. Similarly, no significant difference was seen in the surface conductance between the two cell lines. However, Table 3.5 and Figure 3.11 highlighted a difference in the cyoplasmic conductivity. K562 had a lower cytoplasmic conductivity relative to its MDR counterpart, K562AR (0.23 and 0.50 S/m, respectively), indicating a higher ionic content in the cytoplasm of the resistant cell.

The increase in the cytoplasmic ionic content in K562AR may be attributed to a number of possible mechanisms, most of which involve the increased expression of activity of certain ion channels or pumps, contributing to an increase in the quantity of ions present in the cytoplasm of K562AR cells relative to those in the parent K562. The expression of P-gp itself may be one mechanism for this

increase in cytoplasmic conductivity. P-gp has variously been reported to be a Cl^- channel (Valverde et al, 1992; Altenberg et al, 1994 and reviewed by Wadkins and Roepe, 1997) or bifunctional with one function as a Cl^- channel and another as a peptide transporter (Gill et al, 1992; Zhang and Ling, 1995). It has also been noted that P-gp shares homology with the cystic fibrosis transmembrane conductance regulator (CFTR) (Welsh et al, 1992 and as reviewed by Gadsby and Nairn, 1999), a known Cl^- channel, and also with sulphonyl-urea regulator (SUR). CFTR and SUR proteins have also been implicated with the regulation of other ions in the cytoplasm, including Na^+ and Ca^{2+}, respectively, as reviewed by Wadkins and Roepe (1997). Belhoussine et al (1999) showed that the vesicular pH was more acidic in K562AR cells (pH=5.90) relative to the parent (pH=6.02), while the cytoplasmic pH was more alkaline in K562AR relative to K562 (pH= 7.06 and 6.94, respectively). The lower pH seen in sensitive cells (K562) was suggested to correlate with disruption in the trans-Golgi network (TGN). The organisation of TGN appeared more compact in MDR cells (Simon and Schindler, 1994; Altenberg et, 1993; Schindler et al, 1996; Altan et al, 1998) including K562AR (Belhoussine et al, 1999). Belhoussine et al (1999) noted that drug sensitive cells had a lower number of acidified vesicles, suggesting a diminished capacity of cells to remove protonated drugs from the cytoplasm to secretory compartments followed by their secretion through the activity of the recycling pathways. The same pattern of acidified vesicular pH and alkaline cytoplasmic pH was observed in the doxorubicin resistant breast cancer cell line, as discussed later in this section.

In MCF-7 and MCF-7TaxR (Table 3.6 and Figure 3.12), there was no significant difference in the membrane parameters between the two cell lines. However, a significant difference in the cytoplasmic conductivity was observed, where MCF-7TaxR had a much lower conductivity relative to the parent (0.14 and 0.23 S/m, respectively). This indicates that MCF-7taxR has a lower ionic content relative to the parent MCF-7. This change is surprising when compared with K562AR, as both cell lines overexpress P-gp. The mechanism by which MCF-7TaxR loses its conductivity is uncertain, but a number of suggestions can be made. P-gp has also been described as a regulator of other channels, e.g. Cl^- channels in the membrane (Gill et al, 1992; Valverde et al, 1992; Hardy et al, 1995). A regulator may not necessarily mean an activator of the Cl^- channel, as it could similarly de-activate it, this may cause a reduction in the inflow of Cl^- into the cytoplasm, thereby reducing the ionic content.

The results mentioned earlier highlight the possibility of different mechanisms taking place to account for the different patterns seen in the data. In the case of the MDR cell lines K562AR and MCF-7TaxR, both cell lines showed an overexpression of P-gp relative to their parental lines. Furthermore, MTT results showed similar (at least 14 and 15 fold) increases in resistance were obtained for K562AR and MCF-7TaxR. Also, for both lines, resistance was reversed by the use of the P-gp specific modulator XR9576 indicating that P-gp was the sole source of resistance. However, the cell lines exhibited opposite cytoplasmic conductivity shifts relative to their parental cells. The cytoplasmic conductivity was higher in K562AR relative to the parent. One mechanism that could be proposed for K562AR, relative to K562, is that P-gp is acting as a Cl^- channel. P-

gp has been known to act as a drug transporter, which expels anticancer drugs to the outside of the cell, as well as being and regulating Cl^- channels (as reviewed by Wadkins and Roepe, 1997). In acting as a Cl^- channel, the Cl^- ions are permitted to enter the cytoplasm, thus causing an increase in the number of ions present and giving the evident high cytoplasmic conductivity seen from the DEP data. Other possible contributors to this high cytoplasmic conductivity might involve the low level of activity of the Na^+/H^+ (NHE) and the Cl^-/HCO_3^- anion exchanger. A high level of activity of the NHE pump may cause an accumulation of Na^+ ions in the cytoplasm.

In the case of MCF-7TaxR, lower cytoplasmic conductivity was obtained despite the overexpression of P-gp relative to the parent MCF-7. P-gp has been speculated to have different toplogical structures that are modulated by specific cytoplasmic factors (Zhang and Ling, 1995); another study (Luker et al, 2001) showed P-gp function is not affected by membrane potential in the same cell line. It is known that free cytoplasmic Mg^{2+} is removed by binding to ATP, RNA and by the Na^+/Mg^{2+} antiport (Wolfe, 1993). It is be possible that the overexpression of P-gp (an ATP driven pump) could result in the over-expenditure of the free Mg^{2+}, causing a deficit in the cytoplasm and reducing the overall ionic content, as it forms the basis of Na^+/Mg^{2+} pump function.

MCF-7DoxR showed significantly different MTT and Western immunoblotting results (Table 3.1, and Figure 3.10, respectively), showing 5 fold resistance and lacking the expression of P-gp. It was positive for the expression of BCRP, as was the parent MCF-7. The Western blot (Figure 3.11) indicated a similar level of

BCRP expression in both MCF-7 and MCF-7DoxR. Despite BCRP being a member of the ABC transporter family (formally designated ABCG2) it is not usually used as a marker for MDR in the same way as P-gp, and is expressed in some drug sensitive breast cancer cell lines. This is confirmed by the presence of BCRP in the drug sensitive (parent) MCF-7 (Figure 3.11). Furthermore, XR9576 is known to act on BCRP as well as P-gp (Robey et al, 2004), but treatment only marginally (17%) reversed resistance in MCF-7DoxR, indicating that only BCRP plays a small role in conferring resistance in MCF-7DxoR.

It has been noted in literature that not only does MDR involve the expression of different ABC proteins, but is also associated with drug sequestration and compartmentalisation inside vesicles and cytoplasmic organelles away from the target site (Sognier et al, 1994; Slapak et al, 1992; and reviewed in Dietel, 1991). Sognier and co-workers suggested the possibility of the simultaneous existence of multiple resistance mechanisms inside the same cell. The group found that the drug sequestration phenomenon correlates with the level of drug resistance and occurs rapidly following exposure to doxorubicin.

From the results obtained, it is evident that MCF-DoxR, grown in our study, operates a MDR mechanism that is non-P-gp related. It is therefore suggested that the MDR mechanism operating in these cells is that of drug sequestration and secretion. It has been reported that a MCF-7DoxR cell line has an alkaline cytoplasmic pH (Warburg, 1956; Simon and Schindler, 1994), while the vesicular pH is more acidic in resistant than sensitive cells. The change in the sensitive cells was also correlated with the disruption of the trans-Golgi network (TGN)

(Altenberg et al, 1993, Schindler et al, 1996, Altan et al, 1998, Belhoussine et al, 1999). Schindler et al (1996) explained that sensitive cells exhibited a diminished capacity to remove cytotoxic drugs from the cytoplasm by sequestration of protonated drugs within the vesicles. The group indicated that protonation, sequestration and secretion are the principal elements of the primary mechanism for doxorubicin resistance in MCF-7 breast cancer cell line.

Studies (Warburg, 1956; Simon and Schindler, 1994; Altenberg et, 1993; Schindler et al, 1996; Altan et al, 1998; Belhoussine et al, 1999 and reviewed in Larsen et al, 2000) have shown that the vesicular pH was more alkaline in the drug sensitive breast cancer cells (MCF-7) than the doxorubicin resistant breast cancer cells and normal healthy cells from the breast, while the cytoplasmic pH was acidic in the sensitive MCF-7. On the other hand, the cytoplasmic pH was more alkaline in the doxorubicin resistant cells and the normal breast cells relative to the sensitive MCF-7 cells (Figures 3.4B for a normal breast cell, 3.5A for the drug sensitive MCF-7 and 3.5B for the MDR doxorubicin resistant breast cancer cells). In the sensitive cells, the defect, as described by Larsen (2000) and Schindler et al, 1996, was correlated with disruption in the Golgi network and was due to a diminished capacity of cells to remove drugs from the cytoplasm.

Weak base drugs such as doxorubicin (pKa= 8.34, Raghunand and Gillies, 2000) may be expected to be protonated in the more acidic cytoplasm of drug sensitive cell lines, and sequestered in the more acidic vesicles of drug resistant cell lines (Wadkins and Roepe, 1997). The zwitterionic drug paclitaxel (Taxol), on the other hand has no ionisable groups (Raghunand and Gillies, 2000 and private

communication with Bristol-Myers Squibb, Nottingham, UK) and the cell may therefore adopt a different mechanism to resist this drug.

It has been suggested the some MDR cell lines overexpress a subunit of the vacular-type H^+ - ATPase (V-type) (Ma and Center, 1992). The plasma membrane V-ATPase activity and an increase in the rates of endosomal turnover have been reported in the MDR MCF-7 variants (Martinez-Zaguilan et al, 1993). As with K562AR, NHE overexpression may also play a role. These act to regulate the internal pH of the cytoplasm, as H^+ ions are either expelled from the cell or into vesicles, making cytoplasm more alkaline and the vesicles more acidic. Aharonovitz and co-workers suggested that NHE activity is very sensitively dependent of the intracellular and extracellular concentrations of Na^+ and H^+. They also found that NHE1 activity is modulated by Cl^-, where the interaction of the intracellular Cl^- and the carboxylic terminus of the NHE1 is essential for optimal activity. On the basis of this finding, it is possible that MCF-DoxR has a defect in this type of NHE due to the lack of P-gp. The lack of P-gp may imply a lower Cl^- concentration in cell, in turn causing an accumulation of the Na^+ ions in the cytoplasm.

The results collectively indicate the possibility for there being at least two mechanisms by which the cytoplasmic conductivity changes between MDR cells relative to parent cells. One mechanism is P-gp dependent, whereby the P-gp is acting as a Cl^- channel causing an influx of Cl^- into the cell and raising the cytoplasmic conductivity as it is in the case of K562AR relative to the parent. In the case of MCF-7TaxR, where P-gp is overexpressed but the cytoplasmic

conductivity is lower than the parent, the mechanism may be that P-gp is not acting as a Cl^- channel all the time, but acts as a Cl^- channel or a regulator of Cl^- channels and SUR (as reviewed in Wadkins and Roepe, 1997), as P-gp function is not affected by membrane potential (Luker et al, 2001). Another possibility is that of the deficit of Mg^{2+} ions in the cytoplasm as Mg^{2+} binds to ATP and the P-gp pumping action requires ATP expenditure. A third possibility may involve the overexpression of the vacular type H^+ -ATPase, which has been reported to be overexpressed in MDR breast cell line. This takes part in controlling the cytoplasmic pH by reducing the number of H^+ ions in the cytoplasm. If this ATPase is overexpressed, a reduction of the total cytoplasmic ionic content may be possible.

In the case of MCF-DoxR, cytoplasmic conductivities change is non - P-gp – dependent. Schindler et al (1996) indicated that protonation, sequestration and secretion are the principal elements of the primary mechanism of doxorubicin resistance in MCF-7 breast cancer cells. The same pattern for MCF-7 and MCF-7DoxR as well as K562 and K562AR, as well as TGN organisation and how the resistant cells showed a more compact and organised TGN, were shown by Belhoussine et al (1999).

A study by Aharonovitz et al (2001) reported Cl^- to be critical for the action of NHE and the ion modulates the action of NHE1. The lack of P-gp in MCF-7DoxR may imply a lower Cl^- if any. This defect may cause an accumulation of Na^+ in the cytoplasm, hence the high cytoplasmic conductivity.

Considering both K562AR and MCF-7DoxR together, results may indicate a potential defect in the NHE pumps both in K56AR and MCF-DoxR, resulting in Na^+ accumulation, and in the case of K562AR, the overexpression of P-gp could have the potential of having more Cl^- inside the cells, if P-gp is acting as a Cl^- channel. In MCF-7DoxR, however, the principal drug resistance mechanism is that of drug sequestration, lack of Cl^- could affect the activity of NHE, as Cl^- is crucial for NHE activity, so a defect could cause more Na^+ in the cytoplasm. As for MCF-7TaxR, though there is an overexpression of P-gp, it may only behave as a Cl^- regulator rather than a channel, thereby affecting the influx of Cl^- by deactivating the other Cl^- channels, resulting in a lower total ionic strength inside the cell.

The DEP results have interestingly demonstrated how two different cell lines of the same parent drug sensitive cell line can have a dramatically differing dielectric properties. This is evident in the cytoplasmic conductivities of MCF-7TaxR and MCF-7DoxR (0.14 and 0.40 S/m, respectively) (Tables 3.6, 3.7, respectively), relative to the parent (0.23 S/m). Also, around 30% increase in the specific membrane capacitance was seen in MCF-7TaxR relative to MCF-7DoxR (8.3 and 6.4 mF/m^2) if compared to the slightly lower specific capacitance of the parent MCF-7 (6.0 mF/m^2), indicating possible membrane morphology differences.

3.4.2. Effects of MDR modulation

Using the membrane potential sensitive dye (DIOC5) K562 had a much higher fluorescence emitted, producing a more pronounced shift to the right (Figure 3.15) in comparison to the K562AR peak (with GM values of 124.04 and 36.42, respectively). In the case of the breast cancer cell lines, a similar pattern was seen, whereby MCF-7 had a much higher fluorescence than the resistant counterpart, MCF-7TaxR (83.87) (Figure 3.16). This, according to the work of Vayuvegula et al (1988) indicates a higher membrane potential in the parent cells K562 and MCF-7 relative to their resistant counterparts K562AR and MCF-7TaxR. The modulator XR9576 did not have an effect on the green fluorescence intensity in the parent cells, with GM values remaining more or less the same before and after treatment with XR9576. On the other hand, the use of XR9576 with the MDR cell lines produced a pronounced increase in the fluorescence emitted relative to that before treatment. K562AR had a GM of 36.42 and 491.15, before and after treatment, respectively (Figure 3.15). A similar, yet less dramatic effect was seen in MCF-7TaxR, as it had a GM of 83.87 and 162.44, before and after treatment, respectively (Figure 3.16). It can be seen from the DEP data in Table 3.5 that the drug sensitive K562 appears to exhibit a lower cytoplasmic conductivity (0.23 S/m) than its MDR counterpart K562AR (0.50 S/m), before and after treatment with XR9576. This indicates different ionic strengths or content in the cytoplasm of the parent cells compared to MDR cells. Conversely, MCF-7 parental cells exhibited a higher cytoplasmic conductivity (0.23 S/m) relative to their MDR counterpart, MCF-TaxR (0.14 S/m). Furthermore, there was a notable difference in the trends for the specific membrane capacitance of these breast cancer cell lines. Whilst K562 (3.9 mF/m^2) and K562AR (3.5 mF/m_2) displayed

no differences in their specific membrane capacitance, MCF-7 had a lower specific membrane capacitance of (6.0 mF/m^2) relative to MCF-7TaxR (8.3 mF/m^2). Specific membrane capacitance is related to membrane permittivity and surface area but is independent of membrane thickness, so that changes in membrane morphology (e.g. blebbing or foldings which alter surface area) cause changes in the specific capacitance. In the case of MCF-7TaxR (Table 3.6), the capacitance has increased, indicating differences in the membrane morphology, possibly due to more membrane foldings (Wang et al, 2002).

In spite of the presence of P-gp in both K562AR and MCF-7TaxR, the DEP results for K562AR indicate that the electrical properties remained largely the same after treatment with XR9576 in both parental K562 and the resistant counterpart K562AR. In the case of MCF-7TaxR, the specific membrane capacitance increased after XR9576 modulation to 10.5mF/m^2, giving more than 25% increase relative to MCF-7TaxR before treatment (8.3mF/m^2). This possibly indicates that XR9576 has caused changes in the membrane morphology such as foldings after treatment.

On the other hand, K562 exhibited a significantly lower cytoplasmic conductivity than K562AR (0.23 S/m *versus* 0.50 S/m, respectively) (Table 3.5) indicating a lower cell ionic content, while the reverse was seen for MCF-7 relative to MCF-7TaxR (0.23 and 0.14 S/m, respectively) (Table 3.6). Thus, these data have discriminated the cell lines according to their different dielectric properties. DEP has, therefore, brought attention to differences in the cytoplasm, a part of the cell that is not often considered in MDR.

By comparing the results obtained from DEP and flow cytometry, it can be seen that DEP results clearly do not agree with those obtained by flow cytometry. However, examination of these differences can yield useful information. The DEP results showed that neither the cytoplasmic nor the membrane parameters were altered in the presence of XR9576 for K562AR, but the membrane specific capacitance changed and increased for MCF-7TaxR (Table 3.6); in spite of P-gp expression. However, flow cytometry data (Figure 3.15), suggested an increase in membrane potential following modulator treatment for K562AR and MCF-7TaxR. This contradictory result may indicate that without the modulator, the P-gp could be pumping DIOC5 dye out of the cell, giving an artefactual result.

The contradictory results can be resolved if XR9576 is considered to be blocking the P-gp pump and thus preventing the efflux of the dye. In this regime, the fluorescent dye entering the membrane of the drug-resistant cells was pumped out, resulting in an artificially low fluorescence and implied low membrane potential. When P-gp is blocked, this pumping action does not occur and the high fluorescence level truly reflects the high cytoplasmic ionic strength. This resolves the differences between the two results, and also highlights the P-gp blocking effect of the XR9576 compound. This mechanism of action is illustrated in Figure 3.17 overleaf.

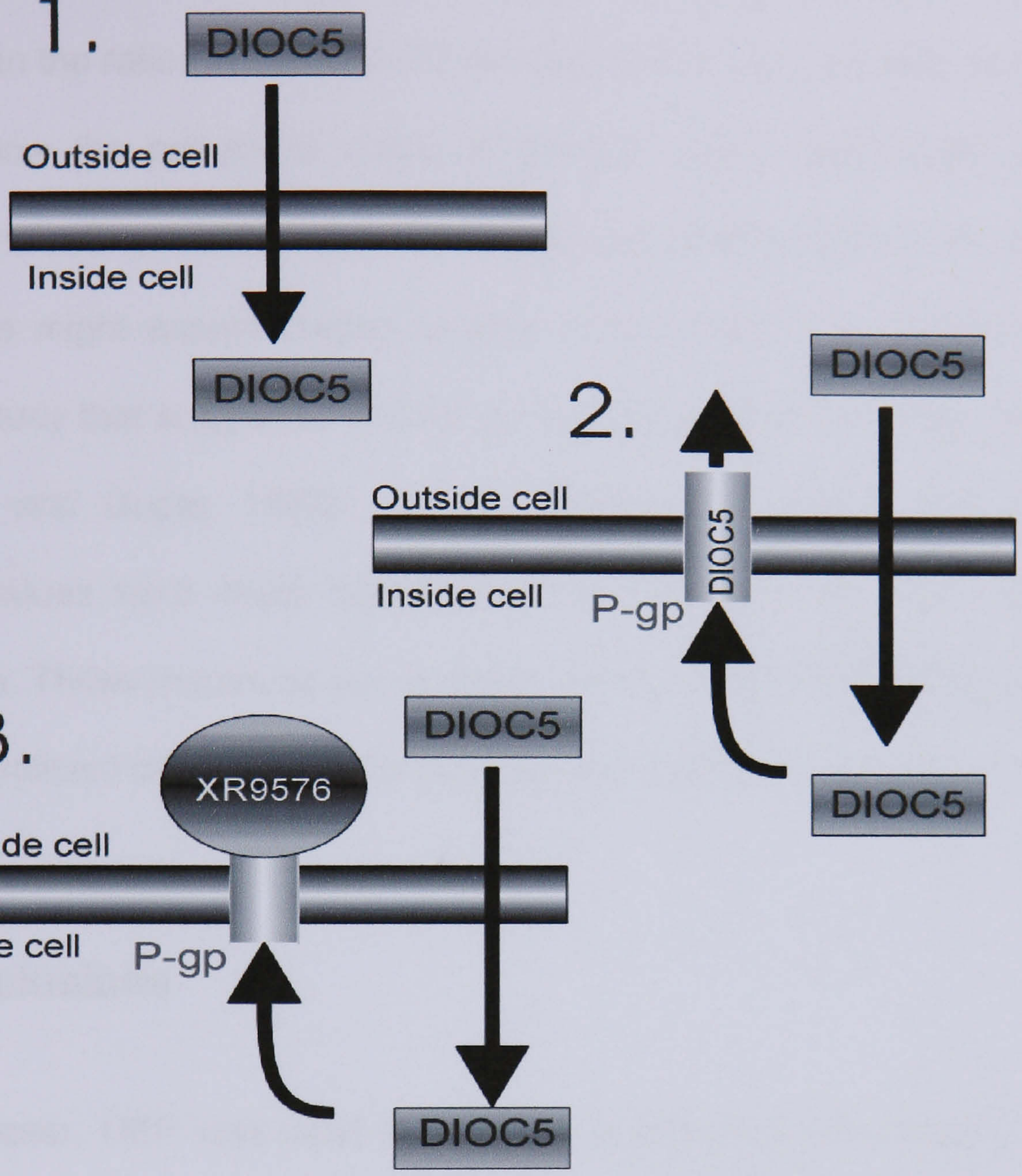

Figure 3.17: The mechanism proposed for P-gp. (1) A drug sensitive cell, where DIOC5 dye permeates the membrane, thus giving a high level of fluorescence (indicative of membrane potential) (2) A drug resistant cell prior to XR9576 treatment; DIOC5 permeates the membrane, but is then expelled from the cell via P-glycoprotein, thus giving an artefactually low level of fluorescence (indicating low membrane potential) (3) A drug resistant cell subsequent to XR9576 treatment, hence XR9576 blocks P-glycoprotein and therefore prevents DIOC5 from being extruded, thus giving rise to increased cellular fluorescence relative to (2)-increased, true membrane potential.

When the pump is blocked, we suggest that as the DIOC5 is no longer efluxed, flow cytometry gives an accurate reading of the membrane potential. Notably, the trends in the ratios of cytoplasmic conductivity for parental and resistant lines closely follow the pattern of ratios of the GM values and hence membrane potential, indicating that the membrane potentials and cytoplasmic conductivities are as one might expect closely related. This finding is in agreement with a previous study that suggested DIOC5 as being a substrate for ABC transporters (Gollapudi and Gupta, 1992). In the presence of XR9576, the membrane potential values were much higher than that seen for those cell lines before modulation. These results do not coincide with the DEP data obtained, as there was no significant difference in the biophysical properties after treatment.

3.5. Conclusions

In this chapter, DEP was used to reveal any dielectric differences in resistant MDR chronic myelogenous leukaemia (K562AR) and breast cancer (MCF-7TaxR and MCF-7DoxR) cell lines relative to the parent drug sensitive cell lines. The results obtained point to significant differences in the cytoplasmic ionic content with no significant differences seen in the membrane parameters. However, the change in polarisation state differs in the leukaemic cell lines; K562AR is hyperpolarised relative to K562, whilst MCF-7TaxR is depolarised and MCF-7DoxR hyperpolarised in comparison to the parental line, MCF-7. The results suggest that these dielectric changes are due to different cellular processes and/ or mechanisms. Two mechanisms have been suggested, one of which is P-gp dependent and relies on the pump acting as a Cl^- channel, as in K562AR. It is

worth noting that the dielectric changes may not be P-gp related. MCF-7TaxR showed an evident overexpression of P-gp, but we suggest that it is behaving more like a regulator, which could imply a deactivating role in the Cl^- channels, possibly resulting in a reduction of the total ionic content and the lower cytoplasmic conductivity relative to the parent. The third mechanism is non- P-gp –dependent, as in MCF-7DoxR, where the principal mechanism of drug resistance is that of drug sequestration and vesicular trafficking, the cytoplasmic conductivity was higher than the parent. This MDR cell line lacked the expression of P-gp, and the potential mechanism of this might involve a defect in the Na^+/H^+ ATPase (NHE), resulting in the accumulation of Na^+ in the cytoplasm. This warrants further research with regards to the presence and activity of the channels, such as P-gp, Cl^- channels and NHE pumps.

We have also shown that DEP can be used as a technique to probe any biophysical differences between cell lines before and after modulation. XR9576, a P-gp specific modulator did not exert any effects on the cytoplasm or membrane parameters in K562 and K562AR, but altered the membrane morphology in MCF-7TaxR after treatment. Our data, therefore, show no significant changes in the biophysical properties of drug sensitive or drug resistant cancer cells following modulator therapy, with the exception of MCF-7TaxR. There has been a disparity between DEP and flow cytometry results. DEP and flow cytometry in combination indicated that DIOC5 is a substrate for P-gp. Furthermore, DEP has provided a more informative and a rigorous approach in revealing that it is the cytoplasm that varies between MDR and drug

sensitive cells. The study has demonstrated the application of DEP as a novel approach to aid a better understanding of the MDR phenotype in cancer cells.

3.6. References

Abraham, J. Edgerly, M. Wilson, R. et al. A phase I study of the novel P-glycoprotein (Pgp) antagonist, XR9576 in combination with vinorelbine. (2001) *Proceedings of the Annual Meeting of the American Association for Clinical Oncologists*, **20**: 287.

Aharonovitz, O. Kapus, A. Szaszi, K. et al. Modulation of Na^+/H^+ exchange activity by Cl^- (2001) *American Journal of Physiology*, **281**: C133-C141.

Altan, N. Chen, Y. Schindler, M. et al. Defective acidification in human breast tumour cells and implications for chemotherapy (1998) *Journal of Experimental Medicine*, **187**: 1583-1598.

Altenberg, G.A. Vanoye, C.G. Han, E.S. et al. Relationships between rhodamine-123 transport, cell volume, and ion channel function of P-glycoprotein (1994) *Journal of Biological Chemistry*, **269** (10): 7145-7149.

Altenberg, G.A. Young, G. Horton, J.K. et al. Changes in intra- or extracellular pH do not mediate P-glycoprotein-dependent multidrug resistance (1993) *Proceedings in the National Academy of Science USA*, **90**: 9735-9738.

Bakewell, D.J. Morgan, H. Measuring the frequency dependent polarisibility of colloidal particles from dielectrophoretic collection data (2001) *IEEE transactions on dielectric and electrical insulation*, **8** (3): 566-571.

Bates, S. Kang, M. Meadows, B. et al. A phase I study of infusional vinblastine in combination with the P-glycoprotein antagonist PSC 833 (valspodar). (2001) *Cancer*, **92**: 1577-1590.

Belhoussine, R. Morjani, H. Sharonov, S. et al. Characterisation of intracellular pH gradients in human multidrug resistant tumour cells by means of scanning microspectrofluorometry and dual emission ratio probes (1999) *International Journal of Cancer*, **81**: 81-89.

Brett, C.L. Wei, T. Donowitz, M. et al. Human Na^+/H^+ exchanger isoform 6 is found in recycling endosomes of cells, not in mitochondria (2002) *American Journal of Physiology- Cell Physiology*, **282**:C1031-1041.

Burt, J. Gascoyne, P.R.C. Becker, F. Dielectrophoretic characterisation of friend murine erythroleukaemic cells as a measure of induced differentiation. (1990) *Biochimica et Biophysica Acta*, **1034**: 93-101.

Cole, SPC. Bhardwaj, G. Gerlach, J.H. et al. Overexpression of a transporter gene in multidrug-resistant human lung cancer cell line (1992) *Science* **258** (5088): 1650-1654.

Dano, K. Active outward transport of daunomycin in resistant ehrlich ascites tumor cells (1973) *Biochemica et Biophysica Acta*, **323**, 466-483.

Dantzig, A.H. Shepard, R.L. Law, K.L. et al. Selectivity of the multidrug resistance modulator, LY335979, for P-glycoprotein and effect on cytochrome P-

450 activities. (1999) *Journal of Pharmacology and Experimental Therapeutics*, **290** (2): 854-862.

De Luise, M. Blackburn, G.L. Flier, J.S. Reduced activity of the red cell sodium pump in human obesity (1980) *New England Journal of Medicine*, **303** (18): 1017-1022.

Dietel, M. What's new in cytostatic drug resistance and pathology (1991) *Pathology Research Practice*, **187**: 892-905.

Ferry, D. Price, L. Atsmon, J. et al. A phase IIa pharmacokinetic and pharmacodynamic study of the P-glycoprotein inhibitor, XR9576 in patients treated with doxorubicin chemotherapy. (2001), *Proceedings of the Annual Meeting of the American Association for Cancer Research* **42**: 950.

Fischer, V. Rodriguez-Gascon, A. Heitz, F. et al. The multidrug resistnace modulator valspodar (PSC 833) is metabolised by human cytochrome P450 3A: implications for drug-drug interactions and pharmacological activity of the main metabolite. (1998) *Drug metabolism and disposition*, **26**: 802-811.

Gadsby, D.C. Nairn, A.C. Regulation of CFTR Cl- ion channels by phosphorylation and dephosphorylation (1999) *Advances in second messenger and phosphoprotein research*, **33**: 79-106.

Gascoyne PRC, Wang XB, Huang Y et al. Dielectrophoretic separation of cancer cells from blood.(1997) *IEEE Transactions on industry applications*, **33** (3): 670-678.

Gill, D.R. Hyde, S.C. Higgins, C.F. et al. Separation of drug transport and chloride channel functions of the human multidrug resistance P-glycoprotein (1992) *Cell*, **71** (1):23-32.

Gollapudi, S. Gupta, S. Lack of reversal of daunorubicin resistance in HL60/AR cells by cyclosporine A. (1992) *Anticancer Research*, **12** (6B): 2127-2132.

Gottesman, M.M. Fojo, T. Bates, S.E. Multidrug resistance in cancer: role of ATP-dependent transporters. (2002) *Nature Reviews Cancer*, **2**: 48-58.

Gottesman, M.M. Pastan, I. The multidrug transporter, a double-edged sword. (1988) *Journal of Biological Chemistry*, **263**, 12163 – 12166.

Griffith, A.W. Cooper, J.M. Single cell measurements of human neutrophil activation using electrorotation. (1998) *Analytical Chemistry*, **70** (13): 2607-2612.

Hardy, S.P. Goodfellow, H.R. Valverde, M.A. et al. Protein kinase C mediated phosphorylation of the human multidrug resistance P-glycoprotein regulates cell volume-activated chloride channels (1995) *European Molecular Biology Organisation (EMBO) Journal*, **14**: 68-75.

Huang, Y. Hölzel, R. Pethig, R. et al. Differences in the AC electrodynamics of viable and non viable yeast cells determined through combined dielectrophoresis and electrorotation studies. (1992) *Physics in Medicine and Biology*, **37**: 1499-1517.

Hübner, Y. Hoettges, K.F. Hughes, M.P. Water quality test based on dielectrophoretic measurements of fresh water algae Selenastrum capricornutum (2003) *Journal of Environmental Monitoring*, **5** (6): 861-864.

Hughes, M.P. Morgan, H. Rixon, F.J. Dielectrophoretic manipulation and characterisation of herpes simplex virus-1 capsids (2001) *European Biophysical Journal*, **30**(4): 268-272.

Hughes, M.P. Morgan, H. Rixon, F.J. et al. Manipulation of herpes simplex virus type 1 by dielectrophoresis (1998) *Biochemica et Biophysica Acta*, **1425**(1): 119-126.

Hughes, M.P. Morgan, H. Rixon, F.J. Measuring the dielectric properties of herpes simplexvirus type 1 virions with dielectrophoresis (2002) *Biochemica et Biophysica Acta*, **157**1(1): 1-8.

Irimajiri, A. Hanai, T. Inouye, V.A. Dielectric theory of "multi-stratified shell" model with its application to lymphoma cell. (1979) *Journal of Theoretical Biology*, **78**: 251-269.

Ishikawa, T. Tien Kuo, M. Furuta, K. et al. The human multidrug resisitnace associated protein (MRP) gene family: from biological function to drug molecular design (2000) *Clinical Chemistry and Laboratory Medicine*, **38** (9): 893-897.

Jirsch, J. Deeley, R.G. Cole, S.P.C. et al. Inwardly rectifying K^+ channels and volume regulated anion channels in multidrug resistant small cell lung cancer cells (1993) *Cancer Research*, **53**(18): 4156-4160.

Johari, J. Hübner, Y. Hull, J.C. et al. Dielectrophoretic assay of bacterial resistance to antibiotics. (2003) *Physics in Medicine and Biology*, **48** (14): N193-N198.

Juliano, R.L. and Ling V. A surface glycoprotein modulating drug permeability in Chinese hamster ovary cell mutants (1976) *Biochemica et Biophysica Acta*, **255**, 152-162.

Kim, J.H. Lingwood, C.A. Williams, D.B. et al. Dynamic measurement of the pH of the Golgi complex in living cells using retrograde transport of the verotoxin receptor (1996) *Journal of Cell Biology*, **134**: 1387-1399.

Krishna, R. Mayer, L.D. Multidrug Resistance (MDR) in cancer:Mechanisms, reversal using modulators of MDR and the role of MDR modulators in influencing the pharmacokinetics of anticancer drugs. (2000) *European Journal of Pharmacological Science*, **11**: 265-283.

Larsen, A.K. Escargueli, A.E. Skaldanowski, A. Resistance mechanisms associated with altered intracellular distribution of anticancer agents (2000) *Pharmacology &Therapeutics*, **85**: 217-229.

Luker, G.D. Flagg, T.P. Sha, Q. et al. MDR1 P-glycoprotein reduces influx of substrates without affecting membrane potential (2001) *The Journal of Biological Chemistry*, **276** (52): 49053-49060.

Ma, L. and Center, M.S. The gene encoding the vacular H+ - ATPase subunit C is overexpresed in multidrug resistant HL-60 cells (1992) Biochemical and Biophysical Research Communications, **182** (2): 675-681.

Marquardt, D. and Center, M.S. Involvement of vacuolar H^+ adenosine triphosphate activity in multidrug resistance in HL-60 cells. (1991) *Journal of the National Cancer Institute*, **83**: 1098-1102.

Martin, C. Berridge, G. Mistry, P. et al. The molecular interaction of the high affinity reversal agent XR9576 with P-glycoprotein. (1999) *British Journal of Pharmacology*, **128** (2): 403-411.

Martinez-Zaguilan, R. Lynch, R.M. Martinez, G.M. et al. Vacuolar type H+-ATP-ases are functionally expressed in plasma membranes of human tumour cells (1993) *American Journal of Physiology*, **265**: C1015-C1029.

Mistry, P. Stewart, A.J. Dangerfield, W. et al. In vitro and in vivo reversal of P-glycoprotein-mediated multidrug resistance by a novel potent modulator, XR9576. (2001) *Cancer Research*, **61** (2): 749-758.

Mosmann, T. Rapid colorimetric assay for cellular growth and survival-application to proliferation and cytotoxicity assays. (1983) Journal of Immunological Methods, **65**: 55-63.

Pinedo, H. M., Giaccone, G. P-Glycoprotein - A Marker of Cancer-Cell Behaviour (1995).*New England Journal of Medicine* **333**: 1417-1419.

Pohl, H. Dielectrophoresis. (1978), Cambridge University Press, Cambridge.

Raghunand, N. Gillies, R.J. pH and drug resistance in tumours (2000) *Drug Resistance Updates* **3**: 39-47.

Robey, R.W. Steadman, K. Polgar, O. et al. Pheophorbide a is a specific probe for ABCG2 function and inhibition (2004) *Cancer Research*, **64**(4): 1242-1246.

Roe, M. Folkes, A. Ashworth, P. et al. Reversal of P-glycoprotein- mediated multidtug resistance by a novel anthranilamide dervivatives. (1999) *Bioorganic & Medicinal Chemistry Letters*, **9** (4): 595-600.

Roepe,P.D. Wei, L.Y. Cruz, J. et al. Lower electrical membrane potential and altered pHi homeostasis in multidrug resistant (MDR) cells: further characterisation of a series of MDR cell lines expressing different levels of P-glycoprotein (1993) *Biochemistry*, **32**: 11042-11056.

Rowinsky, E.K. Smith, L. Wang, Y.M. et al. Phase I and pharmacokinetic study of paclitaxel in combination with biricodar, a novel agent that reverses multidrug resistance conferred by overexpression of both MDR1 and MRP. (1998) *Journal of Clinical Oncology*, **16** (9): 2964-2976.

Scheper RJ, Broxterman HJ, Sheffer GL et al. Overexpression of a M(r) 110,000 vesicular protein in non-P-glycoprotein mediated multidrug resistance (1993) *Cancer Research*, **53** (7): 1475-1479.

Schindler, M. Grabski, S. Hoff, E. et al. Defective pH regulation of acidic compartments in human breast cancer cells (MCF-7) is normalised in Adriamycin-resistant-resistant cells (MCF-7adr) (1996) *Biochemistry*, **35**: 2811-2817.

Schinkel,AH. Smit, JJ. Van Tellingen, O. et al Disruption of mouse mdr1a p-glycoprotein gene leads to a deficiency in the blood-brain barrier and to increased sensitivity to drugs (1994) *Cell*, **77**: 491-502.

Seksek, O. and Bolard, J. Nuclear pH gradient in mammalian cells revealed by laser microspectrofluorimetry (1996) *Journal of Cell Science*, **109**: 257-262.

Seksek, O. Biwersi, J. and Verkman, A.S. Direct measurement of trans-Golgi pH in living ells and regulation by second messengers (1995) *Journal of Biological Chemistry*, **270**: 2967-4970.

Simon, S.M. Schindler, M. Cell biological mechanisms of multidrug resistance in tumors (1994) *Proceedings of the national Academy of the United States of America*, **91** (9): 3497-3504.

Slapak, C.A. Lecerf, J-M. Daniel, J.C. et al. Energy dependent accumulation of daunorubicin into subcellular compartments of human leukaemia cells and cytoplasts (1992) *The Journal of Biological Chemistry*, **267** (15): 10638-10644.

Sognier, M.A. Zhang, Y. Eberle, R.L. et al. Sequesteration of doxorubicin in vesickes in a multidrug resistant cell line (LZ-100) 1994 *Biochemical Pharmacology*, **48** (2): 391-401.

Stewart, A. Steiner, J. Mellows, G. et al. Phase I trial of XR9576 in healthy volunteers demonstrates modulation of P-glycoprotein in CD56+ lymphocytes after oral and intravenous administration. (2000) *Clinical Cancer Research*, **6** (11): 4186-4191.

Teboekhorst, P.A. van Kapel, J. Schoester, M. et al. Reversal of typical multidrug resistance by cyclosporine and its non-immunosuppressive analogue SDZ PSC833 in Chinese hamster ovary cells expressing mdr1 phenotype. (1992) *Cancer Chemotherapy and Pharmacology*, **30**: 238-242.

Thomas, H. Coley, H. Overcoming multidrug resistnace in cancer: An update on the clinical strategy of inhibiting P-Glycoprotein. (2003) *Cancer control*, **10** (2): 159-165.

Thomas, H. Steiner, J.A. Mould, G.P. et al. A phase IIa pharmacokinetic study of the P-glycoprotein inhibitor, XR9576, in combination with Paclitaxel in patients with ovarian cancer. (2001) *Proceedings of the Annual Meeting of the American Association for Clinical Oncologists*, **20**: 288.

Twentyman, P.R. Bleechen, N.M. Resistance modification by PSC-833, a novel non-immunosuppressive cyclosporine A. (1991) *European Journal of Cancer*, **27**: 1639-1642.

Valverde, MA. Diaz, M. Sepulveda, F.V. et al. Volume-regulated chloride channels associated with the human multidrug-resistance P-glycoprotein (1992) *Nature*, **355** (6363): 830-833.

van Zuylen, L. Nooter, K. Sparreboom, A. et al. Development of multidrug resistance convertors: sense or nonsense? (2000) *Investigational New Drugs*, **18** (3): 205-220.

Vayuvegula, B. Slater, L. Meador, J. et al. Correction of altered plasma membrane potentials- a possible mechanism of cyclosporine A and verapamil reversal of pleiotropic drug resistance in neoplasia. (1988) *Cancer Chemotherapy and Pharmacology*, **22** (2): 163-168.

Wadkins, R.M. Roepe, P.D. Biophysical aspects of P-glycoprotein-mediated multidrug resistance (1997) *International Review of Cytology*, **171**: 121-165.

Wang, X. Becker, F.F. Gascoyne, P.R.C. membrane dielectric changes indicate induced apoptosis in HL60 cells more sensitively than surface phosphatidylserine expression or DNA fragmentation. (2002) *Biochimica et Biophysica Acta*, **1564**: 412-420.

Warburg, O. On the origin of cancer cells (1956) *Science* **123**:309-14.

Welsh, M.J. Anderson, M.P. Rich, D.P. et al. CFTR: a chloride channel with novel regulation (1992) *Neuron*, **8**: 821-829.

Wolfe, S.L. Molecular and cellular biology (1993), Wadsworth Publishing Company, Belmont, California.

Yanagisawa, T. Newman, A. Coley, H. et al.Biricodar (vx-710; incel): an effective chemosensitiser on neuroblastoma. (1999) *British Journal of Cancer*, **80**: 1190-1196.

Yang, J. Huang, Y. Wang, X.B. et al. Dielectric properties of human leukocytes subpopulations determined by electrorotation as a cell separation criterion. (1999) *Biophysical Journal*, **76**: 3307-3314.

Zhang, J.T. Ling, V. Involvement of cytoplasmic factors regulating the membrane orientation of P-glycoprotein sequences (1995) *Biochemistry*, **34** (28): 9159-9165.

4. A rapid assay of apoptotic progress in a mixed population by dielectrophoresis (DEP)

4.1. Introduction

Apoptosis is a process that plays a critical role in the embryonic stage of development and tissue homeostasis. In humans dysfunction of this process has been linked to pathogenesis of cancer and other diseases (Thompson, 1995). The term was first described by Kerr et al (1972) in a landmark paper in which they described the morphological features of cell death during development and tissue homeostasis characterised by nuclear and cytoplasmic shrinkage. They termed this process 'apoptosis' (derived from the Greek word meaning 'falling off', as of autumn leaves from a tree). Before the term was coined, this mode of cell death was referred to as 'shrinkage necrosis'.

Initially, it was generally accepted that all programmed cell deaths were of apoptotic morphology, whilst accidental, non-physiological passive cell death displayed features of what was called cell necrosis (from the Greek word for 'dying') or defined by Majno and Joris (1995) as oncosis (from the Greek word *onkos*, meaning swelling). This classification of cell death has made crucial contribution into the research of programmed cell death and providing clear-cut morphological clues to study the mechanisms behind cell death. Recently, it has been suggested (Hughes and Mehmet, 2003) that necrotic cell death also occurs during normal cell physiology and development and necrotic-like cell death is also regulated by a cellular intrinsic death programme.

The morphological changes in apoptotic and necrotic cells have been described (Hughes and Mehmet, 2003), where in apoptotic cells the main changes occur in the nuclear compartment with initial marked condensation in the chromatin. This is accompanied by convolution in the nuclear and cellular outlines and nuclear fragmentation. Surface protuberances separate from the plasma membrane and then re-seal to form membrane-*bound apoptotic bodies* that may or may not contain nuclear fragments. Due to cell shrinkage, the cell also loses its normal cell contacts and some surface elements, such as microvilli and cell-cell junctions, well before cellular budding and fragmentation takes place. Nuclear and cytoplasmic fragmentation is restricted in cells with a high nucleo-cytoplasmic ratio, such as thymocytes. Significantly, these apoptotic bodies were not found to provoke inflammation, but are phagocytosed by adjacent healthy cells or by professional phagocytes (Hughes and Mehmet, 2003).

In necrotic cell death, the most prominent feature is the early disruption of the plasma membrane and the spilling of the contents to the surrounding. Swelling of necrotic cells and disintegration of the cytoplasmic organelles are apparent microscopically. The mitochondria become swollen and often contain granular densities, while ribosomes detach from their associated membranes. The chromatin in the nucleus condenses and ill-defined patches occur close or occupy the entire area in the nuclear membrane in apoptotic cells. At late stages of cell necrosis the chromatin disappears, an event called karyolysis. As opposed to the swelling in necrotic cells, there is a marked shrinkage in the apoptotic cells due to the extrusion of ions and contraction of the cytoskeleton (Hughes and Mehmet, 2003).

If we consider in more detail the events in the cell that mediate apoptosis, we find that the mitochondrion plays an important role. In the mid-1990s, speciallised caspases were discovered and were found to be responsible for apoptotic morphology, drawing increased interest towards the cytoplasmic events seen towards the later stages of apoptosis.

The mitochondrion has now become the centre of death control, as it controls the release of multiple death-triggering proteins that lead to the execution phase of apoptosis (as reviewed in Green and Reed, 1998). Among these proteins is cytochrome *c*, but there are also other important proteins, summarised in Figure 4.1. The mitochondrion also contains pro-caspases which are released into the cytosol during apoptosis (such as pro-caspases-3, -2 and –9), as suggested by Hughes and Mehmet (2003). In addition to the liberation of pro-apoptotic factors and activation of the caspase cascade, a typical early characteristic of apoptosis is mitochondrial membrane permeabilisation followed by dissipation of the mitochondrial transmembrane potential ($\Delta\psi_m$). This potential is due to the asymmetric distribution of protons and other ions on either side of the inner mitochondrial membrane, which gives rise to a chemical (pH) and an electrical gradient, both of which are essential for the function of the mitochondria, for example in ATP synthesis. Disruption of $\Delta\psi_m$ has been detected in cells undergoing apoptosis, indicating pemeability transition pore (PT) opening. However, the exact relationship (such as cause or consequence) between $\Delta\psi_m$ and release of apoptotic factors is still a matter of debate.

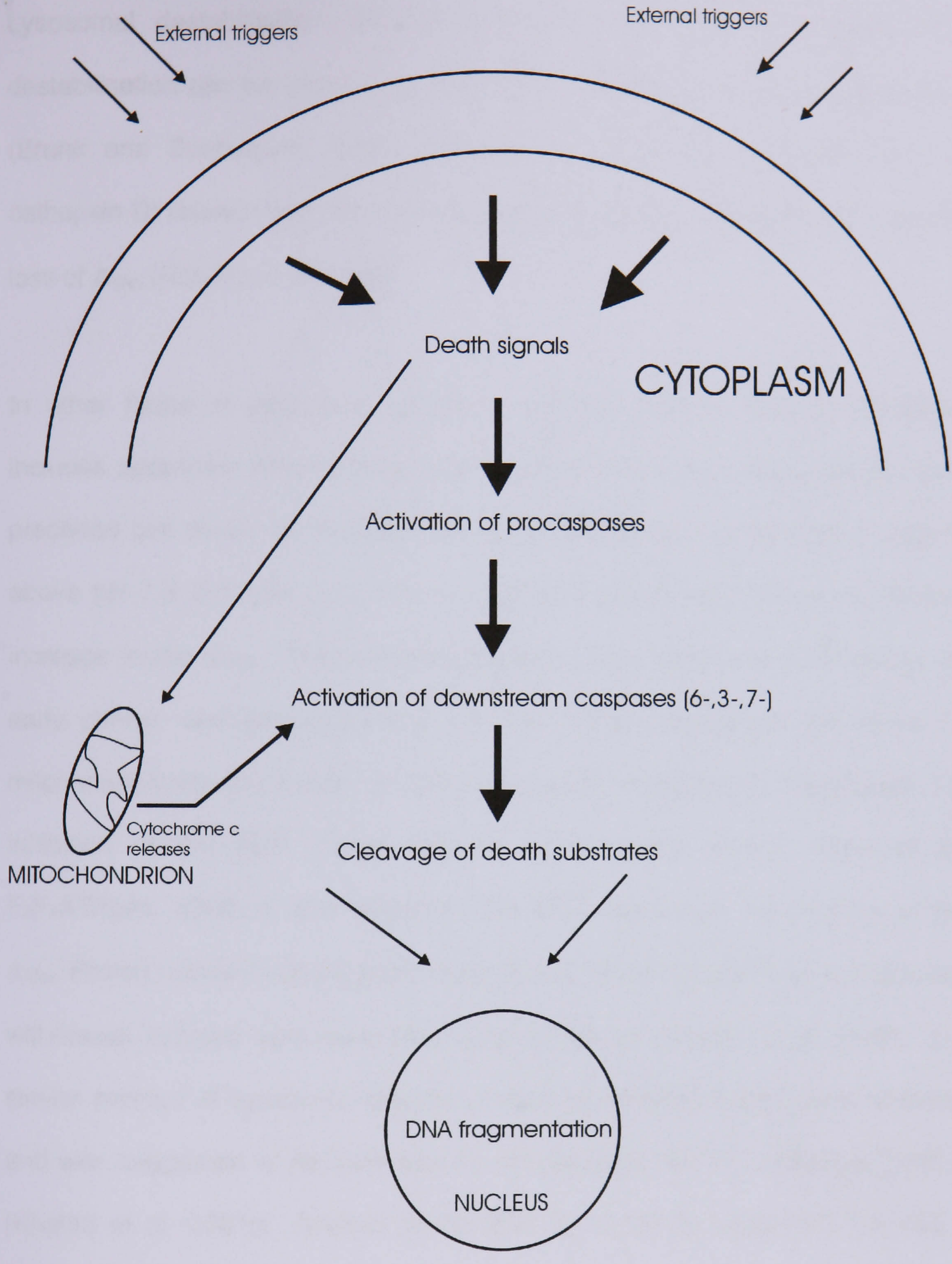

Figure 4.1: A schematic of the factors involved in the apoptotic cascade, the external triggers can include heat shock, infection or drug treatment such as staurosporine. Procaspases can include 8, 9 and 10.

Lysosomal destabilisation also plays an important role in apoptosis. The destabilisation can be initiated by a number of factors, such as oxidative stress (Brunk and Svenssson, 1999). Interestingly, lysosomal proteases (such as cathepsin D) release was found to precede the release of cytochrome c and the loss of $\Delta\psi_m$ (Roberg et al, 1999).

In other forms of apoptosis induction, such as that of cytokine withdrawal includes apoptosis, Khaled et al (2001a) found that early stress-related events preceded cell death. Intracellular rise in pH (alkalinisation) took place peaking above pH 7.8 2-3 hour post interleukin-3 withdrawal, and induced a transient increase in the $\Delta\psi_m$. The authors noticed a sharp decline of ATP during this early period, and suggested that the rise in the intracellular pH inhibit the mitochondrial import of ADP, which consequently limits the ATP synthesis. The inhibition of the ADP import into the mitochondria, in turn reverses the F_0F_1ATPase, which in turn consumes the ATP and pumps out protons, raising $\Delta\psi_m$. Proton outward pumping and the inactivity of the F_0F_1ATPase, in a cytokine withdrawal induced apoptosis, was reported earlier (Khaled et al, 1999). In a similar method of apoptosis induction, intracellular alkalinisation was observed and was suggested to be mediated by pH regulator Na^+/H^+ exchanger (NHE1) (Khaled et al, 2001b). Another study (Kim et al, 2003) suggested the rise in cytosolic pH to be mediated by the Cl^-/HCO_3^- anion exchanger, where Cl^- ions are moving out in exchange for HCO_3^- ions moving in.

The ionic influx/efflux plays an important role in apoptosis and some ions mediate the change in cell volume. The principle ion in question is K^+, where its

intracellular concentration has been widely reported to be diminished during the apoptotic process. K^+ is pumped out of the cell and cell shrinkage takes place, and the role of this ion is pivotal in the cell death programme (Bortner et al, 1997; Yu et al, 1997; Yu et al, 1999). Also, a transient increase in intracellular Na^+ has been reported prior to the loss of cell volume (Bortner and Cidlowski, 2003). An increased generation of reactive oxygen species has been reported (Li et al, 1999), which leads to the transient increase in $\Delta\psi_m$. At later stages of apoptosis, the $\Delta\psi_m$ was found to decrease as the mitochondria depolarises. In these late stages, massive Ca^{2+} influx takes place (Dallaporta et al, 1998), as well as mitochondrial swelling prior to cell lysis (Wyllie et al, 1980). Furthermore, alterations in Ca^{2+} signalling can affect the survival and functioning of cells reviewed by Kass and Orrenius (1999). Table 4.1 summarises the sequence of events associated with apoptosis described above, based on the information cited in the literature.

In this chapter, we examine the use of DEP to shed light on these findings by looking at the changes in the dielectric properties over a period of 48 hours following induction of apoptosis in K562 cells using staurosporine. A study by Wang et al (2002) demonstrated the use of DEP in detecting changes in membrane dielectric properties of cultured human promyelocytic leukaemia (HL-60) during the early stages of apoptosis after treatment with genistein. We extended this by examining changes in both the cytplasm and membrane over longer incubation periods with staurosporine, and demonstrate that a broader range of effects can be observed.

Event	Reference
1) Alkalinisation, as pH ↑, ADP import is inhibited, limited ATP synthesis in mitochondria, inactivation of F_0F_1ATPase and protons are pumped out.	Khaled et al, 1999 and 2001a
The ↑ in pH was mediated by the activation of NHE1.	Khaled et al, 2001b
The ↑ in pH also mediated by the Cl^-/HCO_3^- anion exchanger (Cl^- out) and (HCO_3^- in).	Kim et al, 2003
A transient increase in Na^+	Bortner and Cidlowski, 2003
Membrane capacitance declines	Wang et al, 2002
2) ↑ K^+ efflux, cell shrinks, phosphatidyl serine residues exposed	Bortner et al, 1997; Yu et al, 1997; Dallaporta, 1998; Yu et al, 1999
3) ↑ reactive oxygen species	Li et al, 1999
4) At later stages, $\Delta\psi_m$ depolarises	Dallaporta, 1998
5) Massive Ca^{2+} influx, mitochondrial swelling prior to cell lysis	Wyllie et al, 1980 Dallaporta,1998

Table 4.1: Summary of the sequence of events associated with apoptosis from the literature

4.2. Materials and methods

4.2.1. Chemicals and reagents

Staurosporine (Alexis Corporation, Nottingham, UK) was dissolved in dimethyl sulfoxide (DMSO), and stored frozen as a 1 mM stock solution and thawed prior to use. The other chemicals used in this chapter were provided as part of

commercially produced kits and their sources mentioned in the text.

4.2.2. Cell culture and the induction of apoptosis

Human chronic myelogenous leukaemia (K562) cells were cultured under the same conditions mentioned in Chapter 3. Briefly, cells were grown in 20mM HEPES modified RPMI-1640 medium supplemented with 10% heat-inactivated foetal calf serum (FCS), (Invitrogen, Paisley, UK), 2mM L- glutamine and 100units/ mL penicillin-streptomycin, and passaged in non-vented flasks in a standard tissue culture incubator 37°C. All cell culture reagents were obtained from Sigma Aldrich (Poole, UK).

The cells were treated with an apoptosis inducing agent (staurosporine) (from Sigma Aldrich, Poole, UK) at 1 μM or 2 μM concentration depending on the density of cells and incubation period used. The incubation period included five time points (4, 8, 12, 24 and 48 hours). For the earlier incubation time points (4 and 8 hours), a density of 6×10^5/ mL at 1μM staurosporine was used. For the later time points (12, 24 and 48 hours), a density of 3×10^5/ mL at 2 μM was used. This procedure was adopted in order to account for cell growth encountered in cultures at the longer time points and to have enough pharmacological exposure to staurosporine.

4.2.3 DEP experiments

K562 cells were centrifuged at room temperature at 190 ×g for 5 minutes. The pellet was washed and resuspended in isotonic medium consisting of 8.5% (w/v) sucrose plus 0.3% (w/v) dextrose buffer (Gascoyne et al. 1997), as described in the previous chapter. The final conductivity of the medium was adjusted to 2.5 mS/m using PBS and the final conductivity, before use, was verified with a conductivity meter (RS components Ltd, London, UK). The final cell population, depending on the incubation time point used, was counted using a haemocytometer and adjusted to approximately $3x10^5$ cells/ ml (±15%) for DEP measurements. As before, a range of different frequencies (10 kHz-20 MHz) was used. The experiments were repeated many times (generally 4-6) with different populations, which were summed prior to modelling. The same set up and electrode arrangement were used as that in Chapter 3.

4.2.4. Flow cytometry

A Coulter Epics XL flow cytometer was used to measure fluorescence emitted by individually labelled cells using the following techniques:

4.2.4.1. Annexin V assay

In normal viable cells, the phosphatidylserine (PS) molecules are located on the cytoplasmic surface of the cell membrane. When apoptosis is induced, rapid alterations in the organisation of the phospholipids can occur leading to the

exposure of PS on the cell surface (Fadok et al, 1992; Martin et al, 1995). For these experiments, the rapid Annexin V-FITC detection kit (Oncogene, Boston, USA) was used. The assay principle uses a fluorescently labelled probe, a fluorescein isothiocyante (FITC) conjugate of Annexin V, to detect restructuring of the plasma membrane and apoptosis by flow cytometry. Necrosis is characterised by membrane pemeabilisation, necrotic cells bind to Annexin V-FITC. Propidium iodide (PI) was used to distinguish viable, early apoptotic cells and necrotic or late apoptotic cells. Viable cells do not bind to Annexin V-FITC or PI. Early apoptotic cells have exposed PS but will still have intact membranes, and will bind Annexin V-FITC but exclude PI. Necrotic or apoptotic cells in the late terminal stages will bind both Annexin V-FITC and PI, as the PS groups will be exposed and externalised.

Using the instructions provided in the 'Rapid Annexin V binding' assay kit, briefly, a population of around 0.5×10^6 cells in culture media was mixed with 10 μL of media binding reagent followed by 1.25 μL Annexin V-FITC. The mixture was incubated for 15 minutes at room temperature in the dark. The suspension was then centrifuged at 1000 x g for 5 minutes and the supernatant was removed. The cells were then resuspended in 1 x binding buffer. 10 μL of PI was added to the suspension, and the samples were then placed away from the light and on ice ready for immediate analysis using flow cytometry.

The analysis was performed using a flow cytometer emitting an excitation light at 488 nm from laser. The detection was made using FL1 (FITC detector) at 518 nm and FL2 at 620 nm for PI detection. Adjustments were made to minimise

overlap between these two measurements. The log of the fluorescence made by Annexin V-FITC was displayed on the x-axis and the log of PI fluorescence was on the Y-axis. The evaluation of the results was based on the visualisation of a cytogram. As shown in Figure 4.2, the cytogram consisted of a set of 4 squares (quadrants), the square in the bottom left hand corner corresponded to viable cells, bottom right hand corner was that of cells in the early apoptotic stage and the top right hand corner was that of late apoptotic or necrotic cells. In the corner of each quadrant, a percentage number was displayed conferring to the percentage of cells in that category.

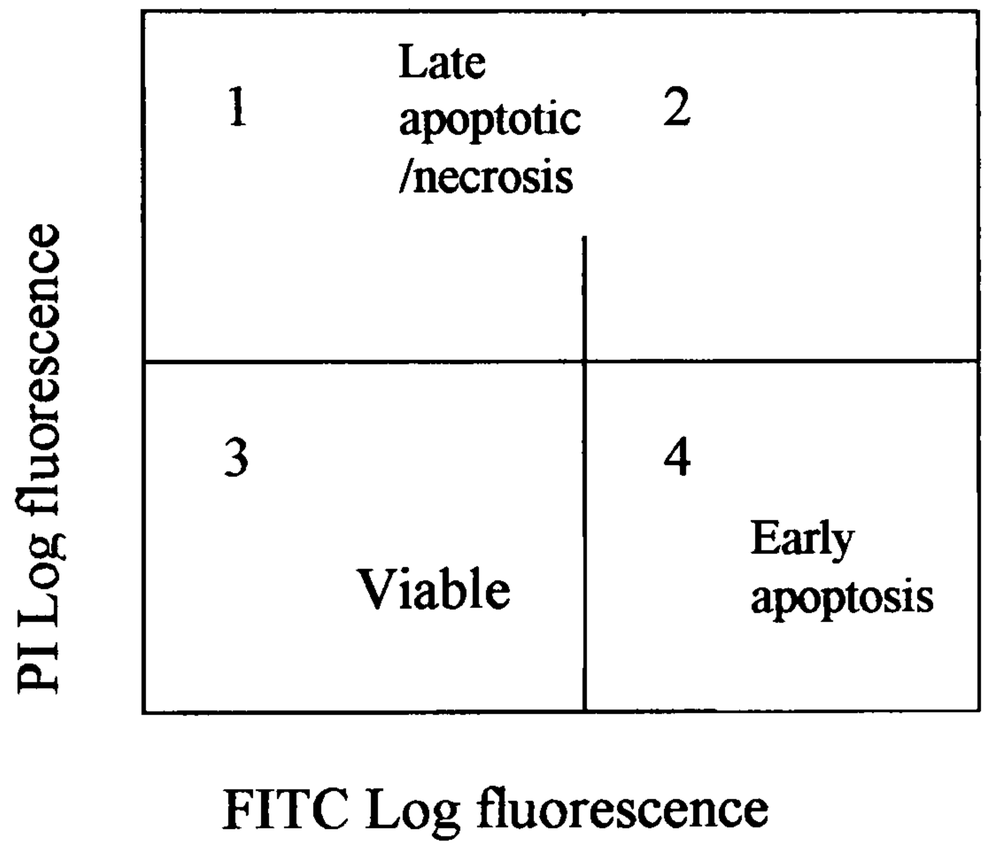

Figure 4.2: A representation of a cytogram in the evaluation of annexin V results by flow cytometry

4.2.4.2. TMRE (tetramethylrhodamine ethylester) assay

TMRE (purchased from Molecular Probes, Leiden, The Netherlands) is a highly fluorescent permeant cationic and a lipophilic dye. It is used as a fluorescent

probe to monitor the membrane potential of mitochondria, as it accumulates in the negatively charged mitochondrial matrix according to the Nernst equation potential (Ehrenberg et al, 1988). TMRE stock was prepared at a concentration of 1mM made with DMSO and stored at -20°C and thawed prior to use. The cultured K562 cells, at a density of approximately 2.5×10^5/ mL were grown overnight, under the usual cell culture conditions (as described in Chapter 3) and then treated with 1μM staurosporine on the following day. Cells were exposed to the drug for a number of hours using the time points (4, 8, 12, 24 and 48 hours). A working stock solution of 10μM of TMRE was made. After each time point, the cells were centrifuged at 200 × g for 3 minutes and the pellet was resuspended in a medium containing PBS supplemented with 2 g/L D-glucose. This was done in order to reproduce the usual conditions cells normally grow in. The cells were then incubated with TMRE (at a final 100nM concentration) for 40 minutes away from light, and again under the normal cell culture conditions. The cells were centrifuged at × 190g for 3 minutes, after which the pellet was resuspended in 500 μL of the PBS medium (with 2 g/L D-glucose). A positive control TMRE sample was also prepared, which involved following the same procedure described earlier, except that an uncoupler carbonyl cyanide m-chlorophenylhydrazone (CCCP) was added at 10 μM final concentration before adding TMRE (100nM final concentration) to the cells, and the cells were then incubated for 3 minutes at room temperature. All samples were then analysed using a flow cytometer using fluorescence at 548nm. CCCP is a protonophore, which depolarises the mitochondria by abolishing the proton gradient across the inner mitochondrial membrane (Martin et al, 1991; Gartner et al, 1995). Different

samples were set up and analysed, these were: control non- TMRE- treated K562 cells, cells that have been treated with staurosporine at different incubation times and a positive TMRE control sample.

In order to assess the mitochondrial membrane potential ($\Delta \Psi_m$) of cells, the shift of the FL3 peak was compared to control (K562 untreated) and to that of positive control TMRE cells. The peak shift gives an indication of the extent of membrane hyperpolarisation or depolarisation (shifting the peak to the right and left, respectively).

4.3. Results

4.3.1. DEP experiments

Table 4.2 summarises the biophysical properties of K562 before and after treatment with staurosporine. The table shows the different time points of incubation with staurosporine, after which DEP data were collected. The results show insignificant changes in the cytoplasmic permittivity, as using any value between 40-80 gave the same best fit curve.

After treatment with staurosporine, more significant changes were seen in the cytoplasmic conductivity at different time points. After 4 hours of treatment, the cells were showing signs of mitochondrial membrane hyperpolarisation, as the cytoplasmic conductivity increased from 0.23 to 0.40 S/m before and after treatment, respectively (Figures 4.3 and 4.4). Hence, the data were suggestive of

an increase in the ionic concentration of the cytoplasm after 4 hours of incubation with staurosporine. The hyperpolarisation pattern appeared to continue at this elevated level, with values remaining as high as 0.45 and 0.42 S/m after 8 and 12 hours of incubation, respectively. Table 4.2 also shows that the specific membrane capacitance (C_{spec}), which provides an indication of the membrane morphology state, varied between these time points. After 4 hours of treatment with staurosporine, C_{spec} was increased from 3.9 to 4.1mF/m^2. K562 cells then demonstrated an elevated C_{spec} at 7.4 mF/m^2 after 8 hours of incubation (Figure 4.5). This parameter remained at this level for the remainder of this study (Figure 4.6). The increase in C_{spec} indicates an increase in the membrane morphology which could be the result of more blebbing taking place in the membrane of these cells. C_{spec} is calculated by taking surface area into account, hence blebbing increases the surface area, which may account for the increase in C_{spec} seen after 8 hours of staurosporine treatment.

After 24 hours of incubation with stauropsporine, the DEP results (Figure 4.7) highlighted the possibility of more than one population accounting for the different dielectric properties obtained. As shown in Table 4.2, each population exhibited different cyoplasmic conductivity. Values started from 0.5 S/m, for population 1, indicating that these cells possessed a high ionic strength. Population 2 demonstrated a reduced cytoplasmic conductivity of 0.03 S/m, which might indicate cells later in their life cycle, or apoptosis, whilst population 3 showed a cytoplasmic conductivity of 0.003 S/m, indicating that the cells have probably gone into the necrotic stage.

	DEP data			
	Cytoplasm		Membrane	
	σ (S/m)	ε	K_s (S)	C_{spec} (mF/m^2)
Incubation conditions of K562 cells before treatment with staurosporine	0.230 (0.220-0.240)	40-80	0.009 (0.008-0.010)	3.9 (3.3-3.6)
Hours of incubation with staurosporine				
4	0.400 (0.30-0.50)	40-80	0.008 (0.007-0.009)	4.1 (3.8-4.2)
8	0.450 (0.44-0.46)	40-80	0.09 (0.007-0.010)	7.4 (6.9-7.8)
12	0.420 (0.41-.43)	40-80	0.006 (0.005-0.007)	7.5 (7.2-8.2)
24				
Population 1	0.500 (0.400-0.600)	40-80	0.01	7.0 (6.9-7.1)
Population 2	0.030 (0.02-0.040)	40-80	0.01	7.0 (6.9-7.1)
Population 3	0.003 (0.002-0.004)	40-80	0.01	7.0 (6.9-7.1)
48				
Population 1	0.003 (0.002-0.004)	40-80	0.01	6.9 (6.8-7.0)
Population 2	0.150 (0.140-0.160)	40-80	0.01	7.6 (7.5-7.7)

Table 4.2: DEP results summarising the dielectric parameters measured after different incubation periods with staurosporine

The parameters in Table 4.2 were obtained using the radius measurements in Table 4.3 below:

Conditions of incubation with staurosporine	*Average K562 radius measurements (μm)*
Before incubation	9.0
After incubation (hours)	
4	8.0
8	7.6
12	7.6
24	6.7
48	6.8

Table 4.3: K562 cell radius measurements used for modelling and obtaining the parameters in Table 4.2 at different incubation periods with staurosporine

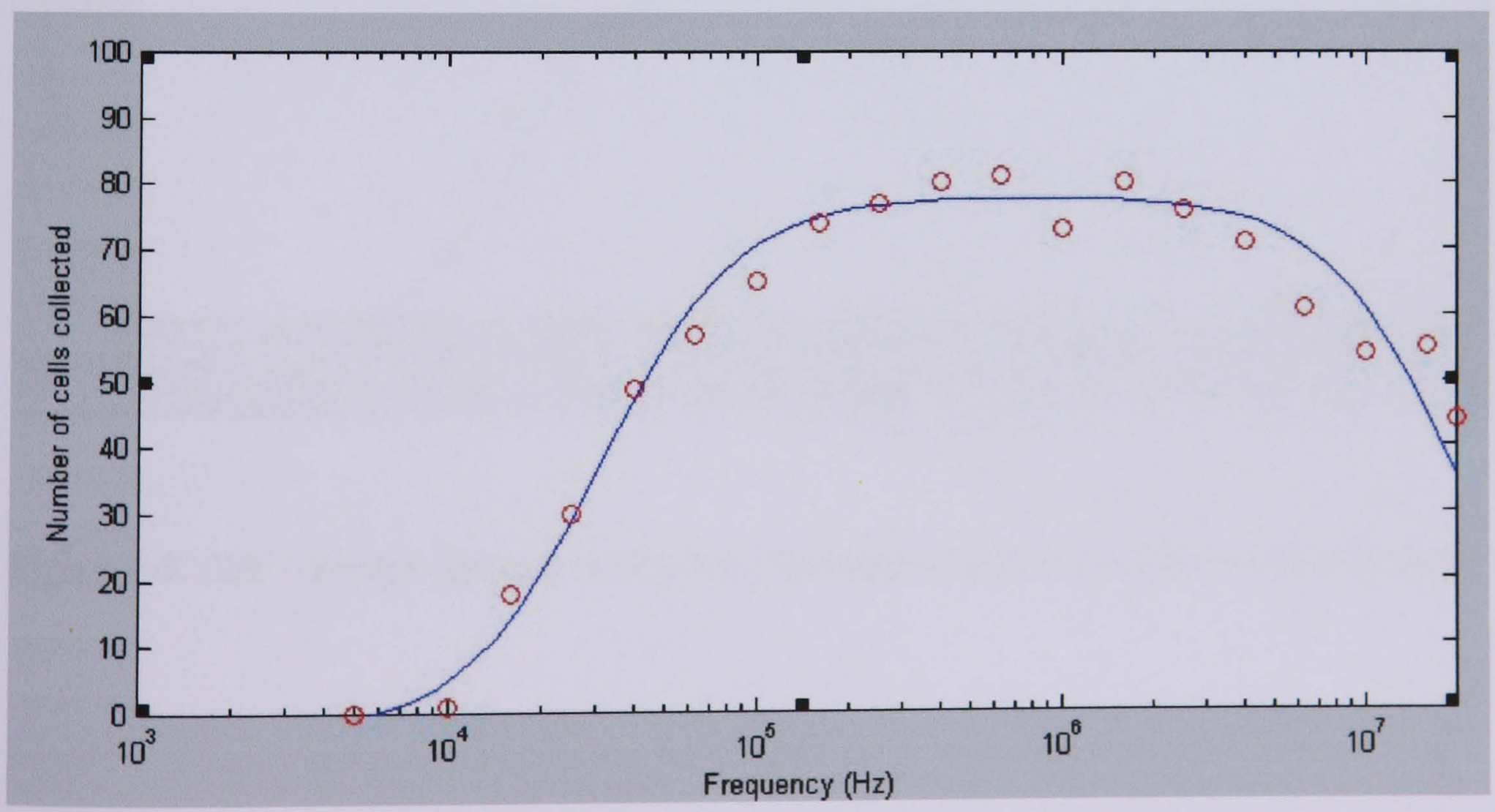

Figure 4.3: DEP collection spectra of control (untreated) K562 cells

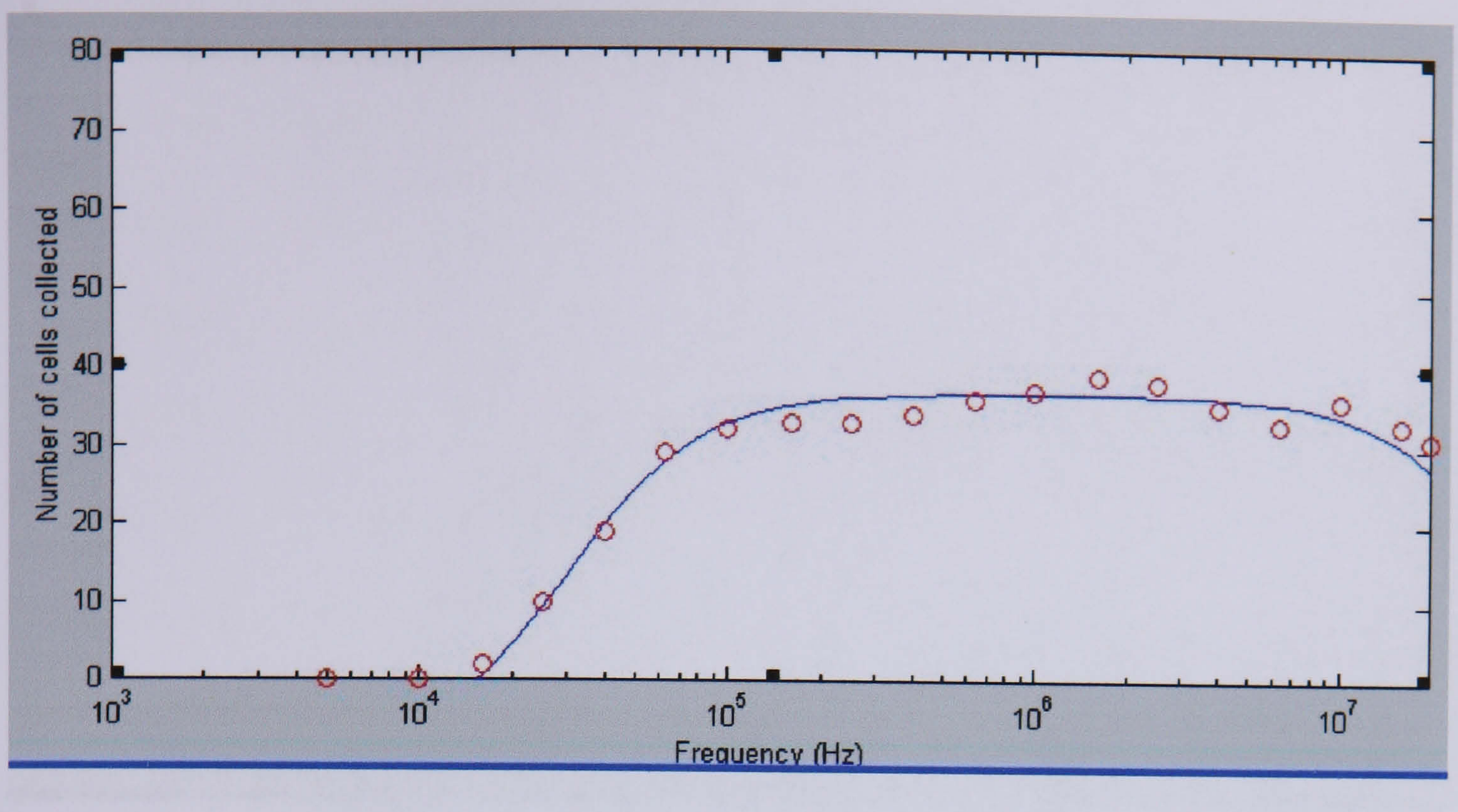

Figure 4.4: DEP collection spectra of K562 cells following 4 hours treatment with staurosporine

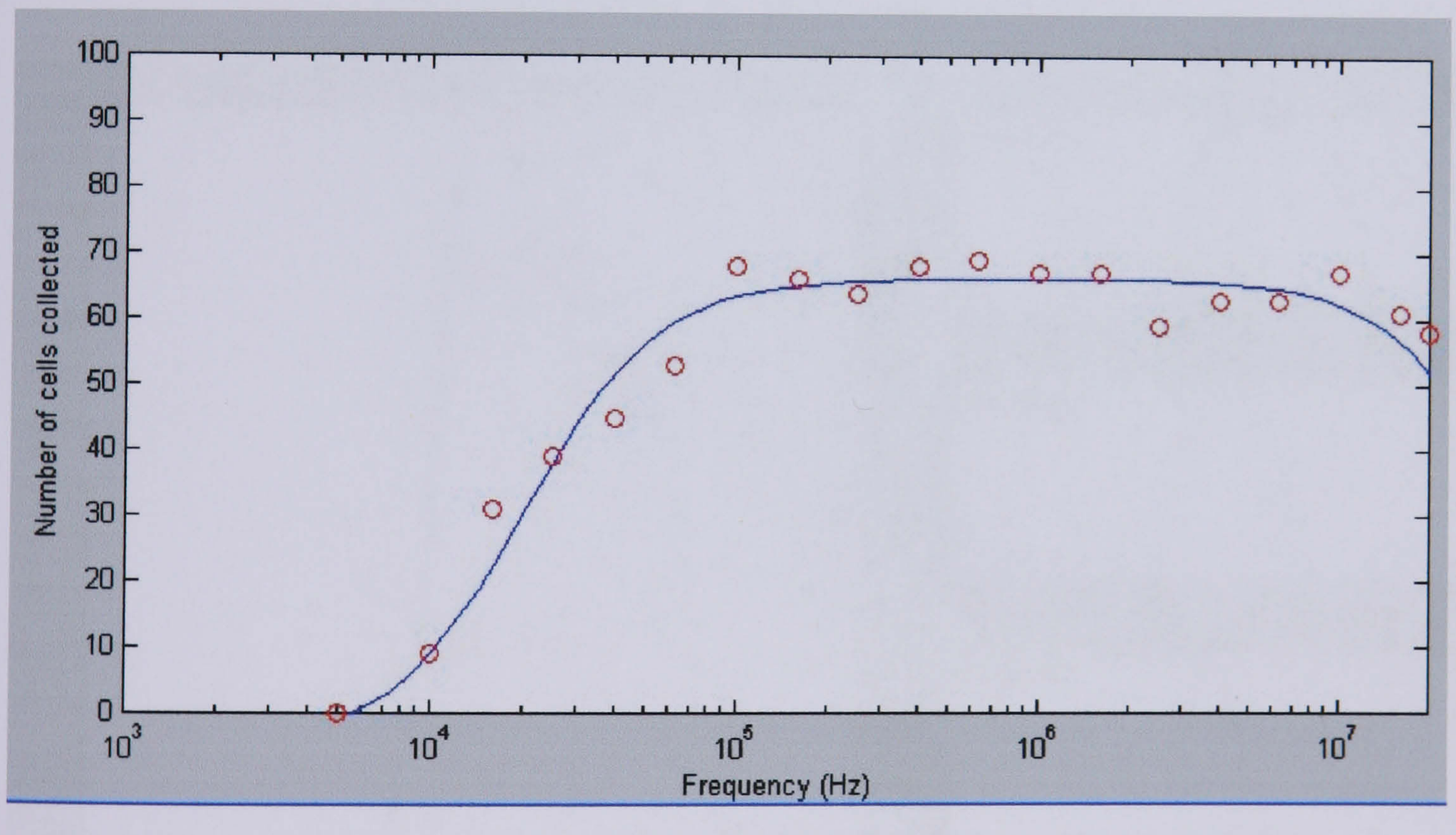

Figure 4.5: DEP collection spectra of K62 cells following 8 hours treatment with staurosporine

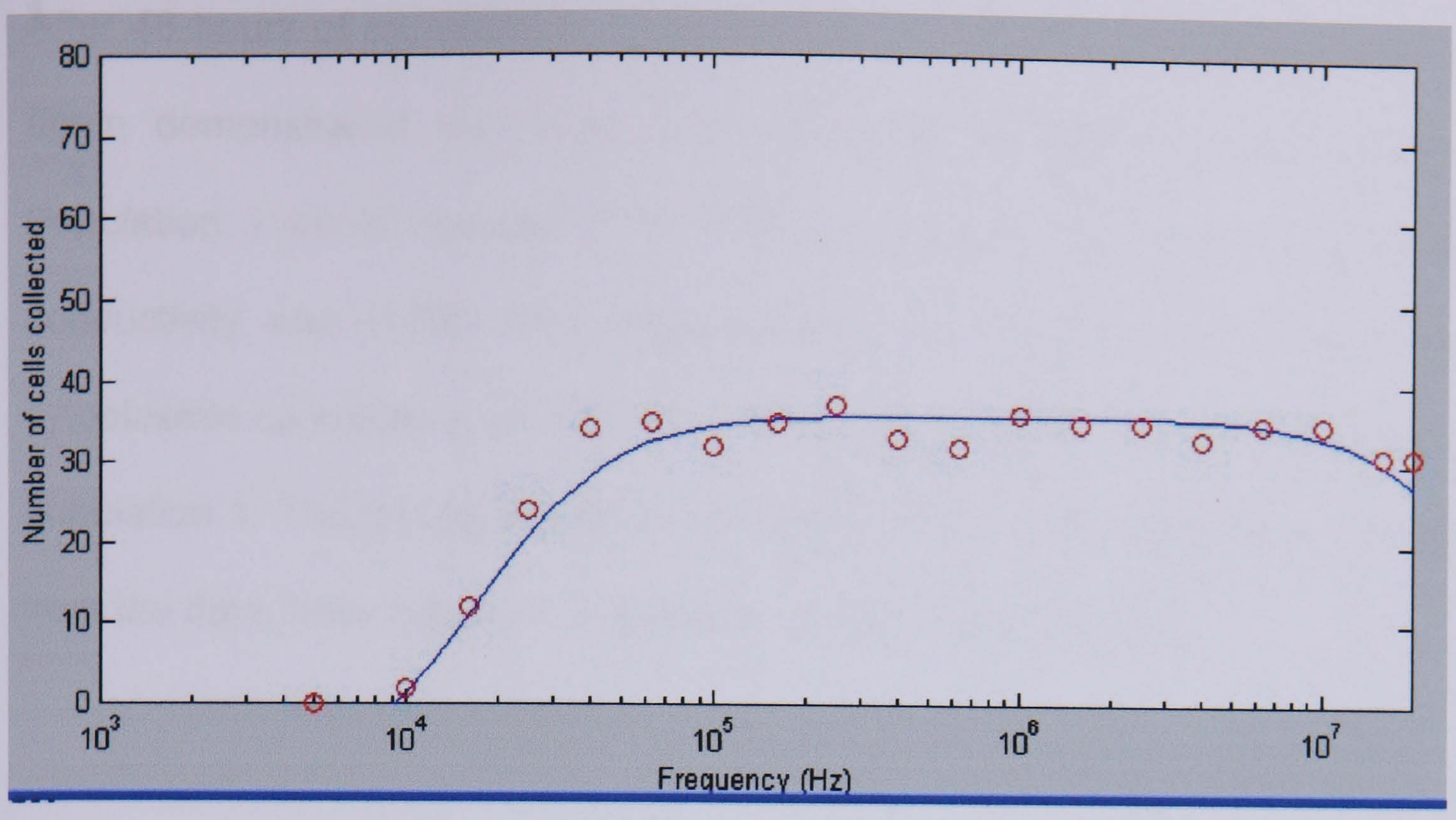

Figure 4.6: DEP collection spectra following 12 hours treatment with staurosporine

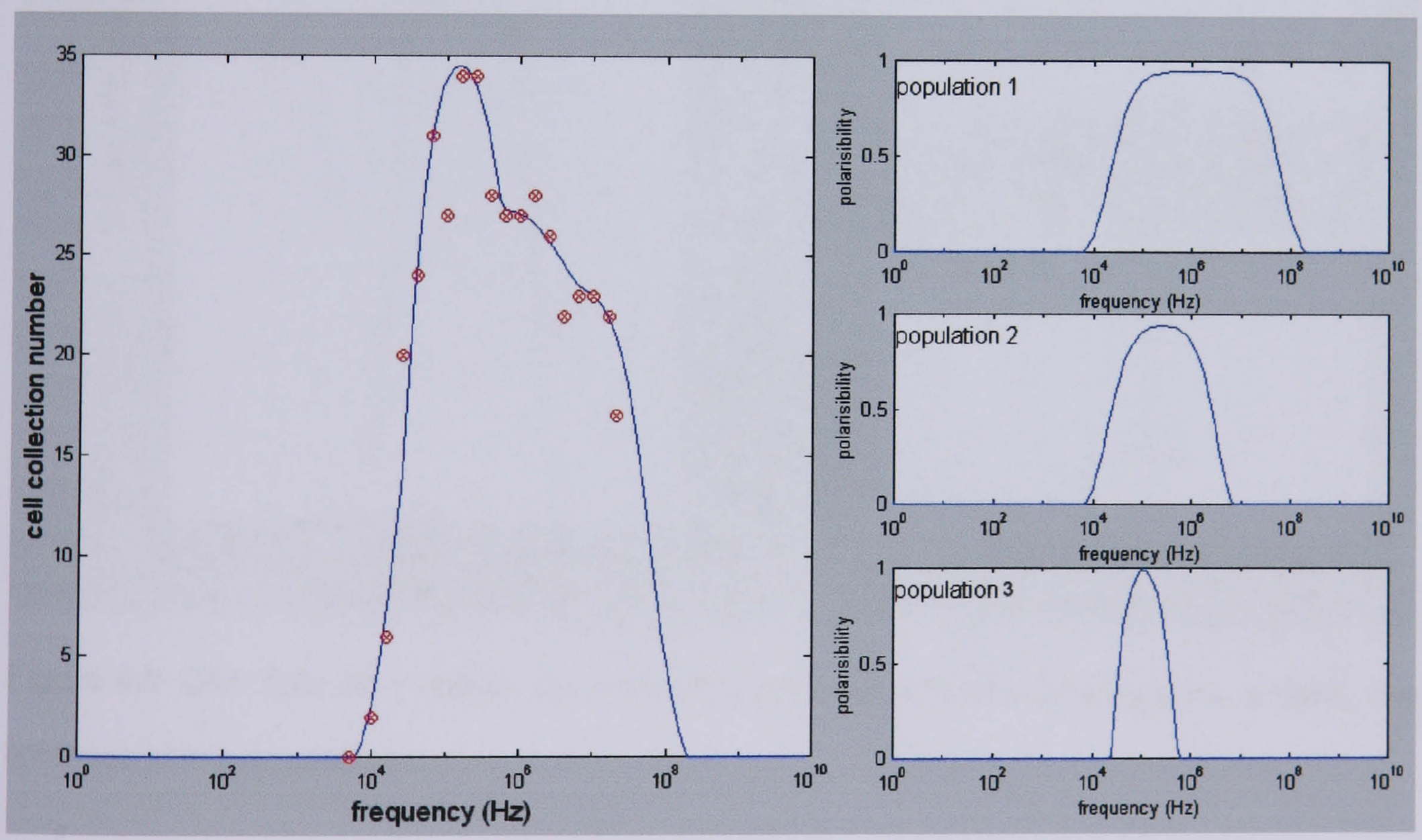

Figure 4.7: DEP collection spectra following 24 hours of treatment showing the presence of more than one population

After 48 hours of exposure to staurosporine, the DEP results (Figure 4.8) have again demonstrated that more than one cell population could be present. Population 1 could represent the dead or necrotic cells, as the cytoplasmic conductivity was 0.003 S/m. Population 2, on the other hand, exhibited a cytoplasmic conductivity of 0.15 S/m, indicating a higher ionic content relative to population 1. The results shown in these figures, and the parameters calculated from the data, have been the average of at least 6 experiments.

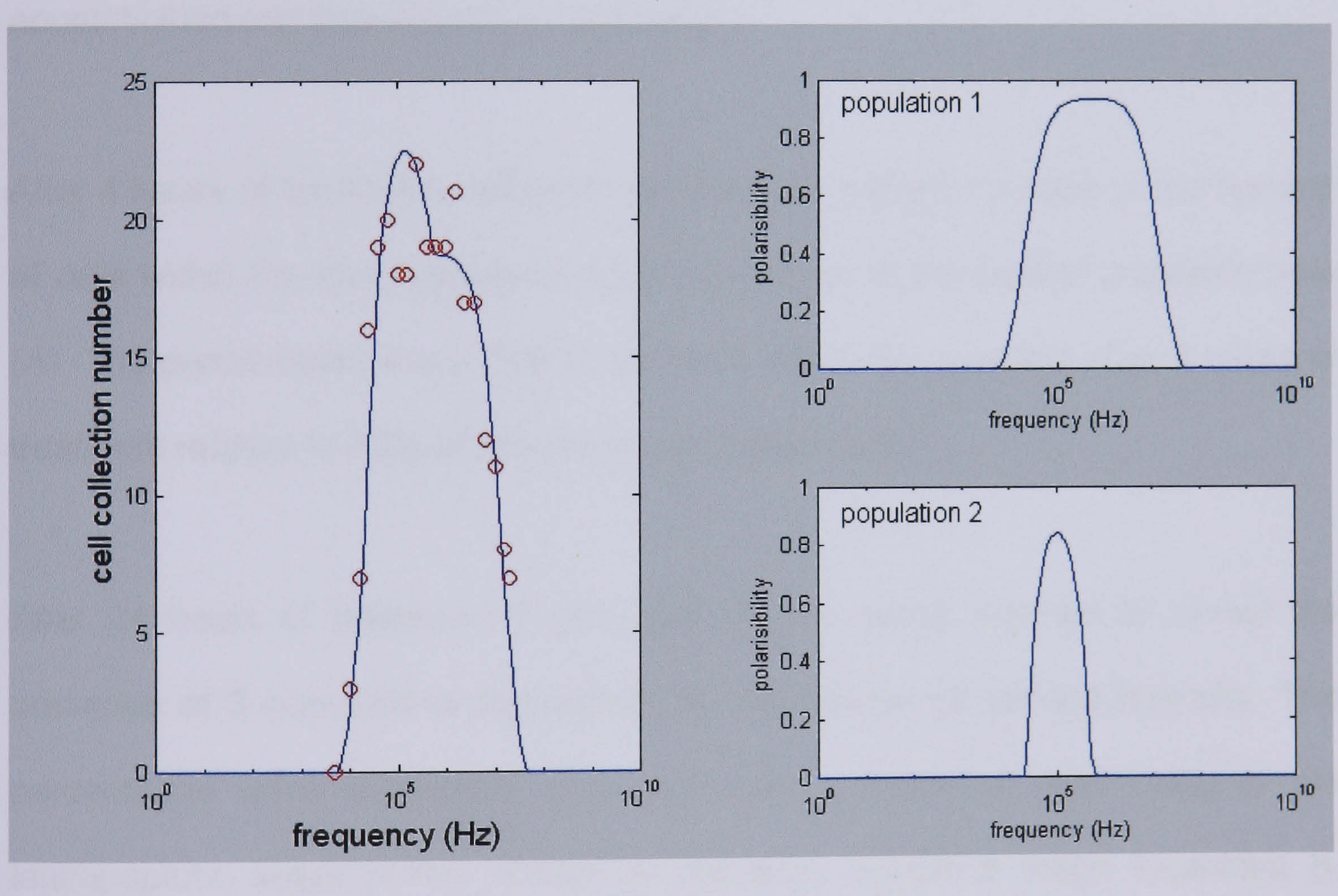

Figure 4.8: DEP collection spectra following 48 hours treatment with staurosporine showing the presence of two populations

4.3.2. Flow cytometry

4.3.2.1. Annexin V results

Figure 4.9 shows the annexin V data for K562 at different incubation periods with staurosporine. The control untreated cells showed a reasonable number of viable cells with a dense population in the viable quadrant. This was demonstrated by the percentage in the bottom left hand quadrant, that being 84%, with very low and insignificant numbers in the other quadrants (12% and 4%, for early and late apoptotic/necrotic populations, respectively).

After 4 hours of treatment, cytogram (B) showed a slight increase in the number of cells within the early apoptotic quadrant relative to the control untreated cells (A). The percentages were 35% in the early apoptotic quadrant after 4 hours of treatment relative to 12% of the control untreated cells.

After 24 hours of treatment (Figure 4.9 C), the assay seemed to reveal the presence of 3 populations highlighted by the 'clouds' of varying intensity. The percentages were suggestive of a significant number of cells being in the late/apoptotic stage (44%) relative to the early apoptotic stage (quadrant B, 11%). At this time point, approximately 50% of the population seemed to be viable (56%).

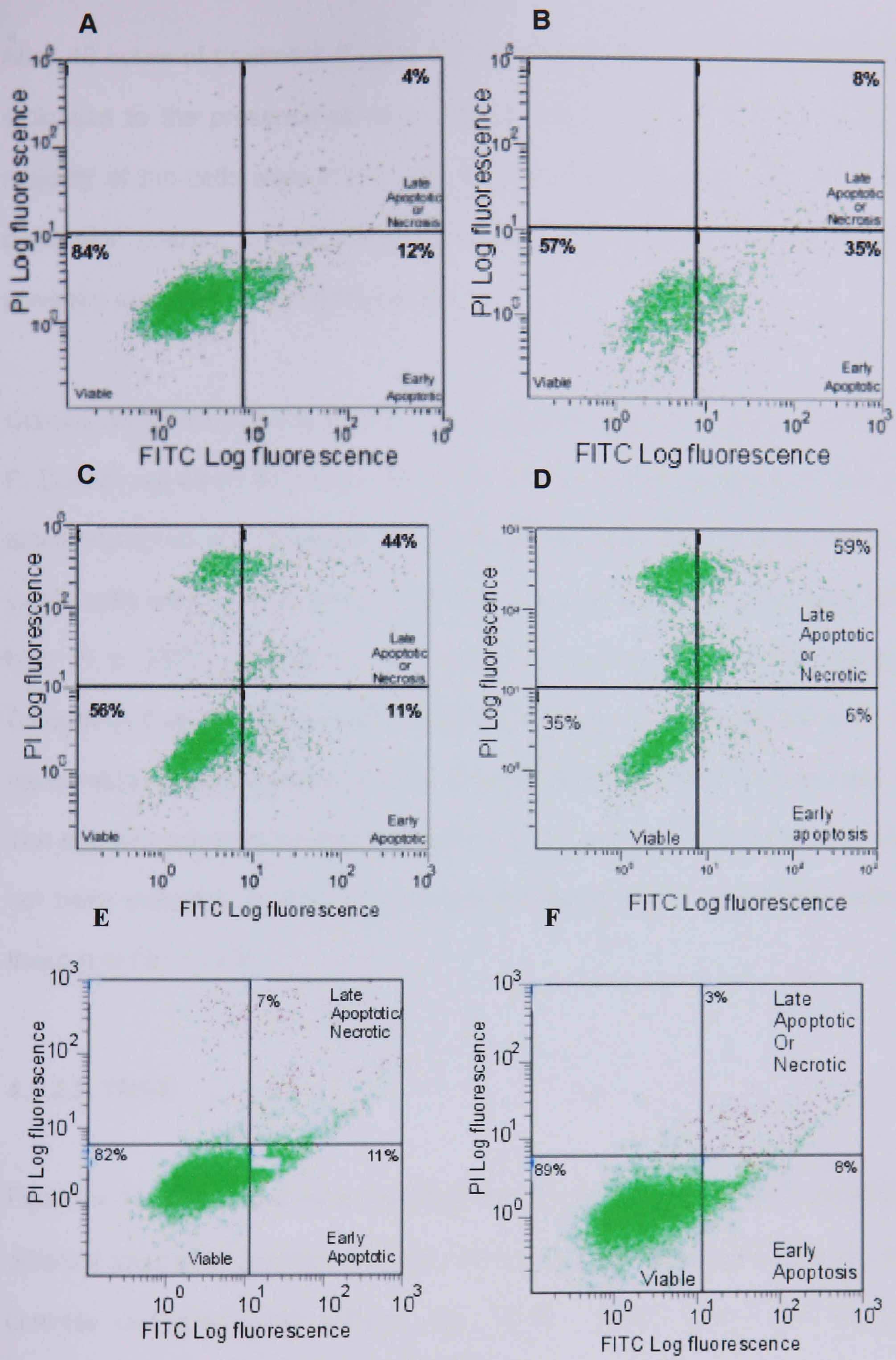

Figure 4.9: Annexin V cytograms showing the stages of apoptosis at different incubation periods with staurosporine: control (A), 4 hours (B), 24 hours (C) and 48 hours (D). Experimental controls on untreated K562 with PI only (E) and FITC only (F).

After 48 hours of treatment (Figure 4.9 D), the cytogram gave a slightly clearer indication to the presence of more than one population and showed that the majority of the cells were in the late apoptotic/necrotic stage, with 59% of the population present in that quadrant, compared to 6% in the early apoptotic quadrant and 35% in the viable quadrant.

Control untreated cells were used in the experiment, shown in Figure 4.9 E and F. Control untreated cells were incubated with PI alone (cytogram E) and FITC alone (cytogram F). Untreated cells are expected to have a high number of viable cells with a low number in the early apoptotic stage. Viable cells do not bind PI or FITC, reflected in the lower left hand quadrant in the cytogram. Cytograms E and F demonstrated that the majority of the control untreated cells were viable with percentages of 82% and 89% for PI and FITC, respectively.

The experiments were repeated at least 3 times, the results of all of which have not been included, as they all provided the same pattern, a representation of these is in Figure 4.9.

4.3.2.2. TMRE

Figure 4.10 shows the mitochondrial membrane potential ($\Delta\Psi_m$) changed at different incubation periods with staurosporine. The first plot (A) showed K562 controls untreated cells without the TMRE, which showed no significant fluorescence emitted. After using TMRE (B), the cells exhibited a shift in the peak indicating that they have taken up TMRE and fluorescence was emitted. As a different control, the cells were incubated with the uncoupler (protonophore),

which depolarised the mitochondria by abolishing the proton gradient across the inner mitochondrial membrane, producing a peak that shifted to the left relative to CCCP untreated cells. Figure 4.10 C has evidently shown the effect of using CCCP, as the peak has shifted to the left indicating a reduction in $\Delta\Psi_m$ (depolarisation) relative to the CCCP untreated cells (B). Incubating the cells with staurosporine has demonstrated changes in the $\Delta\Psi_m$, after 4 hours of exposure to staurosporine (D), the peak shifted slightly to the right in comparison with the TMRE only treated cells (B), showing a slight increase in $\Delta\Psi_m$ that corresponds to a slight hyperpolarisation state. This state appears to have continued after 8 hours of exposure (E). However, a small sub-population was apparent at this time point that exhibited a depolarisation state (i.e. it is displaced to the left). After 24 hours of exposure (F), the results indicate the presence of more than one population, one of which produced a peak shift to the right (hyperpolarisation) and the other had a peak that shifted to the left (depolarisation) relative to (B).

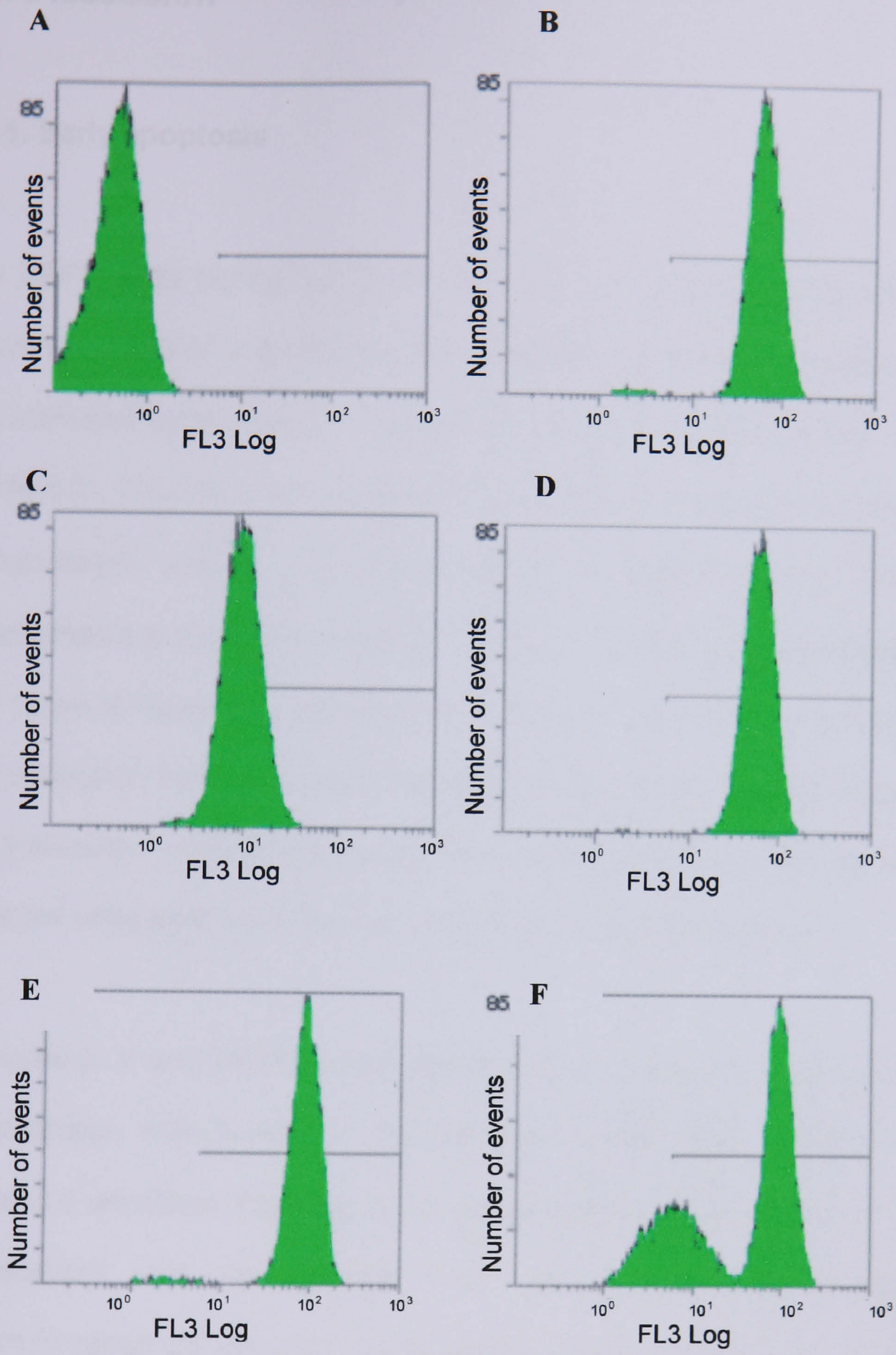

Figure 4.10: Flow cytometric plots showing changes in the mitochondrial membrane potentials. K562 control cells without TMRE (A), control K562 with TMRE but without staurosporine (B), K562 with no staurosporine but with the uncoupler CCP (C), K562 with TMRE following staurosporine exposure: 4 hours (D), 8 hours (E) and 24 hours (F).

4.4. Discussion

4.4.1. Early apoptosis

The DEP results highlighted an increased ionic concentration in the cytoplasm following 4 hours of incubation with staurosporine relative to untreated cells. This was indicated by the rise in conductivity from 0.23 S/m to 0.4 S/m, respectively (Table 4.2). The rise in the cytoplasmic conductivity was persistent after 12 hours of incubation with 1 μM staurosporine. Furthermore, the TMRE assay demonstrated a slight mitochondrial membrane (MMP) hyperpolarisation for up to 8 hours of treatment. This was evident in the peak shifting to the right hand side relative to the TMRE untreated cells (Figure 4.10 B and D). The annexin V assay showed that early apoptosis was evident after 4 hours of treatment relative to control untreated cells (Figures 4.9 B and 4.9 A, respectively).

The annexin V and TMRE results collectively have indicated that at early stages of apoptosis, mitochondrial hyperpolarisation took place. Furthermore, DEP revealed a persistent increase in the cytoplasmic conductivity for up to 12 hours of treatment with staurosporine. This early mitochondrial hyperpolarisation pattern in apoptosis was reported in several previous studies (Green and Reed, 1998; Marzo et al, 1998; Li et al, 1999). A recent study (Kim et al, 2003) showed that Lactacystin-induced apoptosis in rat retinal pigment epithelial cell line (RPE)-J, is closely associated with an early mitochondrial hyperpolarization induced by intracellular alkalinisation. The increase in the cytoplasmic conductivity may possibly be caused by one or more mechanism. One such mechanism may

involve the increased generation of reactive oxygen species (ROS), a phenomenon reported in a study by Li et al (1999). In their report, they showed that p53-induced apoptosis caused an increase in ROS leading to a transient increase in the MMP. Other studies (Khaled et al, 1999, 2001a, 2001b; Belaud-Rotueau et al, 2000) have described the involvement of an increased intracellular pH in mitochondrial hyperpolarisation as a consequence of cytokine withdrawal induced apoptosis. A more recent study (Kim et al, 2003) aimed to investigate whether mitochondrial hyperpolarisation, in a different apoptosis-induced model, was evoked by cytosolic alkalinisation. The authors found that early mitochondrial hyperpolarisation indeed a consequence of intracellular alkalinisation which was mediated by Cl^-/HCO^-_3 anion exchanger. Those findings supported the idea that the intracellular alkalinisation preceded and induced mitochondrial hyperpolarisation. The idea that the rise in intracellular pH induces mitochondrial hyperpolarisation was similar to the finding by Khaled et al (2001a) using a model of cytokine withdrawal-induced apoptosis.

Another possible mechanism may counterintuitively involve ionic efflux. Although the early events triggering apoptosis are still poorly understood (Porcelli et al. 2003), a number of studies reported a dramatic decrease in the intracellular ions during apoptosis, primarily K^+ and Na^+ (McCarthy and Cotter, 1997). The loss of K^+ was up to 95% (Hughes et al, 1997), the intracellular K^+ was reduced from 150 to 50 mM in a fibroblast cell line (Barbiero et al, 1995) and K^+ concentration was found to be as low as 35 mM in shrunken apoptotic thymocytes (Hughes Jr and Cidlowski, 1999). In support of a low K^+ concentration was the study by Montague et al (1999), where shrunken cells, of lymphocytes treated with

glucocorticoid, were shown to be K^+ depleted.

A decrease in Na^+ has also been reported in apoptotic lymphoma cells (Bortner et al, 1997) and in Jurkat cells (Gomez-Angelats et al, 2000). The loss of Cl^- content has been associated with cell volume decrease (Yu and Choi, 2000; Okada and Maeno, 2001. The efflux of K^+ accompanied by the efflux of Cl^- permits the osmotic movement of water out of the cell, generating a characteristic loss of cell volume (apoptotic volume decrease, AVD) (Porcelli et al, 2003; Lang et al, 2000). In a staurosporine induced apoptosis study, the data by Poreclli et al (2003) suggested that upregulation of Cl^- and K^+ channels might be a very early event required for the subsequent onset of AVD that results in apoptosis. Apoptotic cell shrinkage has also been associated with a decrease in the intracellular K^+ and Na^+ (McCarthy and Cotter, 1997). This loss of cytosolic K+ occurs before cell shrinkage, consistent with a role for K^+ efflux in cell volume reduction, and K^+ was also seen before the production of ROS (Dallaporta et al, 1998).

Concomitant with the loss of intracellular ions is a dramatic reduction in cell size characteristic of apoptosis. For example Maeno et al (2000) reported an approximately 30% loss in cell volume in HeLa and U937 cells 4 hours after treatment with staurosporine. This suggests another possible mechanism of increase in cytoplasmic conductivity, which relies on the loss of cell volume. The increase in the conductivity (which is proportional to ionic concentration, and hence inversely proportional to cytoplasmic volume) seen from the DEP data may be caused by the loss of the cell volume as a result of ionic efflux and water

loss causing the remaining ions to become more concentrated inside the cell. Although the 30% decrease in cell volume does not completely account for the near-doubling of the cytoplasmic conductivity seen in our data, this can be accounted for if approximately 40% of the cell is composed of material which does not contribute to volume loss (for example, the organelles and cytoskeleton). This is illustrated in the schematic below (Figure 4.11).

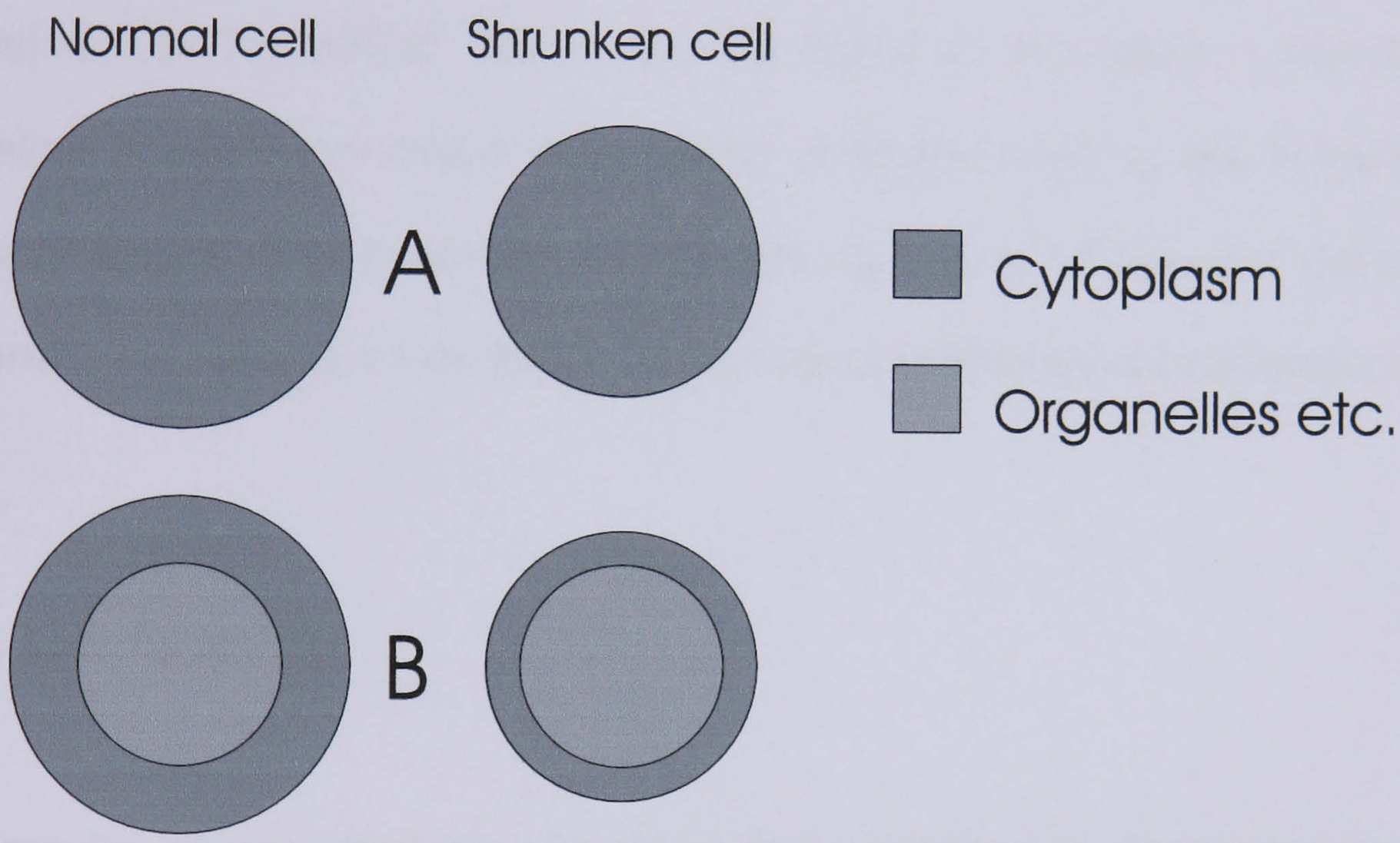

Figure 4.11: During apoptosis, cells shrink by 30% of their normal volume; however the observed change in conductivity suggest that the volume has halved. If the cell consists only of cytoplasm (A), the 30% loss of volume does not correspond to a sufficiently great increase in conductivity. However, if we account for organelles and other cell bodies (B), indicated in the same loss of cell volume gives a much more significant decrease in the volume of the cytoplasm, and hence a more significant rise in conductivity.

The proposed mechanism goes in agreement with an earlier study (Wyllie et al, 1980 and reviewed in Trump and Berezesky, 1996). They reported that in apoptosis, cells shrink with densification of the cytosol, more extreme clumping of nuclear chromatin, formation of large cytoplasmic blebs and changes in mitochondria similar to initial condensation.

Interestingly, the DEP results highlighted significant changes in the specific membrane capacitance, which increased following staurosporine treatment from around 4.1 to 7.4 mF/m^2 (for 4 and 12 hours of incubation, respectively), indicating possible membrane morphology changes, such as the formation of apoptotic bodies. The capacitance remained high up to 12 hours of incubation. Generally, the surface conductance did not vary significantly during apoptosis.

4.4.2. Late Apoptosis

DEP results revealed that after 24 hours of incubation with staurosporine, more than one population was present; multiple populations were also seen after 48 hours of incubation with staurosporine. The dielectric parameters extracted from these populations at the two time points are summarised in Table 4.2. After 24 hours of treatment, DEP results (Figure 4.7) showed the presence of 3 populations, believed to be dead or necrotic cells where the cytoplasmic conductivity was very low; a depolarized population with low cytoplasmic conductivity consisting of possibly late apoptotic cells, and a highly-conductive population that is still behaving as if in early apoptosis. The cytoplasmic

conductivities of these three populations were 0.003, 0.03 and 0.50 S/m, respectively.

Comparing DEP data with those obtained using Annexin V (Figure 4.9 C), three populations could also be observed with similar properties and with greater percentages lying in the quadrants corresponding to viable (56%) and late apoptotic or necrotic cells (44%). On the other hand, TMRE data showed the presence of a second population with depolarised MMP in addition to the hyperpolarised population (Figure 4.10 F). When the treatment was prolonged to 48 hours, the DEP results revealed the presence of 2 populations, one corresponding to dead or necrotic cells and the second to a depolarised population with cytoplasmic conductivities of 0.003 and 0.150 S/m, respectively (Table 4.2). The quadrants from the Annexin V data showed a clearer representation of the cells distribution, with the majority lying in the late apoptotic or necrotic quadrant (59%) (Figure 4.9 D).

The populations of cells seen at 24 hours treatment showed different dielectric properties, principally cytoplasmic conductivities, relative to that of the control untreated cells (0.23 S/m) (Table 4.2). Possible explanations for this include the continuous efflux of the K^+ and Na^+ while the cell volume was still shrinking. The remaining ions are, therefore, still relatively more concentrated, thus giving a hyperpolarised population 1. Population 2 was strongly depolarised as it is possibly reaching the end of its apoptotic cycle and close to dying, so the ionic efflux is over-riding. Population 3 represented the dead necrotic cells, which had ruptured.

After 48 hours of treatment, one population corresponded to (dead) necrotic cells as the cytoplasmic conductivity was very low and the second was weakly depolarised with a cytoplasmic conductivity of 0.15 S/m. This population might reflect the last stages of apoptosis where ionic influx has been reported. The intracellular Ca^{2+} has been reported to increase and can result from the influx from the extracellular space, or from redistribution from intracellular stores shortly before lysis (Wyllie et al, 1980; Dallaporta et al, 1998). Also, Trump and Berezesky (1996) hypothesised the increase in intracellular calcium stimulate the K^+ loss and shrinkage prior to cell death. Ca^{2+} is known to be the key regulator of many enzymatic reactions in the cell. The mitochondrion alone has 3 Ca^{2+} transport systems (a Ca^{2+} uniport, Ca^{2+}/H^+ antiport and Ca^{2+}/Na^+ antiport) responsible for influx and efflux of Ca^{2+}. Mitochondria also have non-specific channels called permeability transition pores (PTP) which may also take part in Ca^{2+} release. Mitochondria are usually present in close contact with endoplasmic reticulum (where Ca^{2+} is stored) (reviewed in Skulachev, 1999). It might be possible that the cytoplasmic conductivity seen for the 0.15 S/m population at the end of the 48 hours incubation with staurosporine was due to the high Ca^{2+} content coming from the mitochondria, as they swell prior to cell death (Trump and Berezesky, 1996). Another contributor might be the increased intracellular Na^+ as reviewed by Yu (2003).

As indicated in the previous section, the specific membrane capacitance (C_{spec}) of the two populations after 48 hours treatment retained an elevated value. These particular data might further reflect the membrane morphology and size changes seen in this population with regards to blebbing or folding (Trump and Berezesky, 1996).

If we attempt to map the events described in this chapter with other known apoptotic events described in the literature, we can obtain an overall sequence of apoptotic processes similar to those shown in Table 4.4. As can be seen, the events indicate that the processes attributed to the DEP data are entirely within the realms of what is known about the progress of apoptosis, whilst also shedding new light on these key cellular events.

Event	**Corresponding findings** (from DEP, annexin V & TMRE) after staurosporine treatment
1) Alkalinisation, as pH ↑, ADP import is inhibited, limited ATP synthesis in mitochondria, inactivation of F_0F_1ATPase and protons are pumped out. The ↑ in pH was mediated by the activation of NHE1. The ↑ in pH also mediated by the Cl^-/HCO_3^- anion exchanger (Cl^- out) and (HCO_3^- in). A transient increase in Na^+	(4-12 hours) Increased cytoplasmic conductivity (ionic concentration) as the cell shrinks, ions become more concentrated
2) ↑ K^+ efflux, cell shrinks, phosphatidyl serine residues exposed	
3) ↑ reactive oxygen species	
4) At later stages, $\Delta\psi_m$ depolarises	(24-48 hours)
5) Massive Ca^{2+} influx, mitochondrial swelling prior to cell lysis	Multiple populations occur as cells depolarise and die. The influx of Ca^{2+} may be reflected by populations seen with intermediate cytoplasmic conductivity

Table 4.4: A table summarising the results obtained collectively from DEP, annexin v and TMRE shown in parallel with the information in literature (as discussed in Table 4.1)

4.5. Conclusions

DEP can be used as a rapid, non-invasive technique to detect early dielectric changes in apoptosis, where semi-quantitative results can be obtained. Furthermore, it can be used to differentiate between multi- populations on the basis of their dielectric properties and, therefore, gives an accurate assessment of key stages within apoptosis.

The DEP results in this chapter indicate that K562 cells increase in cytoplasmic conductivity within the first 4 hours after exposure to staurosporine, which then lasts beyond 12 hours of exposure. The Annexin V assay indicated that this occurred synonymously with early-stage apoptosis. Furthermore, within this time period, TMRE data pointed to hyperpolarisation in the MMP. Although no work exists which directly explains the rise of cytoplasmic conductivity at this stage of apoptosis, a number of known events may explain this behaviour. The most likely cause of this effect is cell shrinkage due to water loss triggered by ion (K^+, Cl^-) efflux, resulting in an increase in the intracellular concentration of the remaining ions

After 24 and 48 hours of incubation with staurosporine, multiple populations were detected by DEP, highlighting the dielectric changes that the cell undergoes before death or necrosis. The Annexin V results showed that the majority of cells were identified as being in the late stages of apoptosis and the TMRE data indicated both depolarised and hyperpolarised MMP in the population. The DEP results at these two time points showed cells with elevated, diminished and

depleted cytoplasmic conductivities after 24 hours of exposure to staurosporine, with the latter two populations only being observed after 48 hours of exposure. The reduction effect might be associated with the later stages of apoptosis. This may be due to cell swelling, causing the cell ionic content to become relatively more dilute and significantly lower in cytoplasmic conductivity relative to control untreated cells. However, this conductivity was significantly higher than the third population (assumed to be dead cells). This could be the result of an increased ionic content, such as an influx of Ca^{2+} and Na^{+} through the membrane channels from the extracellular fluid, and additionally from the mitochondria in the case of Ca^{2+}.

These suggestions may need further and closer examination, by using potential blockers to eliminate for the changes seen, as well as perhaps using other apoptosis-inducing techniques to examine whether similar effects are observed.

4.6. References

Barbiero, G. Duranti, F. Bonelli, G. et al. Intracellular ionic variations in the apoptotic death of L cells by inhibitors of cell cycle progression (1995) *Experimental Cell Research*, **217**(2): 410-418.

Belaud-Rotureau, M.A. Leducq, N. de Gannes, FMP. et al. Early transitory rise in intracellular pH leads to Bax confirmation change during ceramide-induced apoptosis (2000) *Apoptosis*, **5**(6): 551-560.

Bortner, C.D. Hughes Jr, F.M. Cidlowski, J.A. A primary role for K^+ and Na^+ efflux in the activation of apoptosis (1997) *The Journal of Biological Chemistry*, **272**(51): 32436-32442.

Bortner, C.D. Cidlowski, J.A. Uncoupling cell shrinkage from apoptosis reveals that Na+ influx is required for volume loss during programmed cell death (2003) *Journal of Biological Chemistry*, **278** (40): 39176-39184.

Brunk, U.T. Svensson, I. Oxidative stress, growth factor starvation and Fas activation may all cause apoptosis through lysosomal leak (1999) *Redox Report*, **4**(1-2): 3-11.

Dallaporta, B. Hirsch, T. Susin, S.A.et al. Potassium leakage during the apoptotic degradation phase (1998) *Journal of Immunology*, **160**(11): 5605-5615.

Ehrenberg, B. Montana, V. Wie, M.D. et al. Membrane potential can be determined in individual cells from the nernstian distribution of cationic dyes (1988) *Biophysical Journal*, **53**:785-794.

Fadok, V.A. Voelker, D.R. Campbell, P.A. et al. Exposure of phosphatidylserine on the surface of apoptotic lymphocytes triggers specific recognition and removal by macrophages (1992) *Journal of Immunology*, **148**: 2207-2216.

Gartner, F. Voos, W. Querol, A. et al. Mitochondrial import of subunit Va of cytochrome c oxidase characterised with yeast mutants (1995) *The Journal of Biological Chemistry*, **270** (8): 3788-3795.

Gascoyne, P.R.C. Wang, X.B. Huang, Y. et al. Dielectrophoretic separation of cancer cells from blood (1997) IEEE transactions on Industry Applications, **33** (3): 670-678.

Gomez-Angelats, M. Bortner, C.D. Cidlowski, J.A. Protein kinase C (PKC) inhibits fas receptor-induced apoptosis through modulation of the loss of K+ and cell shrinkage (2000) *The Journal of Biological chemistry*, **275**(26): 19609-19619.

Green, D.R. and Reed, J.C. Mitochondria and apoptosis (1998) *Science*, **281** (5381): 1309-1312.

Hughes Jr, F.M. Bortner, C.D. Purdy, G.D. et al. Intracellular K+ suppresses the activation od apoptosis in lymphocytes (1997) *The Journal of Biological Chemistry*, **272**(48): 30567-30576).

Hughes Jr, F.M. Cidlowski, J.A. Potassium is a critical regulator of apoptotic enzymes in vitro and in vivo (1999) *Advances in Enzyme Regulation*, **39**: 157-171.

Hughes, D. Mehmet, H. *Cell proliferation and apoptosis. Advanced methods* (2003) Bios Scientific Publishers Limited. Oxford.

Kass, G.E.N. Orrenius, S. Calcium signalling and cytotoxicity (1999) *Environmental Health Perspectives*, **107**(S1): 25-35.

Kerr, J.F. Wyllie, A.H. Currie, A.R. Apoptosis: a basic biological phenomenon with wide-ranging implications in tissue kinetics (1972) *British Journal of Cancer*, **26**:239-257.

Khaled, A.R. Kim, K. Hofmeister, R. et al. Withdrawl of IL-7 induces Bax translocation from cytosol to mitochondria through a rise in intracellular pH (1999) *Proceedings of the National Academy of Sciences of the United States of America*, **96**(25): 14476-14481.

Khaled, A.R. Reynolds, D.A. Young, H.A. et al. Interleukin-3 withdrawal induces an early increase in MMP unrelated to the bcl-2 family- roles of intracellular pH, ADP transport, and F0F1-ATPase (2001a) *Journal of Biological Chemistry*, **276**(9): 6453-6462.

Khaled, A.R. Moor, A.N. Li, A. et al. Trophic factor withdrawl: p38 mitogen-activated protein kinase activates NHE1, which induces intracellular alkalinization (2001b) *Molecular and Cellular Biology*, **21**(22): 7545-7557.

Kim, J-M. Bae, HR. Park, B.S. et al. Early mitochondrial hyperpolarization and intracellular alkalinisation in lactacystin-induced apoptosis of retinal pigment (2003) *The Journal of Pharmacology and Experimental Therapeutics*, **305** (2): 474-481.

Li, P.F. Dietz, R. von Harsdorf, R. p53 regulates mitochondrial membrane potential through reactive oxygen species and induces cytochrome c-independent apoptosis blocked by Bcl-2 (1999) *European Molecular Biology Organization Journal*, **18** (21): 6027-6063.

Maeno, E. Ishizaki, Y. Kanaseki, T. et al. Normotonic cell shrinkage because of disordered volume regulation is an early prerequisite to apoptosis (2000) *Proceedings of the National Academy of Science of the United States of America*, **97**(17): 9487-9492.

Majno, G. and Joris, I. Apoptosis, oncosis and necrosis. An overview of cell death (1995) American Journal of Pathology, 146(1):3-15.

Martin, J. Mahlke, K. and Pfanner, N. Role of an energised inner membrane mitochondrial protein import (1991) *The Journal of Biological Chemistry*, **266** (27): 18051-18057.

Martin, S.J. Reutelingsperger, C.P.M. McGahon, A.J. et al. Early redistribution of plasma membrane phosphatidylserine is a general feature of apoptosis regardless of the initiating stimulus inhibition by overexpression of bcl-2 and ABL (1995) Journal *of Experimental Medicine*, **182**: 1545-1556.

Marzo, I. Brenner, C. Zamzami, N. et al. Bax and adenine nucleotide translocator cooperate in the mitochondrial control of apoptosis (1998) *Science*, **281** (5385): 2027-2031.

McCarthy, J.V. and Cotter, T.G. Cell shrinkage and apoptosis: a role for potassium and sodium ion efflux (1997) *Cell Death and Differentiation*, **4**: 756-770.

Montague, J.W. Bortner, C.D. Hughes Jr, F.M. et al. A necessary role for reduced intracellular potassium during the DNA degradation phase of apoptosis (1999) *Steroids*, **64**(9): 563-569.

Okada, Y. Maeno, E. Apoptosis cell volume regulation and volume-regulatory chloride channels (2001) *Comparative Biochemistry and Physiology A-Molecular & Integrative Physiology* **130**(3): 377-383.

Porcelli, A.M. Ghelli, A. Zanna, C. et al. Staurosporine induces apoptotic volume decrease (AVD) in ECV304 cells (2003) *Annals of the New York Academy of Science*, **1010**: 342-346.

Roberg, K. Johansson, U. Ollinger, K. Lysosomal release of cathepsin D precdes relocation of cytochrome c and loss of mitochondrial transmembrane potential during apoptosis induced by oxidative stress (1999) *Free Radical Biology and Medicine*, **27**: 1228-1237.

Skulachev, V.P. Mitochondrial physiology and pathology:concepts of programmed death of organelles, cells and organisms (1999) *Molecular Aspects of Medicine*, **20**:139-184.

Thompson, C.B. Apoptosis in the pathogenesis and treatment of disease (1995) *Science*, **267**(5203): 1456-1462.

Trump, B.F. Berezesky, I.K. The role of altered [Ca2+]I regulation in apoptosis, oncosis and necrosis (1996) *Biochemica et Biophysica Acta*, **1313**:173-178.

Vander Heiden, M.G. Chandel, N.S. Williamson, E.K. et al. Bcl-xL regulates the membrane potential and volume homeostasis of mitochondria (1997) *Cell*, **91** (5): 627-637.

Wang, X. Becker, F.F. Gascoyne, P.R.C. Membrane dielectric changes indicate induced apoptosis in HL-60 cells more sensitively than surface phosphatidylserine expression or DNA fragmentation (2002) *Biochemica et Biophysica Acta*, **1564**: 412-420).

Wyllie, A.H. Kerr, J.F.R. Currie, A.R. Cell death: the significance of apoptosis (1980) *International Review of Cytology*, **68**: 251-306.

Yu, S.P. Canzoniero, L.M. Choi, D.W. Ion homeostasis and apoptosis (2001) *Current Opinion in Cell Biology*, **13**(4): 405-411.

Yu, S.P. Choi, D.W. Ions, cell volume, and apoptosis (2000) *Proceedings of the National Academy of Science of the United States of America*, **97**(17): 9360-9362.

Yu, S.P. Regulation and critical role of potassium homeostasis in apoptosis (2003) *Progress in Neurobiology*, **70**: 363-386.

Yu, S.P. Yeh, C.H. Sensi, S.L. et al. Mediation of neuronal apoptosis by enhancement of outward potassium current (1997) *Science*, **278**(5335): 114-117.

Yu, S.P. Yeh, C.H. Strasser, U. et al. NMDA receptor mediated K^+ efflux and neuronal apoptosis (1999) *Science*, **284**(5412):336-339.

5. Conclusion

This work presents a study of the biophysical properties of cancer cells in a range of pharmacological scenarios, focusing on the effects of pharmacological agents both on drug-sensitive and multidrug resistant leukaemic and breast cancer cell lines. In this work, dielectrophoresis has been used as a non-invasive technique to examine dielectric properties of drug resistant and sensitive cancer cells before and after treatment with anti cancer drugs, and with a chemosensitiser. The results of this work have provided a better understanding of the physiology of different types of cancer cells, and allowed direct comparisons of these properties for both the membrane and the cytoplasm.

Dielectrophoresis (DEP) is the motion of particles, (in this case cells), in non-uniform electric field gradients. The non-uniform nature of the field generates Coulombic forces of differing magnitudes at either pole of the cell dipole, resulting a net force and a resultant motion. The gradient of the electric field and the polarisibility of the cell dictate the motion of the cell. The polarisiblity is a function related to the dielectric properties of both the cell and the medium surrounding it. If the cell is more polarisable than the medium, the net motion acts in the direction of highest electric field regions; a phenomenon called *positive dielectrophoresis*, where cells are attracted to the electrodes. If the medium is more polarisable than the cell, net motion acts towards low-field regions; a phenomenon called *negative dielectrophoresis*, as cells are repelled from the electrodes. These properties are dependent on frequency of the applied electric field.

Cancer is one of the biggest causes of death, and common methods of treatment include radiation, local excision and chemotherapy. A significant impediment in the chemotheraputic treatment of cancer is the acquisition of the ability of cancer cells to prevent the drug from reaching its target (typically in the nucleus), thereby rendering the cell resistant to the effects of the drug. The term "multi-drug resistant" (MDR) is used to characterise those cells that have acquired cross-resistance to many anti-cancer drugs having no common structure, but are generally natural product in origin. A number of mechanisms have been suggested by which cells acquire MDR. One of which is the overexpression of membrane glycoproteins, collectively termed as the ABC (ATP-binding-cassette) transporters. A typical example of the ABC transporters is the membrane P-glycoprotein pump (P-gp), which effluxes anti cancer drugs outside the cells, thereby reducing the intracellular accumulation of the drugs and reducing their cytotoxic effects as a result. Another form of MDR is that involving reduced anti cancer drug cytotoxicity, as the drug is sequestered into vesicles, as part of the intricate intracellular trafficking system.

In order to assess the biophysical properties of MDR cells, previous studies have used a membrane potential sensitive dye (DIOC5) and flow cytometry to compare membrane potentials of drug sensitive and resistant cancer cells before and after treatment with a chemosensitiser (agents that are designed to reverse drug resistance). Previously, it was found that the membrane potential was decreased significantly after treating the resistant cell lines with the chemosensitiser. Our DEP data, however, showed no significant changes in the biophysical properties of drug sensitive or drug resistant cancer cells following

modulator/chemosensitiser therapy. The disparity between DEP and flow cytometry results indicated that DIOC5 acts as a substrate for P-gp. Furthermore, the results probed biophysical differences between cell lines, with multidrug resistant (MDR) cells exhibiting a higher cytoplasmic conductivity than the parental cells. These findings are suggestive of a difference in the relative ionic strengths of the tumour cells. The technique has also revealed differences in the membrane morphology of MCF-7 relative to MCF-7TaxR, whilst showing an absence of such membrane differences in K562 relative to K562AR. XR9576, a P-gp specific chemosensitiser/modulator did not exert any effects on the cytoplasm or membrane parameters in K562 and K562AR but altered the membrane morphology in MCF-7TaxR after treatment. DEP has therefore provided a more informative and a rigorous approach in revealing that it is the cytoplasm that varies between MDR and drug sensitive cells. Moreover, using the DIOC5 method of probing membrane potential provides artefactual results, as the dye is a substrate for ABC transporters.

Further studies were then performed to investigate differences between sensitive and drug resistant cell lines. Reports have suggested that MDR can be mediated by the overexpression of an ABC-transporter, which includes P-gp, or by drug sequestration. DEP was used to reveal and compare dielectric properties of ABC- and non- ABC- based modes of MDR. Different cell lines were compared, namely MDR chronic myelogenous leukaemia (K562AR) and breast cancer (MCF-7TaxR and MCF-7DoxR), relative to their parent drug sensitive cell lines. The results pointed to significant differences in the cytoplasmic ionic content with no significant differences in the membrane parameters. The results also

suggested that two mechanisms of drug resistance were present. One of these is P-gp- dependent and relies on the pump acting as a Cl^- channel, as in K562AR. The other mechanism is non- P-gp –dependent, as in MCF-7DoxR, where the principal mechanism of drug resistance is believed to be that of drug sequestration and vesicular trafficking, as the cytoplasmic conductivity was higher than the parent. This MDR cell line lacked the expression of P-gp, and the potential mechanism of this might involve a defect in the Na^+/H^+ ATPase (NHE), resulting in the accumulation of Na^+ in the cytoplasm. In MCF-7TaxR, however, a low cytoplasmic conductivity was detected relative to the parent, despite its overexpression of P-gp. We believe that P-gp is behaving more like a regulator in the MCF-7TaxR, implying a deactivating role in the Cl^- channels, hence possibly resulting in a reduction of the total ionic content, giving a lower cytoplasmic conductivity relative to the parent.

Another aspect of the interaction between cancer cells and pharmacological agents is the induction of *apoptosis* (programmed cell death). This was the third focus point of this research. A recent study reported the use of DEP to detect early stages of apoptosis and found a significant decrease in the specific membrane capacitance after 4 hours of apoptosis induction. DEP was used to study apoptosis by examining the cytoplasm as well as the membrane parameters at early, and extending the study to look at later stages of apoptosis. Other well established flow cytometry based techniques, namely annexin V were used to characterise the stage of apoptosis, and the mitochondrial membrane potential was investigated and compared by using the TMRE assay. DEP results indicated that K562 cells had an increased cytoplasmic conductivity within the

first 4 hours after exposure to staurosporine, which then lasted beyond 12 hours of exposure. The Annexin V assay indicated that this occurred simultaneously with early-stage apoptosis. Furthermore, within this time period, TMRE data pointed to hyperpolarisation in the MMP. Although no work exists which directly explains the rise of cytoplasmic conductivity at this stage of apoptosis, a likely cause of this effect that can be suggested is that of cell shrinkage due to water loss trigger by ion (K^+, Cl^-) efflux, causing concentration of the remaining ions. Interestingly, after 24 and 48 hours of incubation with staurosporine, multiple populations were detected by DEP, highlighting the eventual dielectric changes that the cell undergoes before death or necrosis. The Annexin V results showed that the majority of cells were identified as being in the late stages of apoptosis and the TMRE data indicated both depolarised and hyperpolarised MMP in the population. The DEP results at these two time points showed cells with elevated, diminished or effectively lost cytoplasmic conductivities after 24 hours of exposure to staurosporine, with only the latter two populations being observed after 48 hours of exposure. The reduction effect might be associated with the later stages of apoptosis. This may be due to cell swelling, causing the cell ionic content was becoming more dilute and the significantly lower cytoplasmic conductivity obtained relative to control untreated cells. However, this conductivity was significantly higher than the third population (assumed to be dead cells). This could be the result of an increased ionic content, such as an influx of Ca^{2+} and Na^+ through the membrane channels from the extracellular fluid, and additionally from the mitochondria in the case of Ca^{2+}.

Further work will be required in order to further explore some of these hypotheses produced from the results obtained. Firstly, activities of certain ionic channels should be investigated to address the changes in the cytoplasmic conductivity of the ABC- and non- ABC mediated MDR. This could be performed by the use of channel blockers, and investigating overexpression of these channels to eliminate for the changes seen. Examples may include Ba^{2+} and quinine for K^+- channel, 5-nitro 2-(3-phenylpropylamine) benzoic acid (NPPB) for Cl^- channel blockers and 4-acetoamido-4'-isothiocyanostilbene-2,2'-disulfonic acid (SITS) for Cl^-/HCO_3^- channel blockers. This work could also be extended by investigating the cytoplasmic pH using the fluorescent pH indicator SNARF 1, and the cytoplasmic ionic composition using techniques such as time-of-flight secondary ion mass spectrometry (TOF-SIMS). The work on apoptosis can be extended by increasing the time resolution by including additional staurosporine incubation periods, and test other modes of apoptosis induction, such as UV radiation or dexamethasone on the cell lines used.

Publications arising from this work

Book chapters:

AC Electrokinetics of particles

MP Hughes, K Hoettges, FH Labeed, HO Fatoyinbo

Handbook of Engineering, ed. RC Dorf, CRC Press (Boca Raton), 2004 *(book chapter)*

Refereed journals:

Assessment of multidrug resistance reversal using dielectrophoresis and flow cytometry

FH Labeed, HM Coley, H Thomas, MP Hughes

Biophysical Journal 2003; 85: 2028-2034

Major dielectric differences in the cytoplasm at different stages of apoptosis

FH Labeed, MP Hughes, H Thomas, HM Coley

Biophysical Journal (submitted)

Anticancer drugs change the dielectric properties of multidrug resistant cancer cells

FH Labeed, MP Hughes, H Thomas, HM Coley

Clinical Cancer Research (submitted)

Dielectrophoresis reveals major biophysical differences in multidrug resistance in cancer

FH Labeed, MP Hughes, H Thomas, HM Coley

Journal of Biological Chemistry (submitted)

Extraction of dielectric properties from dielectrophoretic collection spectrum data

L Broche, FH Labeed, MP Hughes

Physics in Medicine & Biology (submitted)

Dielectrophoresis in drug discovery (review)

FH Labeed, MP Hughes, H Thomas, HM Coley

Biotechnology (in preparation)

Conference papers:

Differences between drug-resistant and sensitive cancer cells studied using flow cytometry and dielectrophoresis

FH Labeed, MP Hughes, H Thomas, HM Coley

1st European Workshop on Electrokinetics and Electrohydrodynamics in Microsystems (Glasgow, UK, 2001).

Dielectrophoretic assessment of modulator action on drug-resistant and sensitive cancer cells

FH Labeed, MP Hughes, H Thomas, HM Coley

Electromagnetic methods in Pharmacy and Medicine (Canterbury, UK, 2002).

Assessment of modulator action on drug-resistant and sensitive cancer cells using dielectrophoretic methods

FH Labeed, MP Hughes, H Thomas, HM Coley

British Association for Cancer Research Annual Meeting (Glasgow, UK, 2002).

Dielectrophoresis for assessment of drug action

MP, Hughes, KF, Hoettges, FH, Labeed, HO, Fatyinbo and Y, Hubner

15th International Bioanalytical Forum (University of Surrey, Guildford, UK, 2003).

A rapid assay of apoptotic progress in a mixed population by dielectrophoresis (DEP)

FH Labeed, MP Hughes, H Thomas, HM Coley

94th Annual meeting of the American Association for Cancer Research (Washington DC, USA, 2003).

Dielectrophoretic assessment reveals major differences in the biophysical properties of the membrane and cytoplasm of MDR versus parental lines

FH Labeed, MP Hughes, H Thomas, HM Coley

95th Annual meeting of the American Association for Cancer Research (Orlando, Florida, USA, 2004)